9 Organic gas phase ion chemistry

Tom Waters and Richard A. J. O'Hair *

School of Chemistry, University of Melbourne, Victoria 3010, Australia

1 Introduction

Experimental studies on a wide variety of gas phase organic species such as radicals, neutrals, ions, clusters and aerosols continued in 2001. The focus of this annual review is similar to previous years, with an emphasis on a physical organic approach to understanding the mechanisms of gas phase organic ion–molecule reactions.[1] Despite many impressive advances of 'real world' applications of mass spectrometry (*e.g.* the analysis of species of ever increasing complexity such as bacteria[2] and intact micro-organisms[3]), the burgeoning areas of chemical and biological analytical mass spectrometry are for the most part not reviewed. The following applications of chemical and biological analytical mass spectrometry have been reviewed in 2001: environmental sciences;[4] polymer and polymer surfaces;[5] proteomics;[6–8] other aspects of protein chemistry;[9–11] and lipids.[12]

It has been noted that mass spectrometry has evolved from an art practised by a few to ***a widely used analytical science that produces a billion individual mass spectra daily***.[13] This intense interest in mass spectrometry is reflected in an entire issue of Chemical Reviews being devoted to "Frontiers in Mass Spectrometry",[14] including a review on mass spectrometric studies of organic ion–molecule reactions by Gronert.[15] Details of instrumentation, techniques and past reviews of gas phase organic ion chemistry are not given here – readers are directed to last year's review[1] and previous introductions by Gronert.[16,17]

A number of reviews and books have appeared in 2001 that reflect the rich areas of organic gas phase ion chemistry. Topics covered include: a discussion of the units in mass spectrometry;[18] methods of generating gas phase ions;[19–21] mass analysers;[22,23] coupling of chromatography techniques to MS;[24,25] aspects of unimolecular fragmentation reactions;[26,27] collisions with surfaces;[28] charge permutation reactions[29] including charge stripping of anions;[30] mulitpole bound molecular anions;[31] crossed beam methods;[32] high temperature conditions;[33] complex formation and the influence of vibrations;[34] applications of proton transfer reactions;[35] base induced 1,4 elimination reactions;[36] formation of cumulenes and related systems;[37] the neutral products from gas phase carbocation rearrangements;[38] thermochemistry of ions[39] including proton transfer;[40] photodetachement of multiply charged anions;[41] photodissociation of ions;[42,43] REMPI photoelectron spectroscopy;[44] techniques to probe the "conformational landscape" of small biomolecules in the gas phase;[45] gas phase spectroscopy of

biomolecules;[46,47] aspects of cluster ions;[48,49] use of ion-mobility measurements;[50] molecular recognition and supramolecular chemistry;[51,52] non-covalent complexes in the gas phase including cyclodextrin complexes,[53] RNA and DNA complexes[54] and oligonucleotide complexes with drugs, metals and proteins;[55] computational chemistry as an aid to experiment;[56,57] and aspects of mass spectrometry in drug discovery[58–61] including a book[58] which has a review on fundamental ion chemistry and fragmentation.[59]

The gas phase ion chemistry of inorganic and organometallic systems is sufficiently advanced to warrant a yearly review of the literature, and transition metal inorganic and organometallic gas phase chemistry is not discussed here. A number of reviews have appeared in the previous year, including: the gas phase "solvation" of metal ions;[62–64] gas phase coordination chemistry;[65] doubly charged metal complexes;[66] thermochemistry of metal ions;[67,68] unusual stoichiometries of metal systems;[69] temperature effects in metal ion reactions;[70] transition metal oxides and sulfides[71] and the use of electrospray ionization to study organometallic catalysis in the gas phase.[72]

2 Reactions of carbocations and related cations

Carbocations exhibit a rich and diverse gas phase chemistry, and their rearrangements have been reviewed in 2001.[38] Apart from their central role in many analytical applications, they are thought to play important roles in areas ranging from interstellar chemistry[73] and the atmosphere of Titan[74] through to the formation of diamond-like carbon films.[75] Suprising reactions and processes involving carbocations continue to be discovered. For example, the fragmentation of protonated acetaldehyde to the methyl cation involves mechanisms other than the simple direct cleavage to yield hydroxycarbene.[76] The remainder of this Section reviews papers published in 2001 involving the formation, reactivity and stability of carbocations and radical cations.

A Carbocation ion–molecule reactions

The field of gas phase carbocation chemistry is sufficiently advanced that existing thermochemical data has been used to develop a model of the atmosphere of Titan in which clustering of N_2 to ionic species such as CH_5^+, $HCNH^+$ and HN_2^+ is thought to play an important role.[77]

Tsuji and co-workers have continued their studies on the reactions of CH_5^+, $C_2H_5^+$ and $C_3H_5^+$ ions with organic compounds using a quadrupole ion trap, most recently focusing on C8–C18 1-alkenes.[78] Alkyl and alkenyl ions were observed in all reactions, with distributions peaking at C4 or C5 and C7 for the long-chain alkenes. Based on the observed distributions and calculated thermochemical data, it was concluded that: (i) CH_5^+ reacts *via* proton transfer to the C=C bond to give alkyl cations or *via* hydride-ion abstraction to yield alkenyl ions; (ii) $C_2H_5^+$ reacts *via* proton transfer to the C=C bond to give alkyl cations or *via* alkanide-ion abstraction to yield alkenyl ions; and (iii) $C_3H_5^+$ ions undergo addition to the C=C bond. A theoretical study on the attack of CH_3^+ at carbon atoms of a benzene moiety fused to small rings[79] follows the first experimental examination of the Mills–Nixon (MN) effect discussed in last

year's review. In kinetically controlled reactions the β-position is more reactive than the α-site, supporting the original Mills–Nixon postulate. However, in thermodynamically controlled electrophilic substitution reactions the α-site is slightly preferred for three-, four- and five-membered annelated rings. Differences between the Me cation affinities at the α and β positions were theoretically analysed and resolved into angular strain and cationic resonance contributions. The gas phase reaction of CH_3^+ with Me_3SiNH^iBu has been studied *via* the radiolytic technique and proceeds *via* either condensation or proton transfer.[80]

The unimolecular and bimolecular chemistry of isomeric $C_4H_7^+$ ions formed *via* Cl loss from the radical cations of RCl (where R = cyclopropylcarbinyl, cyclobutyl and homoallyl) have been studied.[81] When R = cyclopropylcarbinyl or homoallyl the cyclopropylcarbinyl cation is formed, while when R = cyclobutyl a substantial amount of the bicylcobutonium ion is formed.

The diastereofacial selectivity (Scheme 1) for the reactions of tertiary 2-adamantyl cations reacting with methanol in the gas phase has been reported.[82] When X = F, addition of CH_3OH proceeds *via* tight transition states with large adverse entropic factors accounting for the preferred *syn* diastereoselectivity. In contrast, when X = Me_3Si entropy plays a minor role in the looser transition state, leading to a preference for *anti* addition.

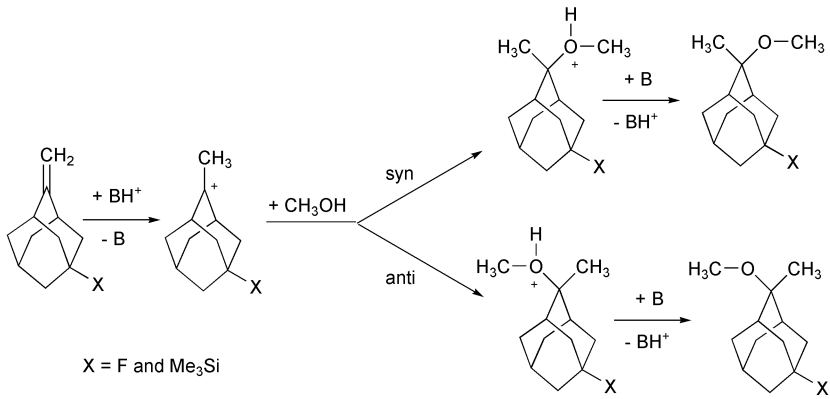

Scheme 1

An ion trap mass spectrometer has been used to examine the ion molecule reactions of fragment ions formed *via* electron impact on 1,1,1- and 1,1,2-trichlorotrifluoroethane with their neutral parent precursors.[83] The $[M - Cl]^+$, Cl_3C^+ and Cl_2FC^+ ions were found to be unreactive, while all other ionic species react *via* halide abstraction to give $[M - Cl]^+$ and, to a far lesser extent, $[M - F]^+$. The competing Cl^- *versus* $Cl^{\bullet}$ abstraction reactions [eqns. (1) and (2)] were postulated to arise from the same intermediate **1**. Two interesting reactivity trends were observed: (i) the monovalent carbenium ions were more reactive than their divalent counterparts, which in turn were more reactive than the trivalent ions [*e.g.* the reaction efficiencies for the fluorinated systems are: $CF^+(0.96) > CF_2^{+\bullet}(0.78) > CF_3^+(0.70)$]; and (ii) within a given family of ions, reactivity increases with the number of fluorine substituents (*e.g.* $CF_2^{+\bullet}$

> $CFCl^{+\bullet}$ > $CCl_2^{+\bullet}$ and CF^+ > CCl^+). Ion–molecule reactions of similar ions have been the subject of two other studies: (i) the dichlorocarbene radical cation reacts with acetone *via* $O^{-\bullet}$ transfer to form a transient radical cation of dimethylcarbene, which undergoes rapid rearrangement to the radical cation of propene;[84] and (ii) CF^+, $CF_2^{+\bullet}$ and CF_3^+ ions undergo halide transfer reactions with CF_3X (X = Br and I), with CF^+ being most reactive.[85]

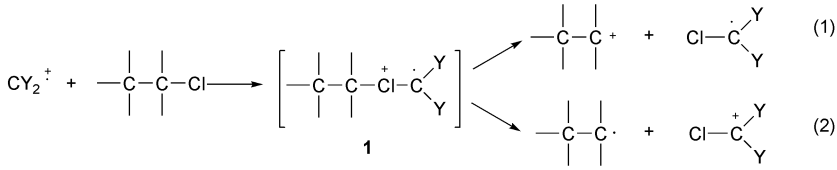

The gas phase reactivities of a range of carboxonium and sulfonium ions towards cyclic acetals and ketals have been compared.[86] While primary carboxonium (H_2C=O^+–R) and carbosulfonium (H_2C=S^+–R) ions (R = CH_3, C_2H_5, Ph) react *via* transacetalization [eqn. (3), X = O or S], acyclic secondary and tertiary carboxonium ions bearing acidic α-hydrogens undergo little or no transacetalization, with proton transfer dominating instead.

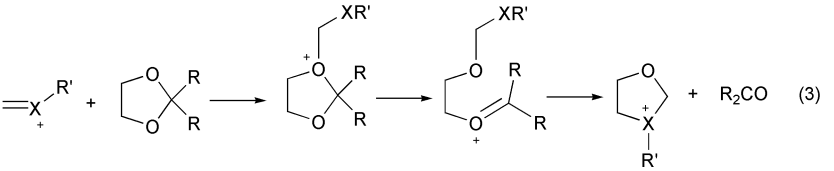

The selectivity of dimethyl ether as a chemical ionization reagent towards anthraquinones has been evaluated in an ion trap mass spectrometer.[87] The two major reagent ions, $CH_3OCH_2^+$ and $(CH_3)_2OH^+$, react to give a series of ions including $[M+CH]^+$, $[M+CH_3]^+$, $[M+CH_3OCH_2]^+$ and $[M+(CH_3)_2OH]^+$. The MS/MS behaviour of these ions was compared to the $M^{+\bullet}$ ion.

Substituted benyzl cations formed *via* fragmentation of electrosprayed benyzylpyridinium salts undergo ion–molecule reactions with background solvent molecules in a quadrupole ion trap mass spectrometer.[88] The kinetics of addition of acetonitrile solvent molecules onto these substituted benyzl cations were found to directly correlate with the Brown parameter σ^+ of the aromatic ring substituent, and therefore with the effective charge density on the α-carbon atom of the benzyl ion. Another gas phase benzyl group migration has been observed in the extrusion of formamide from protonated aminoacylbenzylamines formed *via* ESI.[89]

While the gas phase ion–molecule reactions of phenyl cations have been studied in depth experimentally over the past decades (most recently radiolytic techniques have been used to show that diethylamine reacts with phenyl cations *via* benzyne formation[90]), the theoretical literature on these systems has lagged behind. Thus, the detailed theoretical investigation of the reaction of the phenyl cation with methanol and methyl fluoride using DFT makes a welcome addition.[91] The high exothermicity

of these addition reactions (67 kcal mol^{-1} for CH_3OH and 42 kcal mol^{-1} for CH_3F) can be used to drive a range of reactions. Among the reactant complexes corresponding to the different sites of the phenyl cation attack on the CH_3X molecules ($[C_6H_5{\cdot}CH_3X]^+$ X = OH, F), the addition complex (O-protonated anisole) was most stable for X = OH, followed by the CH insertion complex (*ipso*-protonated benzyl alcohol), while for X = F the CF insertion complex was most stable. Addition and insertion complexes may transform into the ring protonated isomers either *via* proton migrations (with barrier heights in the 1–23 kcal mol^{-1} range) or methyl migrations (with barrier heights in the 5–28 kcal mol^{-1} range). The global minimum corresponds to *para*-protonated anisole for X = OH and *meta*-protonated *ortho*-fluorotoluene for X = F.

Finally, the unimolecular fragmentation reactions of alkoxylated oxonium ions proceed *via* a novel three-component 'ion–neutral–neutral' intermediate consisting of a solvated 1,1-dimethylallyl cation which ultimately decomposes to yield the proton bound dimer [eqn. (4)].[92]

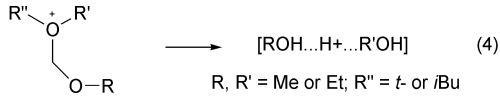

(4)

B Carbocation stability and isomerization

Photoionization–photoelectron experiments provide detailed information on ionization energies, ion dissociation thresholds [eqn. (5)] and ion appearance energies. These quantities allow heats of formation of cations and bond dissociation energies for neutrals and cations to be deduced. A significant recent advance is the implementation of high resolution VUV synchrotron sources to provide highly accurate thermochemical data, including separation of spin-orbit states (allowing spin-orbit coupling constants to be calculated).[93–96] Organic systems studied include CH_4,[93] CD_4,[94] C_2H_2,[93] CH_3X (X = Br and I)[95] and nitrobenzene.[96] The fragmentation processes occurring in nitrobenzene as a result of photoionization are quite complex, and the appearance energies of 18 fragment ions ranging from $C_6H_5NO^+$ to H^+ were determined. While this data has allowed the previously unknown heats of formation for $C_5H_2^+$ and $C_6H_3^+$ to be estimated, the isomers that are formed remains unclear.

(5)

The gas phase bromide ion exchange equilibrium [eqn. (6)] has been used to examine the influence of alkyl substitution on the gas phase stability of 1-adamantyl cations **2**.[97] 1-Adamantyl cations having three methyl groups or up to three *i*-Pr groups

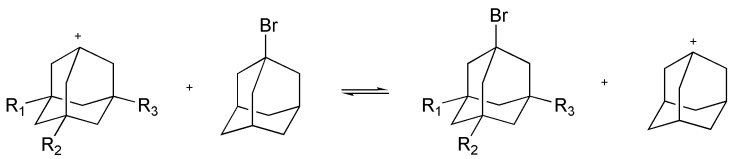

(6)

2

on the 3-, 5- and 7-positions are more stable than the 1-adamantyl cation, and stability increases with the number of *i*-Pr groups. Relative stabilities were compared to the rates of solvolysis of 1-bromoadamantane species in a range of solvents.

The gas phase protonation of cyclopropane by Brønsted acids leads to two distinct $C_3H_7^+$ isomers: cyclic *c*-$C_3H_7^+$ and acyclic *i*-$C_3H_7^+$.[98] Relative abundances of these isomers were determined by analysing the neutral end products from their reactions with benzene *via* radiolytic experiments. Protonation by strong acids leads to a large extent of isomerization to the thermodynamically favoured *i*-$C_3H_7^+$. Deuterium labelling experiments reveal that *c*-$C_3H_7^+$ ions undergo complete randomization of their hydrogen atoms, and high level *ab initio* calculations suggest this scrambling involves the interconversion of corner protonated cyclopropane **3** (thermodynamically favoured) and edge protonated cyclopropane **4**.

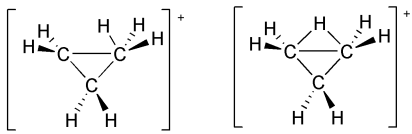

3 **4**

It is well known that ions can isomerize during fragmentation processes. Mormann and Kuck have carried out detailed labelling studies and independantly synthesized proposed intermediates to evaluate the mechanism for ethene loss from protonated 7-ethylcycloheptatriene and related systems.[99] They find that the H ring walk **5** ⟶ **6** ⟶ **7** isomerizes the protonated cycloheptatriene frame to yield isomer **8** (with the bicyclo[3.2.1]octenyl framework) which then undergoes a cycloreversion process to yield protonated toluene (Scheme 2).

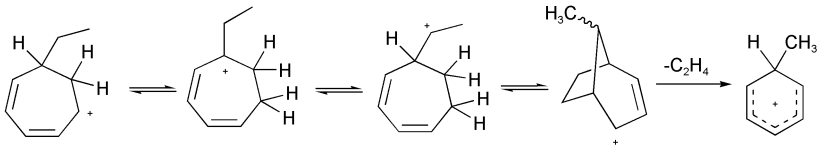

5 **6** **7** **8**

Scheme 2

C Reactivity of conventional radical cations *versus* their isomeric distonic ions

The gas phase reactivity of conventional radical cations as well as their distonic ion counterparts continues to generate considerable interest, especially since these species play a key role in the fragmentation reactions of ions generated under EI conditions. Although the EI literature is so vast that no attempt is made to review the 2001 contributions here, we do note the following: (i) several groups are carrying out careful labelling studies which reveal that many fragmentation reactions of ions under EI conditions are very complex, often involving hydrogen transfers and skeletal or other

isomerizations;[100] (ii) hydrogen and alkyl shifts are often involved which can cause isomerization between conventional radical cations and distonic ion structures;[101] (iii) ion-neutral complexes often play an important role in EI fragmentation reactions[102] as well as the collision induced dissociation (CID) reactions of radical cations;[103] (iv) high-resolution analysis of kinetic energy distributions of fragment ions provides detailed information on their energy content and on the competition between fast and slow fragmentation;[104] (v) several rearrangement and migration reactions under EI conditions have been discussed[105–108] including a gas phase Newman–Kwart rearrangement reaction;[109] (vi) the benzylium/tropylium ion structure and mode of formation saga continues;[110] and (vii) one cannot assume that a fragment ion at a particular *m*/*z* value in an EI mass spectrum has only one structure.[111]

This Section begins with a review of studies that have considered both conventional radical cations and distonic ion structures, before moving onto studies which have considered only the reactivity of conventional radical cation structures or the reactivity of distonic ions. The reactivity of some unusual distonic ions is also discussed in Section 4.

The rich ion chemistry of ionized phenol has been examined *via* experiment and theory.[112] The structures and relative stabilities of 16 six-membered ring isomers were calculated, and several detailed potential energy surfaces for the extrusion of CO were examined (starting from the conventional radical cation **9** which represents the global minimum of all 16 structures). The most favoured of these is shown in eqn. (7) of Scheme 3. The rate determining step is the enol–keto isomerization, which requires a 1,3 H transfer. The keto ion **10** does not undergo concerted CO loss, but rather ring opens to **11**, followed by recyclization to the five-membered ring **12**, leading to the final products. The authors also attempted to generate novel distonic ion structures *via* CID of appropriate precursor ions. The $[M + H]^+$ ion of 4-bromophenol fragments *via* loss of Br to give $[C_6,H_6,O]^{+\bullet}$, which fragments identically to the conventional radical cation structure **9**. The authors suggest this is due to protonation of 4-bromophenol on the ring to give **14**, which fragments to give **9** [eqn. (8)]. This compares with protonation at the O atom to give **15**, which would fragment to give the novel distonic ion **16** [eqn. (9)]. In contrast, the $[M - CO]^{+\bullet}$ ion of salicylaldehyde exhibits a different MS/MS spectrum and it was suggested that this was due to the formation of the novel distonic ion **17** [eqn. (10)].

Anderson's group have continued their studies on how the vibrational state of an ion can influence its gas phase reactivity. A guided ion beam instrument was used to study the combined effects of reactant ion vibrational state and collision energy on the reactions of mode-selectively excited acetaldehyde cations with D_2O,[113] CH_3OH[114] and C_2H_2.[115] Reactions with D_2O proceed *via* proton transfer [eqn. (11)], H/D exchange [eqn. (12)] and CH_3 loss [eqn. (13)].[113] H/D exchange is dominant at low energy collisions, but is inhibited by CH_3CHO^+ vibration as well as increasing collision energy. CH_3 elimination is most energetically favoured, yet is only a minor channel and is strongly suppressed by both collision energy and vibration. The proton transfer reaction shows strongly mode-specific dependence on the CH_3CHO^+ vibrational state. Similar reactions are observed for CH_3OH and its deuterated analogues, with the dominant exoergic proton transfer channel [*cf.* eqn. (11)] being strongly suppressed by collision energy and mildly suppressed by CH_3CHO^+ vibrational excitation.[114] Minor H abstraction reactions from both the CH and OH

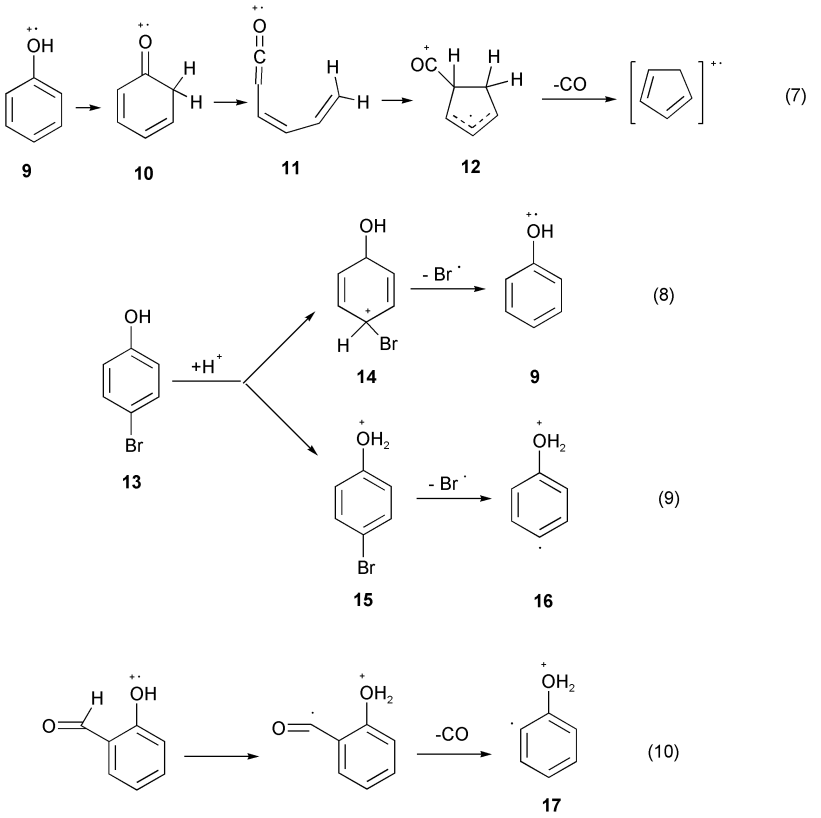

Scheme 3

sites of CH_3OH were also observed. For reaction with acetylene, the dominant hydrogen transfer channel [eqn. (14)], proceeds with >73% efficiency at low energies, and decreases with increasing collision energy. This reaction is also weakly affected by reactant vibration, including the aldehyde CH stretch.[115] CH_3 elimination from a covalently bound complex [eqn. (15)] is the most exoergic reaction, yet accounts for no more than a few percent of the total reaction signal and is strongly (but non-mode specifically) inhibited by vibration.

The chemistry of enol radical cations has been the subject of several recent studies.[116–119] Fourier transform ion cyclotron resonance (FT-ICR) experiments using labelled reactants as well as ab initio calculations have been used to show that the $CH_2CHOH^{\cdot+}$ enol radical cation reacts with *t*-butanol by a simple exothermic proton transfer to yield the ter-body intermediate [$CH_2CHO^{\cdot}$, H_2O, $C(CH_3)_3^+$].[116] This intermediate then undergoes three processes: (i) formation of *tert*-butylvinyl ether with elimination of water [eqn. (16)]; or alternatively, regiospecific proton transfer to isomerize into three different ter-body complexes formed of water, isobutene and ionized enol, which can then react to either form (ii) the solvated enol ion [eqn. (17)]; or (iii) undergo a cycloaddition-cycloreversion process to form a new enol ion [eqn. (18)].

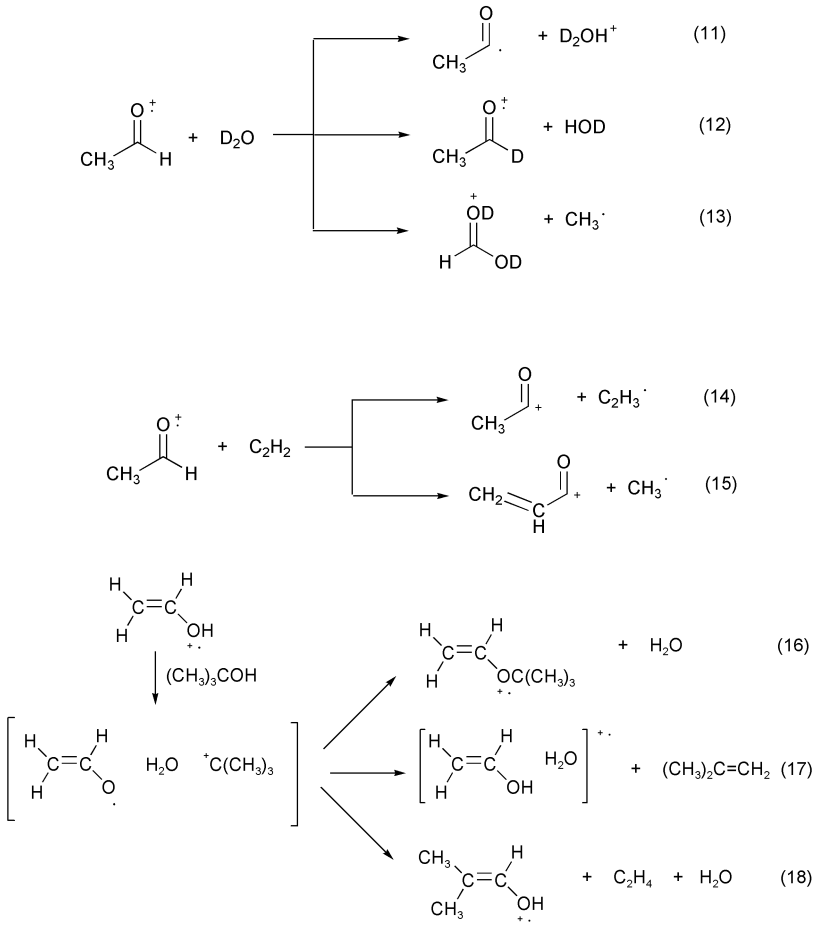

Two different groups have examined the catalysis of keto to enol tautomers of radical cations *via* ion–molecule reactions. Mourgues *et al*. have found that a wide range of compounds (ethers, ketones, nitriles, acids and esters) can be used to isomerize the keto radical cations of acetone into the enol form *via* the 'proton transport' mechanism.[117] The neutral catalyst must be basic enough to abstract a proton from the methyl group of ionized acetone, but not too basic so as to give this proton back to oxygen. Thus, for a catalyst to be efficient, its proton affinity (PA) must lie between the PA of the radical $CH_3COCH_2^{\bullet}$ at the carbon site (PA_C = 185.5 kcal mol^{-1}) and its PA at the oxygen site (PA_O = 195.0 kcal mol^{-1}).

Both the acetamide radical cation, $CH_3C(=O)NH_2^{\bullet+}$, and the acetone radical cation, $CH_3C(=O)CH_3^{\bullet+}$, can be induced to rearrange into their more stable enol isomers, $CH_2=C(OH)NH_2^{\bullet+}$, and $CH_2=C(OH)CH_3^{\bullet+}$ by ion–molecule reactions with benzonitrile under CI conditions.[118] Deuterium labelling and MS^n experiments reveal that while the previously reported acetone/benzonitrile system enolizes by way of a

base-catalyzed 1,3-proton shift, a different mechanism (Scheme 4) operates for the enolization in the acetamide/benzonitrile system.

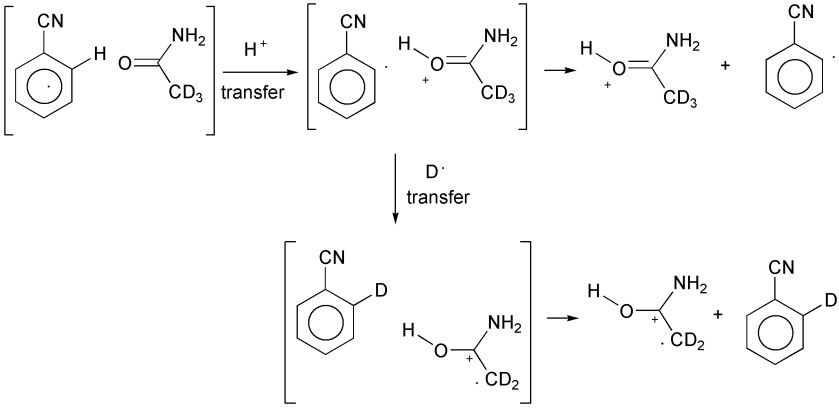

Scheme 4

The gas phase chemistry of the $M^{+\bullet}$ ion of acetamide has also been studied using FT-ICR MS.[119] Two isomers are formed upon direct EI or electron transfer on acetamide: the conventional 'keto' form **18** as well as enol form **19**, which can be independently formed from hexanamide *via* a McLafferty rearrangement. The two isomeric ions exhibit different reactivity towards neutral reagents (Scheme 5).

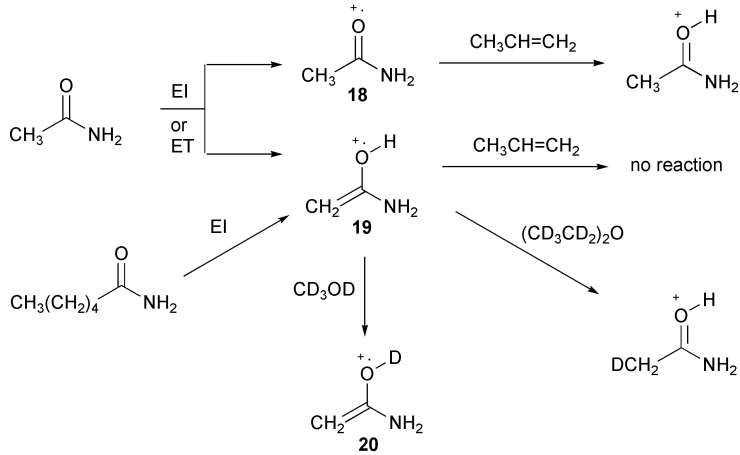

Scheme 5

Differentiation between ionized pyridine **21** and its 1,2-H shift isomer **22** is possible using ion–molecule reactions with CH_3SSCH_3, CH_3OH, H_2O, *i*-C_3H_7I, and *t*-C_4H_9-NC, as **22** exhibits radical-type reactivity characteristic of its distonic nature.[120] An

unambiguous structural characterization of the isomeric $C_6H_7N^{+\bullet}$ 2-methylpyridine **23**, the *N*-methylene pyridinium ylide ion **24**, the 2-methylene-1-hydropyridine ion **25**, and the *N*-methyl-2-dehydropyridine radical cation **26**, can be achieved when all of the above substrates are used in the analysis. The reactions of **22** and **26** with D_2O are remarkable, and involve oxygen atom abstraction [eqn. (19)].

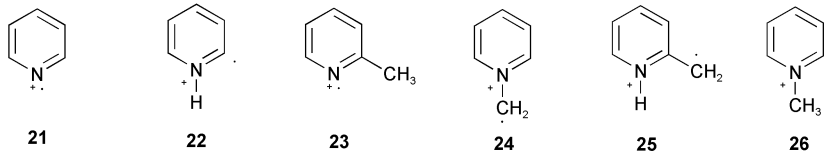

21 **22** **23** **24** **25** **26**

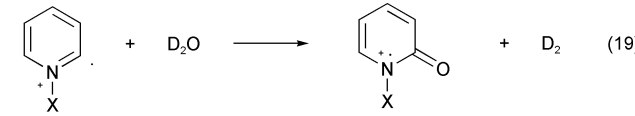

X = H or CH_3 (19)

The gas phase unimolecular reactions of the conventional radical cations of benzonitrile **27** have been compared to the distonic ion structures **28**–**30**.[121] Ion–molecule reactions with NO, *t*-BuONO, acetone and MeSSMe allow isomer distinction between **27** and **28**. The chemistry of the isomeric conventional pyrazole radical cation **31** and distonic ion **32** has also been examined.[122]

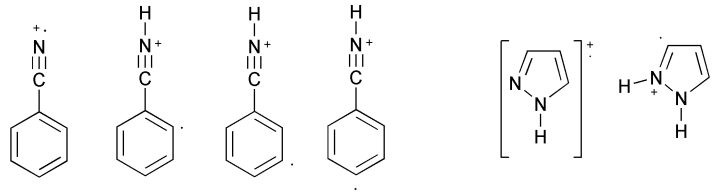

27 **28** **29** **30** **31** **32**

Ionized pyrimidine **33** has been compared to its distonic isomers using a combination of MS/MS experiments and DFT calculations.[123] Four distonic radical cations **34**–**37** were predicted to have stability similar to that of the pyrimidine radical cation. Distonic isomers **34**–**36** were generated and characterized on the basis of their CAD spectra.

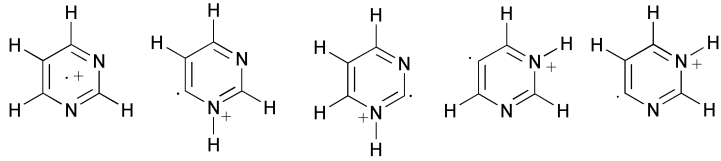

33 **34** **35** **36** **37**

FT-ICR mass spectrometry and *ab initio* calculations have been used to gain insights into the ion–molecule reactions of the radical cations of vinyl chloride, vinyl bromide, 1,2-dichloroethene, 1,2-dibromoethene, 1,1-dichloroethene and 1,1-dibromoethene with methanol and ethanol.[124] Two competing processes are observed: (i) oxidation of the alcohol to protonated aldehyde *via* a formal hydride transfer to the haloethene radical cation; and (ii) substitution of the halide radical by the alcohol. Bromo derivatives of haloethene radical cations react predominantly by substitution, while chloro derivatives tend to react by oxidation. A general mechanism (illustrated in Scheme 6 for the reaction between CH_3OH and $CH_2{=}CHCl^{+\bullet}$) involves fast and reversible addition of the alcohol to the ionized double bond of the haloethene radical cation, thereby generating a β-distonic oxonium **39**. Elimination of the halogen substituent completes the substitution process, while a 1,5 H migration leads to **40**, which ultimately dissociates into the protonated aldehyde and a β-haloethyl radical. Support for reversible addition and hydrogen migrations within a long-lived intermediate was provided by the observation of H/D exchange in reactions with CD_3OH. *Ab initio* calculations were used to provide insight into the energetics of the two reaction channels shown in Scheme 6.

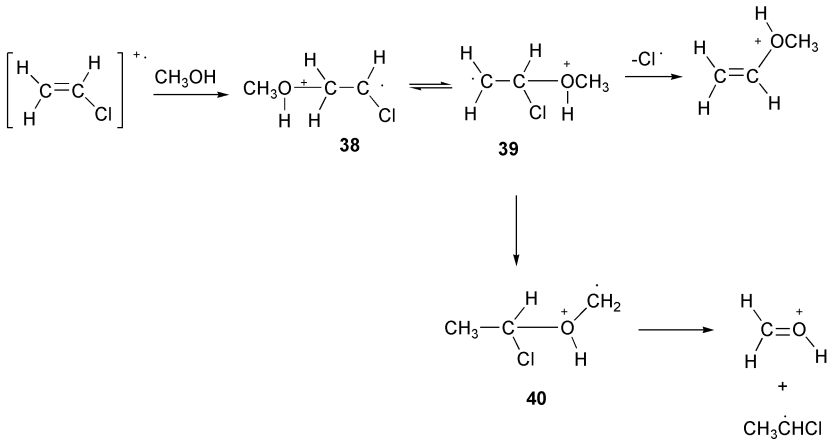

Scheme 6

Polymerization reactions initiated by radical cations have been the subject of two reports. The reactions of cyclopropane with the radical cations of ethylene, propylene and cyclopropane involve a sequence of polymerization reactions which proceed by the addition of three carbons followed by the rapid expulsion of ethylene, resulting in the sequential addition of a methylene unit.[125] The gas phase radical cation polymerization of propene initiated by the radical cation of benzene has been studied by resonance two-photon ionization-high-pressure mass spectrometry (R2PI-HPMS) and selected ion flow tube (SIFT) techniques.[126] At higher concentrations of propene, reaction products are the propene oligomers $(C_3H_6)_n^+$ ($n = 2$–7) and the adduct series $C_6H_6^+(C_3H_6)_n$ ($n \leq 6$).

Several ring closing reactions of radical cations have been examined.[127–129] The radical cation of 1,5-hexadiene is prepared by charge transfer between 1,5-hexadiene

and $CS_2^{+\bullet}$, and spontaneously rearranges to the cyclohexene cation.[127] The mechanism proposed for this process involves a Cope rearrangement to the cyclohexane-1,4-diyl cation, followed by isomerization to the cyclohexene cation. The ring-closing reaction of the hexatriene radical cation has been studied computationally at the B3LYP/6–31G* and QCISD(T)/6–311G*//QCISD/6–31G* levels of theory.[128] The two energetically favoured pathways are: (i) a concerted pathway *via* an asymmetric transition state with an activation barrier $E_a = 16.2$ kcal mol^{-1} and an exothermicity of -23.8 kcal mol^{-1}; and (ii) a stepwise pathway with a rate-determining step involving the formation of the intermediate bicyclo[3.1.0]hex-2-ene with an activation barrier $E_a = 20.4$ kcal mol^{-1}, and an overall exothermicity of -18.6 kcal mol^{-1}.

Under EI conditions, the $M^{+\bullet}$ ions of *N*-(*o*-cyclopropylphenyl)benzamides **41** undergo ring opening and subsequent ring closure to the corresponding 3-aryl-1-alkyl-1-ethyl-1*H*-benzoxazines **42** and isomeric 5-ethyl-2-oxodibenzoazepines **43**.[129] These novel reactions prompted the search for related processes in the condensed phase and *N*-(*o*-cyclopropylphenyl)-4-methylbenzamide was found to yield *N*-(*o*-cyclopropylphenyl)-4-methylbenzamide as the major product and 5-ethyl-2-oxodibenzoazepine as a minor product when treated with sulfuric acid.

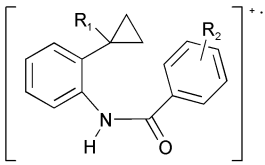

41

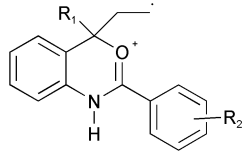

42

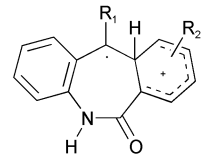

43

Finally, charge exchange ionization has been used to detect the presence of a long-lived excited electronic state of the radical cation of benzene.[130]

3 Reactions involving nucleophilic substitution, addition, elimination or addition/elimination mechanisms

Gas phase substitution and elimination reactions have been extensively studied experimentally over the past decade and have been reviewed in 2001.[15,36] These reactions have also been the focus of a number of theoretical studies. Unfortunately, space constraints mean that the many relevant theoretical studies carried out 2001 are not reviewed here.

Kato *et al*. have re-examined the gas phase 300 K rate coefficients and secondary α-deuterium kinetic isotope effects (KIEs) for some nucleophilic substitution (S_N2) reactions involving halomethanes and halide anions [eqn. (20), X = Cl, Y = Br; X = Cl, Y = I; X = Br and Y = I).[131] Substantial *inverse* KIEs were measured with an improved accuracy: $k_H/k_D = 0.77$ (±0.03), 0.84 (±0.01), and 0.76 (±0.01), respectively, for each of the above systems. These KIEs are found to decrease (*i.e.* become more *inverse*) with

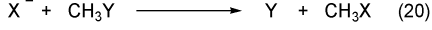

an increase in the transition-state looseness parameter (R_{TS}) for larger halide anions, and show the expected positive correlation with R_{TS} for the lighter methyl halides.

Guided ion beam tandem mass spectrometry techniques have been used to examine the competing chemical dynamics of reactions of fluoride ions with chloromethane as a function of collision energy.[132] The exothermic S_N2 reaction [eqn. (20) X = F, Y = Cl] predominates at the lowest collision energies but decreases at higher collision energy. At higher collision energies, two endothermic product channels are detected [eqns. (21), (22)].

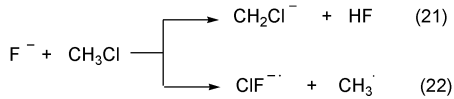

One of the problems with studying the competition between S_N2 and $E2$ reactions between anionic nucleophiles and neutral substrates is that both processes yield the same anionic leaving group. While neutral products could be used to distinguish between S_N2 and $E2$ pathways, these are generally not detected in MS experiments. Gronert has cleverly overcome this problem by using dianionic species as nucleophiles, which yield singly charged product ions characteristic of S_N2 and $E2$ reactions, thus allowing these pathways to be directly observed in an MS experiment. Gronert and co-workers have reported on the branching ratios and rate constants for the competing gas phase S_N2 [eqn. (23)] and $E2$ [eqn. (24)] reactions of benzoate (Y = CO_2) and phenolate (Y = O) containing dianions reacting with a series of β-substituted alkyl bromides in a quadrupole ion trap mass spectrometer.[133] While β-halogens increase both the S_N2 and $E2$ rates, the effect is greater for the latter process and therefore these substituents lead to an increase in the amount of elimination. Analysis of the kinetic data for the S_N2 reactions *via* a two-parameter linear free-energy relationship reveal that field-effects (*i.e.* electron-withdrawing groups) strongly favour the reaction (σ_F = 1.83). In contrast, analysis of the available condensed phase data for these substrates indicates that halogens strongly retard the reaction (σ_F = −2.04). This dramatic reversal in substituent effects can be explained by a simple electrostatic model which suggests that solvation causes the system to shift to a more highly ionized S_N2 transition state.

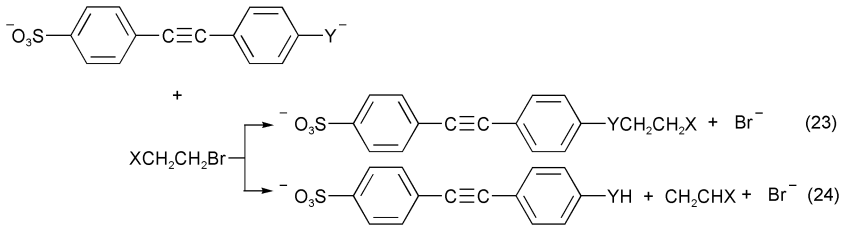

The first gas phase nucleophilic substitution reactions at neutral nitrogen have been reported.[134] S_N2 reactions of chloramine, NH_2Cl [eqn. (25)], were observed for all the nucleophiles studied (HO^-, CH_3O^-, $CH_3CH_2O^-$, $CH_3CH_2CH_2O^-$, $C_6H_5CH_2O^-$, $CF_3CH_2O^-$, F^-, HS^- and Cl^-). These reactions are faster than the corresponding S_N2

reactions of methyl chloride, and take place at nearly every collision when the reaction is exothermic. The thermoneutral identity S_N2 reaction of NH_2Cl with Cl^- occurs approximately once in every 100 collisions, and is more than two orders of magnitude faster than the analogous reaction of CH_3Cl. The significantly enhanced S_N2 reactivity of NH_2Cl is consistent with a previous theoretical prediction about the barrier heights for the S_N2 identity reactions. Competitive proton abstraction to form $NHCl^-$ [eqn. (26)] has also been observed with the more highly basic anions and is the major reaction channel for HO^- and CH_3O^-.

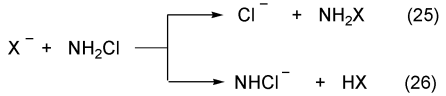

There have been two reports of intramolecular substitution reactions occurring *via* methyl migrations from aromatic systems under CID conditions.[135,136] The *ortho* $[M - H]^-$ anion of methyl phenyl carbonate was found to lose CO_2. Theoretical calculations reveal that this is a stepwise process, involving a methyl migration through a six-centre transition state to give a cresol $[M - H]^-$ ion [eqn. (27)].[135] Migration of a methyl group from a *para* methoxy substituent was reported.[136]

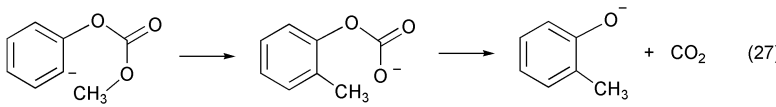

Positive ion S_N2 reactions have undergone a renaissance, with several studies appearing in 2001. The problems with evaluating competition between S_N2 and E2 pathways for singly charged anions are absent for positively charged ions, as the charged products from S_N2 reactions with positive ions directly reveal competing pathways. The groups of McMahon and Mayer have independantly reported on S_N2 reactions involving alcohols proceeding *via* proton bound dimers. These reactions are interesting since they require that isomerization of a more stable proton bound dimer into methyl-bound complex prior to methyl cation transfer and dissociation to protonated monomers are competitive processes (Scheme 7). Thus, the temperature dependence of the rate constants of the methyl cation transfer reactions between methanol and protonated methanol, protonated acetonitrile, and protonated acetaldehyde have been investigated experimentally by low-pressure FT-ICR mass spectrometry.[137] *Ab initio* calculations predict that the barrier for isomerization of the initially produced proton-bound dimer to a methyl-bound complex is significantly lower than the barrier for methyl cation transfer such that it does not interfere with the experimental determination of the latter. Ochran and Mayer have used MS/MS experiments and *ab initio* calculations to investigate the unimolecular decompositions of proton-bound dimers of acetonitrile with *n*- and *i*-propanol.[138] Both systems also undergo the competitive reactions (Scheme 7), including isomerization of the proton-bound dimer to access the S_N2 reaction channel to yield $[(CH_3CNR)(H_2O)]^+$ and then undergo water loss [R = $CH_2CH_2CH_3$ and $CH(CH_3)_2$]. The same group has examined the kinetics of dehydration reactions of protonated alcohols with neutral alcohols.[139]

These systems react *via* an initial proton-bound dimer which isomerizes *via* an internal S_N2 mechanism, leading to the formation of the protonated ether. Reaction rates and RRKM theory reveal that the isomerization activation energies, E_{iso}, for the proton-bound dimers decrease as the size of the alcohols increases, consistent with the S_N2-type rearrangement.

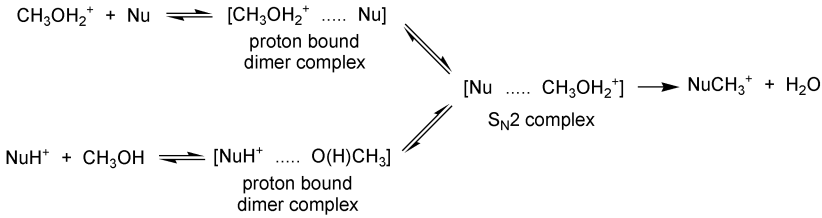

Scheme 7

Fridgen and McMahon have examined the temperature dependence of the low-pressure association reaction of dimethyl ether with protonated dimethyl ether.[140] These reactions follow the same type of mechanistic scheme described above (Scheme 7), whereby the unimolecular dissociation of nascent proton-bound dimers is complicated by two factors: (i) the presence of another unimolecular dissociation route producing trimethyloxonium cation and methanol through a high-energy isomer of the proton-bound dimer; and (ii) the presence of at least two high-energy isomers of the proton-bound dimer *en route* to dissociation of the nascent proton-bound dimer. In a separate study, Fridgen and McMahon used the same techniques to study the temperature and deuterium isotope effects on the S_N2 reaction for the same system.[141] The temperature dependence of this bimolecular reaction yielded thermodynamic information on the energy barrier, $\Delta G^{\ddagger}_{298} = 33.7 \pm 2.1$ kJ mol^{-1}, in good agreement with *ab initio* calculations.

FT-ICR MS and *ab initio* calculations have been used to investigate the reaction between $CH_2O(CH_3)_3^+$ and NH_3.[142] Two main products arise *via* an $E2$ pathway [eqns. (28), (29)], while two minor products are due to a competing S_N2 reaction [eqn. (30)] and an addition/elimination reaction [eqn. (31)].

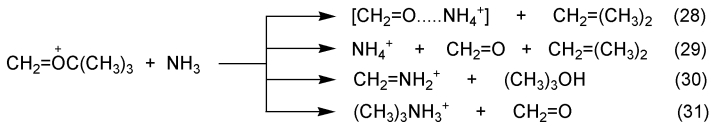

Gas phase ion–molecule reactions between dialkoxyborinium cations (RO–B$^+$–OR) and small organic amides proceed *via* direct addition at boron and a competing S_N2 pathway.[143] Isotopic labelling and CID of the methyl transfer products demonstrate *O*-methylation of the amide. When R = Et, *i*-Pr and *t*-Bu, a new $E2$ pathway dominates reactivity.

The contrasting behaviour between gas phase and condensed phase S_N2 reactions has been highlighted in a recent study of the nicotine analogue. In acetonitrile, methylation with methyl iodide occurs exclusively at the sp^3-nitrogen, while in the gas phase

methylation with trimethyloxonium occurs exclusively at the pyridine nitrogen atom (Scheme 8).[144] Hartree Fock calculations suggest there is an interaction between the side-chain nitrogen and hydrogens on the aromatic ring, which affects both the conformation as well as the relative basicity of the two nitrogens. Calculations also indicate that in the gas phase the pyridine methylated product is thermodynamically favoured.

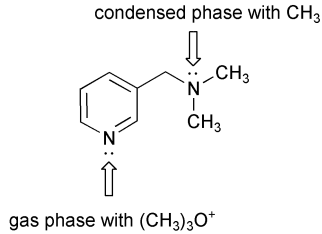

Scheme 8

Gas phase high pressure methods such as the radiolytic technique offer the opportunity to examine the sterochemical outcomes of substitution reactions which proceed *via* alternative pathways (*e.g.* S_N1 mechanisms). The problems associated with using steroechemical data to classify reactions as proceeding *via* either S_N1 or S_N2 mechanisms are clearly highlighted by a recent study by Speranza *et al.*[145] Although the gas phase intracomplex "solvolysis" of the proton-bound complexes between $CH_3{}^{18}OH$ and (*R*)-(+)-1-arylethanols proceeds through the intermediacy of the relevant benzyl cation (*i.e.* a pure S_N1 mechanism), the stereochemical outcome is highly temperature dependent. At $T > 50$ °C, complete racemization occurs, whilst at $T < 50$ °C the reaction displays a preferential retention of configuration (Scheme 9).

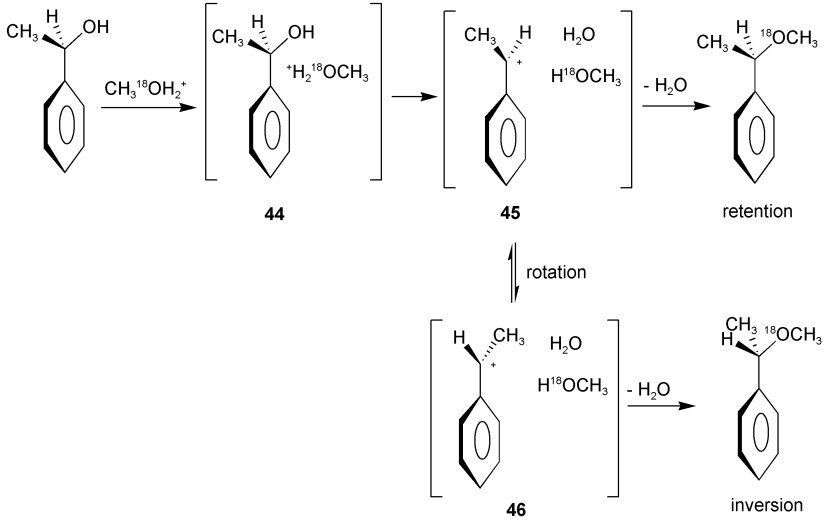

Scheme 9

The initially formed complex **44** dissociates to complex **45** which consists of the benzyl cation and the nucleophile/leaving group pair. At lower temperatures, **45** reacts to give the product resulting from frontside attack, thus yielding preferential retention of configuration. However, at higher temperature, **45** is in equilibrium with **46** (formed *via* rotation of the benyzyl moiety) thereby yielding the racemic mixture. The same technique has been used to examine hindered inversion of chiral ion–dipole pairs.[146]

4.0 Reactions of carbon clusters and unusual species such as distonic radical ions, carbenes, *etc.*

A Reactions of carbon clusters

Interest in gas phase carbon cluster ions and polycyclic aromatic hydrocarbons (PAH) has continued in 2001, and is largely driven by their potential roles in interstellar chemistry. Bierbaum and co-workers have examined the reactivity of a number of cumulene anions, C_n^- (n = 2, 4–10) and C_nH^- (n = 2, 4, 6, 7) with atomic hydrogen using a FA-SIFT apparatus.[147] These species generally react *via* associative detachment, *i.e.* $C_n^- + H \longrightarrow C_nH + e^-$, with rate constants of $\approx 10^{-9}$ cm^3 molecule^{-1} s^{-1}. Reaction with molecular hydrogen was found to be considerably slower ($k < 10^{-13}$ cm^3 molecule^{-1} s^{-1}). Bowie and co-workers have used electronic structure calculations to study a variety of cumulenes and heterocumulenes, C_nH, $C_{n-1}CH_2$ and C_nO (n = 2–10), previously identified in the interstellar medium.[148] These species were predicted to have high electron affinities, and their anionic counterparts are generally predicted to be linear with large dipole moments. This suggests such species may be detectable *via* radio astronomy. One of these species, the propadienylidene anion, H_2CCC^-, has also been studied using photodetachment spectroscopy.[149]

A number of other heteroatom doped carbon cluster anions and cations have also been studied. Linear C_nSe^- clusters (n = 1–11, n = even) were produced *via* laser ablation of selenium and carbon powders.[150] CID of these species resulted in loss of selenium (smaller clusters) or CSe (larger clusters). In accord with experiments, DFT calculations predict that linear structures with even numbers of carbon atoms are more stable than their odd numbered counterparts. $C_nX_p^+$ cations (X = P, S; $n + p = 3$–6) have also been studied theoretically.[151] Linear clusters are again predicted, with the exception of CX_3^+ for which a T-shaped ground state geometry with a central carbon atom was found to be more stable. C_nS^+ cations (n = 1–16) and C_nS^- anions (n = 9–16) are also predicted to be generally linear with the sulfur atom in the terminal position.[152] Multireference configuration interaction calculations have been used to study the low lying excited states of isoelectronic polyacetylene and cyanopolyacetylene species, HC_6H^+, C_6H, HC_5N^+.[153]

A laser photolysis source has been used to generate silicon clusters terminated with hydrogen atoms, $Si_nH_x^+$ ($n \leq 50$).[154] The stoichiometric composition of these clusters was investigated over temperatures ranging from 300K to 950K. Cage-like geometries were proposed.

Flammang and co-workers have used a combination of flash vacuum pyrolysis (FVP), mass spectrometry and matrix isolation IR spectroscopy to generate, detect

and characterize a number of heterocumulene-type species in the gas phase.[155–157] These species include *N*-aryliminopropadienethiones, Ar–N=C=C=C=S[155] [eqn. (32)], *N*-arylaminobutatrienes, Ar–N=C=C=C=C=X (X=Nar, S)[156] and benzoylthioketene and its isomer thiobenzoylketene.[157] Neutralization reionization mass spectrometry (NRMS) experiments confirm the gas phase stability of NCCCS and NCCCCS based radical species.

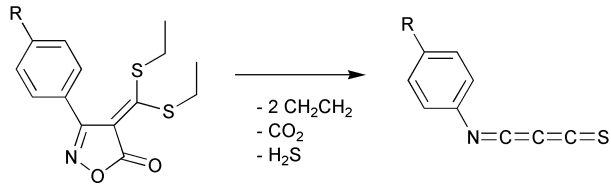

(32)

FT-ICR mass spectrometry has been used to study reactions of PAH radical cations (*e.g.* naphthalene, pyrene) with molecules such as H_2, CO, H_2O and NH_3.[158] These studies provide insights into reactions occurring for PAH species in interstellar environments. Bierbaum and co workers have developed a model based on experimental data predicting the charge states and degree of hydrogenation of PAH species in diffuse clouds.[159] The model incorporates processes such as ionization, photodissociation, electron recombination and reaction with common interstellar species.

Photodissociation of the fluorene cation, $C_{13}H_{10}^+$, results in the loss of up to five hydrogen atoms, resulting in the formation of $C_{13}H_5^+$.[160] Theoretical calculations indicate that the first hydrogen is removed from the sp^3 carbon of the central 5 membered ring, while the remaining four are removed from only one of the aromatic six membered rings.[161] The skeletal structure of fluorene is retained in $C_{13}H_5^+$.

Single and double ionization of corannulene ($C_{20}H_{10}$) and coronene ($C_{24}H_{12}$) has been explored using a number of mass spectrometric based techniques.[162] Photoionization studies provide first ionization energies of 7.83 and 7.21 eV respectively. Second ionization potentials were examined *via* (i) photoionization thresholds from the neutrals to doubly charged cations; (ii) energy-resolved charged stripping mass spectrometry; and (iii) ion–molecule reactions involving electron transfer to the dications. Ionization energies for the monocations were estimated as 12.3 and 11.3 eV respectively.

Fullerenes and related species have again been the subject of a number of studies. $C_{60}H_{18}^-$ was generated using 3 different ionization techniques: laser desorption/ionization, negative ion chemical ionization and resonant free electron capture.[163] This species was estimated to have a lifetime in the range of 1 ms at 600 K. The observation of stable fullerene anions with such a high degree of hydrogen attachment is unprecedented. Photodissociation of transition metal-C_{60} complexes ($M_x(C_{60})_y$, x = 1–5, y = 1,2) has been used to investigate their structure and bonding.[164] Loss of metal atoms suggests that these complexes are exohedral. Lifshitz and co-workers have used MS based techniques to detect a number of new endohedral fullerenes containing diatomic molecules ($N_2@C_{60}$, $N_2@C_{70}$, $^{13}CO@C_{60}$ and $^3He^{22}Ne@C_{70}$).[165] Ion mobility measurements have demonstrated the existence of two structural isomers of endohedral $Sc_2C_{82}^+$.[166] Bohme and co workers have attached Fe^+ cations to buckminsterfullerene and corannulene to generate $C_{60}Fe^+$ and $C_{20}H_{10}Fe^+$ respectively.[167]

The reactivity of these species towards small organic and inorganic neutrals was explored using a SIFT mass spectrometer. In some cases the presence of the C_{60} or $C_{20}H_{10}$ unit led to enhancements of reactivity relative to the bare Fe^+ cation. The degree of sequential ligand attachment relative to Fe^+ was also affected by the presence of the C_{60} or $C_{20}H_{10}$ units. Endohedral fullerene ions containing nitrogen atoms, $N@C_{60}^+$ and $N@C_{70}^+$, were found to fragment with loss of the nitrogen atom.[168]

B Reactions of unusual neutrals

Electron attachment to 1,3-dioxolane-2,5-dione followed by retro-cleavage of H_2CO results in the formation of $[O_2C–CO]^{-\bullet}$ [eqn. (33)].[169] Neutralization–reionization mass spectrometry (NRMS) experiments do not result in a recovery signal for this ion, suggesting that the neutral $O_2C–CO$ has a lifetime of $<10^{-6}$ s. Neutral, cationic and anionic [C_2, O_3] isomers have also been studied theoretically.[170] Anionic and neutral NCCCO species have also been studied experimentally and theoretically.[171]

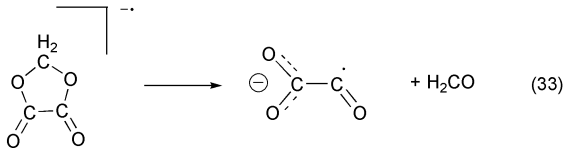

Polasek and Turecek have used NRMS and electron photodetachment–reionization mass spectrometry (PRMS) to examine the nitromethyl radical, cation and anion.[172] $^-NR^-$ experiments show that the radical is stable for >3.7 μs, while $^-NR^+$ experiments and theoretical calculations suggest the cation is unstable with respect to cyclization and dissociation to H_2CO and NO^+ (Scheme 10). A number of [C, H_2, N, O_2] isomers were identified using *ab initio* calculations and investigated experimentally.

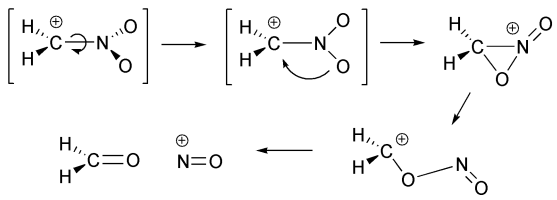

Scheme 10

The stability of various isomers of the nitrobenzene radical cation has been studied using NRMS, CAD and *ab initio* calculations.[173] These isomers include the nitrobenzene radical cation **47**, ylid ions **48**–**50**, the phenyl nitrite cation **51** and the *p*-nitrosophenol cation **52**. *Ab initio* calculations suggest that the *p*-nitrosophenol cation **52** is the most stable of these isomers. NRMS of the phenyl nitrite cation **51** allowed the elusive phenyl nitrite neutral to be generated.

The amino(hydroxy)methyl radical was generated *via* selective protonation of formamide at the oxygen atom, followed by collisional electron transfer with dimethyl

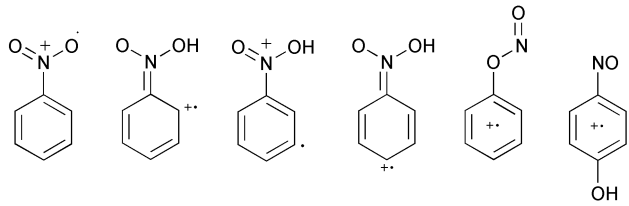

47 48 49 50 51 52

disulfide.[174] Its dissociation was investigated using CAD and NR experiments. Deuterium labelling experiments revealed that NR results in approximately 4:1 loss of H atoms from the O *versus* N positions, while CAD resulted in predominant loss of H (70%) from the C position. RRKM calculations using high level *ab initio* potential energy surfaces were in qualitative agreement with experiment. Bimolecular reactions of H atoms with formamide were also examined theoretically.

Proton transfer (NH_4^+) to the oxygen of pyridine N-oxide followed by collisional electron transfer with dimethyl disulfide allowed the *N*-hydroxypyridyl radical to be generated transiently in the gas phase,[175] although extensive fragmentation from ring cleavage and loss of H and OH in the neutral was observed. High level *ab initio* calculations suggest that exothermic loss of OH proceeds on the ground state doublet potential energy surface, while endothermic dissociations involving ring cleavage and loss of H proceed on excited state potential energy surfaces. H atom addition to the oxygen of pyridine N-oxide catalyses the isomerization to the more stable hydroxypyridines. The same group has utilized NRMS and theory to probe the hydrogen atom adducts of uracil at both the O4 and C5 positions.[176,177] Both adducts are stable, but not surprisingly yield different dissociation products *via* different mechanisms.

FAB of mixtures of LiCl and 18-crown-6 or LiCl and 1,4,8,11-tetraazacyclotetradecane produces $Li^+O{=}CH_2$ and $Li^+NH{=}CH_2$.[178] NRMS experiments on each of these complexes reveal the corresponding neutral counterparts are stable for at least 3 μs in the gas phase. *Ab initio* calculations suggest three bound structures for both complexes: two C-centred radical ion-pair complexes, $Li^+.^-XCH_2$, and an electrostatically bound $Li{-}X{=}CH_2$ complex (X = O, NH). The relative stabilities of these complexes are reversed as X is varied from O to NH.

C Reactions of unusual anions

Kass and co-workers have prepared the acetamide enolate anion **53** *via* the fluoride desilylation of 2-(trimethylsilyl)acetamide.[179] Its reactivity, proton affinity and CID spectra were compared with that of the isomeric amidate anion **54**. Ion–molecule reactions of both anions with various neutrals were investigated using FTMS and FA techniques. The acetamide enolate anion **53** is reactive towards CS_2 [eqn. (34)] while the isomeric amidate anion **54** is unreactive [eqn. (35)]. Bracketing measurements of the proton affinity of the acetamide enolate anion reveal that this carbanion is 11 ± 4 kcal mol^{-1} more basic than the isomeric amidate anion. Heating either isomer to 300 °C resulted in no isomerization, consistent with barrier heights predicted using a variety of theoretical techniques.

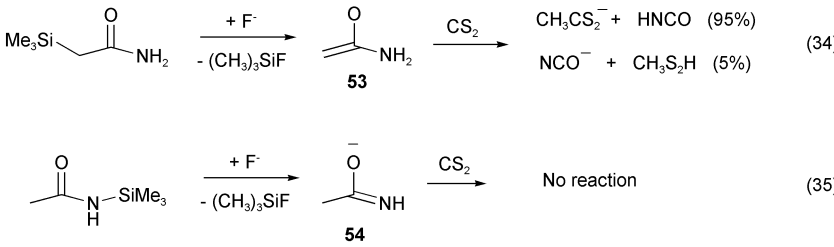

The gas phase reactivity of the atomic oxygen radical anion has again been the subject of a number of studies. Cardoso *et al.* have studied its reactivity towards a number of biologically active arylalkylamines, $R^1C_6H_4CHR^2(CH_2)_nNHR^3$ (R^1 = H, F, NO_2, OH, OCH_3; R^2 = H, OH; R^3 = H, CH_3) using CIMS and CID experiments.[180] Fragmentation pathways of $[M - H + O]^-$ anions were described. The preferred site of oxygen radical anion attachment was found to be the benzylic carbon atom, except for amines with a benzylic hydroxy group, for which attack at the aromatic ring was also observed. Stemmler and co-workers have shown that $O^{-\bullet}$ attacks methyl benzoate at both the carbonyl carbon and the aromatic ring.[181] Attack at the carbonyl carbon resulted in the formation of $C_6H_5CO_2^-$ and $CH_3OCO_2^-$. Stemmler and Segovis have proposed that reaction of $O^{-\bullet}$ with dimethyl glutarates results in the formation of $^{\bullet}CH_2OC(O^-)CR_2$ distonic radical anions (Scheme 11).[182] This distonic anion can be considered an 'electron-bound dimer' of ketene and formaldehyde.

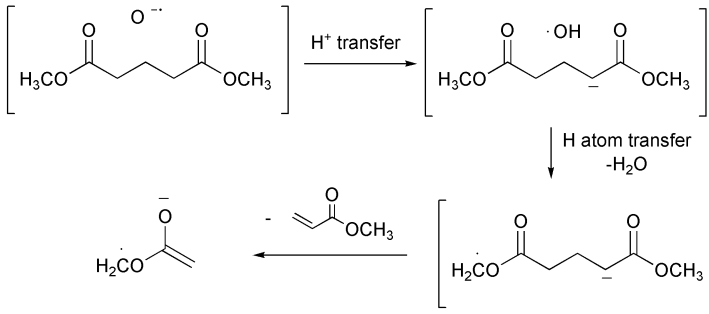

Scheme 11

Gimbert, Arnaud and co-workers have examined the gas phase reactivity of two isomeric 1,3-benzodithiole anions, generated *via* deprotonation of 1,3-benzodithiole at either the dithioacetal carbon **55** or at the *o*-phenylic carbon **56** during negative ion chemical ionization (NICI), *via* experiment and theory.[183] Deuterium labelling at the dithioacetal position allowed these isomers to be distinguished. CID of these species resulted in distinctly different fragmentation products, confirming that the isomers do not interconvert, while ion–molecule reactions with CS_2 resulted in adduct formation for both species. The fragmentation reactions of these adducts were different for both isomers.

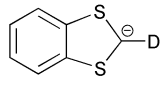

55

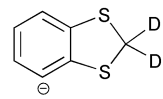

56

Grabowski, Lee and co-workers have studied the gas phase Cope rearrangement of 1,5-hexadiene 3-oxide anions using FTMS and FA techniques.[184] Dimethyl disulfide undergoes characteristic reactions with both the alkoxide **57** [eqn. (36)] and the enolate **58** [eqn. (37)] and was used as a probe reagent to distinguish between these isomers. Based on FTMS measurements, a lower limit on the rate constant for rearrangement of 25 s^{-1} was estimated, providing an upper limit on $\Delta H^{\ddagger}$ of ≈11 kcal mol^{-1}, consistent with DFT predictions.

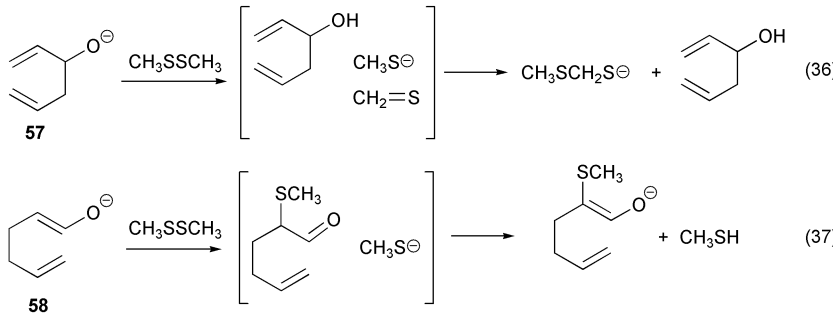

57

58

3-(4-Trifluoromethylphenyl)-3-trimethylsilylcyclopropene **59** reacts with fluoride in the gas phase to form a cyclopropenyl anion **60**, which spontaneously rearranges to form the 6-trifluoromethyl 3-indenyl anion **61**.[185] Reactions of **61** with CH_3OD or CF_3CH_2OD result in a single H/D exchange and isomerization to the more stable indenyl anion **62** (Scheme 12). The identity of **61** and **62** was confirmed *via* comparison of ion–molecule reactions (*e.g.* CS_2, COS) with the authentic species. Despite the instability of its conjugate base, the acidity of 3-(4-methylphenyl)-3-cyclopropenyl was determined by the DePuy kinetic method (ΔH°_{acid} = 398.6 ± 1.4 kcal mol^{-1}). This value is in good agreement with theoretical predictions. Results from this study suggest the previously reported 1,2,3-triphenylcyclopropenyl anion underwent an identical rearrangement to that described for **61**.

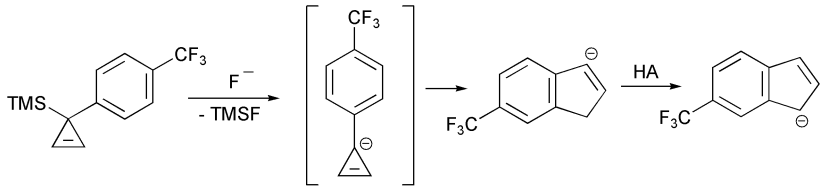

59 60 61 62

Scheme 12

Dua and Bowie have evaluated charge-remote fragmentation of the 3-substituent in 3-substituted adamantane carboxylate anions.[186] The 3-cyclohexenyl system **63** shows

loss of the cyclohexenyl radical, with no charge-remote retro-Diels–Alder fragmentation. The 3-isobutyl ketone system **64** shows loss of CO_2 and charge-remote radical loss of the 3-substituent, while no Norrish II cleavage is observed. The 3-isobutyl ester system **65** shows some loss of propylene (from Norrish II cleavage) in competition with loss of CO_2 and radical loss of the 3-substituent. The inability of these model systems to readily undergo charge-remote reactions is attributed to the carbonyl group of the side chain making radical side chain cleavage thermodynamically favoured over Norrish II type reactions. Bowie and co workers have also examined the rearrangement and fragmentation of five isomeric C_4H_5O anions using collisional activation and charge reversal experiments, as well as *ab initio* calculations.[187]

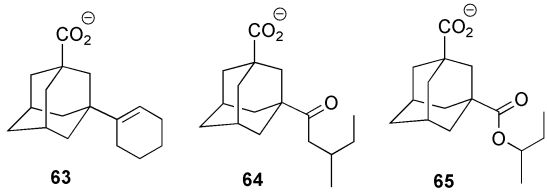

63 **64** **65**

D Reactions of unusual cations

Kenttämaa and co-workers have continued their gas phase FT-ICR studies of the hydrogen atom abstraction reactions of charged phenyl radicals **66**,[188–190] formed *via* the combination of ion–molecule reactions and either collisional activation or photodissociation shown in Scheme 13 (where R = CH_3, H, Br, Cl, COOH, NO_2, CN; X,Y = Br, I).

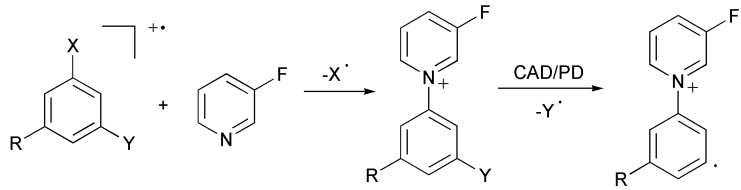

66

Scheme 13

The gas phase reactions of these species towards neutral reagents such as benzeneselenol, thiophenol, benzaldehyde, toluene, aniline and phenol proceed *via* hydrogen atom abstraction and addition to the phenyl ring.[188] The amount of hydrogen atom abstraction was found to vary greatly: it represents the dominant pathway for benzeneselenol (100%) and thiophenol (74–85%) yet is hardly observed for aniline. These trends could be only partially rationalized in terms of the C_6H_6X–H bond dissociation energies of neutrals. Reaction efficiencies were found to increase with increasingly electron withdrawing substituents on the phenyl ring (*i.e.* R, Scheme 13). The reactivi-

ties of a wider variety of charged phenyl radicals towards neutrals such as tributyltin hydride, benzeneselenol, tetrahydrofuran, thiophenol, 4-fluorothiophenol and pentafluorothiophenol were described in a separate study.[189] Although no correlation between reaction efficiency and DFT calculated reaction exothermicity was observed, a strong correlation between both the electron affinity of the phenyl radical and the ionization potential of the neutral substrate and the reaction efficiency was noted. These trends were rationalized in terms of a lowering of the reaction barrier due to an increase in polarity of the transition state. In the third study, a similar range of charged phenyl radicals were allowed to react with allyl iodide, dimethyl disulfide and *tert*-butyl isocyanide, resulting in $I^{\bullet}$, $^{\bullet}SCH_3$ and $^{\bullet}CN$ abstraction.[190] Reactivity for each of these neutrals followed the order $R = CH_3 \approx H < Br \approx Cl \approx COOH < NO_2 \approx CN$ (Scheme 13). Once again, correlations between the polarity of the transition state and the reaction efficiency were noted.

Kenttämaa and co-workers have also examined the gas phase reactivity of *meta*-benzyne analogues carrying charged substituents **67**.[191] Nucleophilic substitution reactions were often observed. For example, reaction of the 3,5-didehydrobenzoyl cation **67** with dimethyl sulfide results in the nucleophilic dimethyl sulfide replacing the acylium charge to generate a new *meta*-benzyne analogue **68**, which can undergo further nucleophilic substitution (*e.g.* reaction with pyridine yields the ion **69**, eqn. (38)). Rates of these charge site substitution reactions were strongly correlated to differences in the proton affinity of the incoming nucleophile relative to the outgoing leaving group. Importantly, the benzoyl cation ($PhCO^+$) is unreactive towards most of the nucleophiles examined, suggesting that the *meta*-benzyne moiety is important in these reactions. A mechanistic rationale involving nucleophilic attack at the *meta*-benzyne moiety followed by elimination of the original charged moiety was supported by 'labelling' of the *meta*-benzyne ring with a chlorine atom, **70**. Only product **71** was formed, with no *ipso* attack being observed, confirming reaction at the *meta*-benzyne moiety [eqn. (39)]. DFT calculations support the formation of a zwitterionic 3,5-bis(pyridinium)benzenide cation **72** as the key intermediate in this reaction [eqn. (40)] and in certain cases this intermediate could be experimentally trapped and its gas phase chemistry explored. Nelson and Kenttämaa have also distinguished the 3,5-didehydophenylium cation **73** and its cyclic **74**,**75** and acyclic **76**,**77** $[C_6, H_3]^+$ isomers on the basis of their reactivity towards 3-fluoropyridine, di-*tert*-butylnitroxide and methanol.[192] Relative energies of these species are provided from previous *ab initio* calculations.

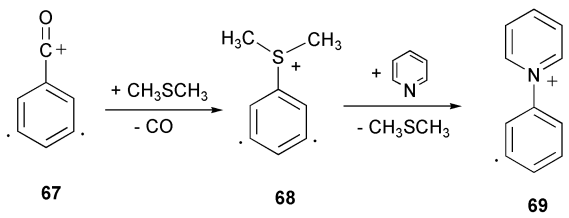

67 **68** **69** (38)

Tichy, Kenttämaa and co-workers have used elaborate experimental approaches to examine the reactivity of triplet *N*-phenyl-3-nitrenopyridinium ion ^{3}**79** (formed *via* CID on **78**) in the presence of other isomers (**80a**,**b** and **81a**,**b**).[193] This is achieved by

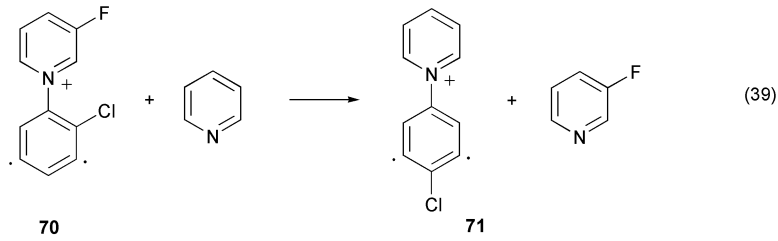

70 **71**

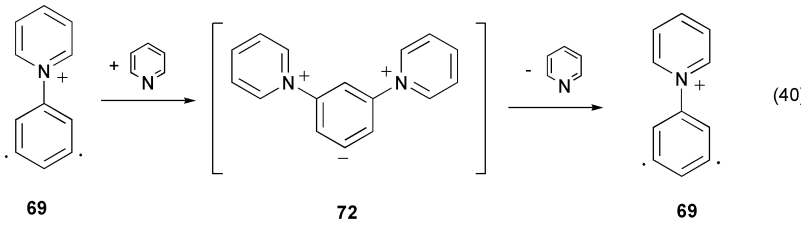

69 **72** **69**

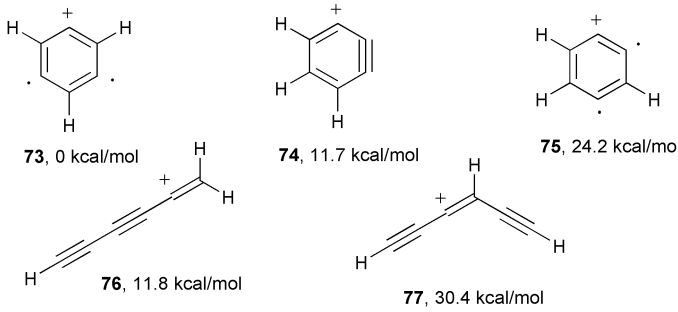

73, 0 kcal/mol **74**, 11.7 kcal/mol **75**, 24.2 kcal/mol

76, 11.8 kcal/mol **77**, 30.4 kcal/mol

titrating out the other isomers *via* ion–molecule reactions (diethyl ether removes **80a**,**b** while triethylamine removes **81a**,**b**). The pure sample of triplet *N*-phenyl-3-nitreno-pyridinium ^{3}**79** thus formed undergoes two sequential H-atom transfer reactions with benzeneselenol and reaction with doublet NO to eliminate N_2O.

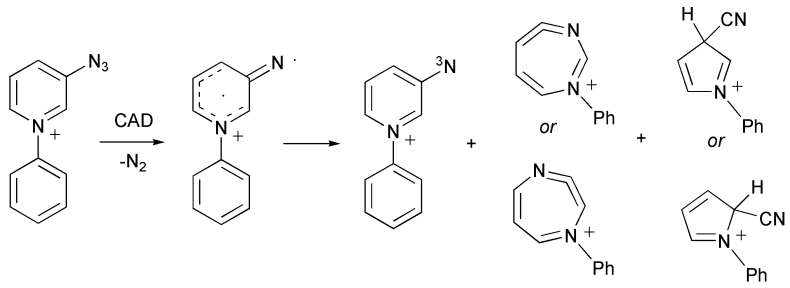

78 ^{1}**79** ^{3}**79** (90%) **80a,b** (5%) **81a,b** (5%)

5 Reactions of organic ions containing heteroatoms

Several studies have investigated the gas phase reactivity of acylium ions.[194–197] Pentaquadrupole mass spectrometry experiments have been used to examine the reactivity of acylium ions CH_3–C^+=O, CH_2=CH–C^+=O, C_6H_5–C^+=O and $(CH_3)_2$N–C^+=O **82** towards nitriles RCN (R = Me, Et, CH_2=CH and Ph).[194] Under multiple collision conditions, proton transfer to the nitrile and addition of one or two nitrile units to the acylium ion were observed. Addition of two nitrile units results in formation of the 1,3,5-oxadiazinium ion **83** [eqn. (41)]. Reaction with two different nitriles results in isomeric 1,3,5-oxadiazinium ions dependent on the order of nitrile addition. CID of 1,3,5-oxadiazinium ions resulted in sequential loss of nitriles *via* two pathways: double retro-addition to form the parent acylium ion or dissociation that promotes group exchange between a nitrile and the acylium ion. Related solvation reactions of acylium ions with commonly used electrospray solvent molecules (*e.g.* water, acetonitrile, aliphatic alcohols) during the electrospray process has been observed. Product ions from these reactions may complicate the interpretation of mass spectra.[195]

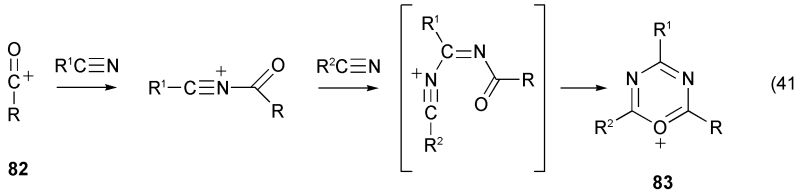

Moraes and Eberlin have studied the reactivity of $(CH_3)_2$N–C^+=O **84** with α-diols and their amino, thiol, ether and thioether analogues and propose that ketalization proceeds *via* the neighbouring acyl group participation [eqn. (42)].[196] Ketalization with $H_2NCH_2CH_2OH$ was found to favour the HO acylated adduct and NH_3 loss. The site selectivity of more complex systems (*e.g.* HO–$CH_2CH(OH)CH_2OCH_3$) was also explored. Finally, the attack by an acyl ion onto a 5-substituted tetrazole ring results in rearrangement and elimination of N_2 to form a 2,5-disubstituted-1,3,4-oxadiazole[197]

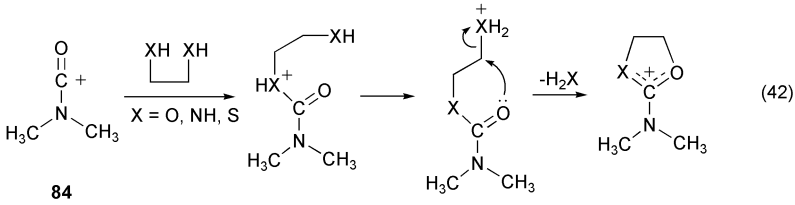

Zheng, Tao and Cooks have observed Eberlin-type reactivity for arenesulfenylium cations reacting with cyclic acetals and ketals.[198] The arenesulfenylium cation **85** reacts with 2,2-dimethyl-1,3-dioxolane to form the 2-phenyl-1,2-oxathietan-2-ium ion **86** [eqn. (43)]. CID of **86** results in cycloreversion reactions eliminating formaldehyde or

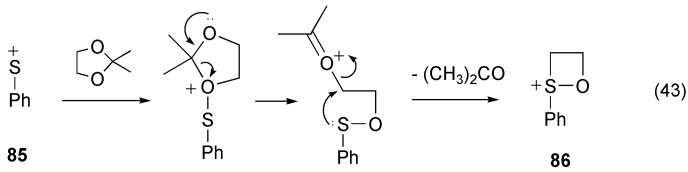

ethylene, to form Ph–S^+=CH_2 or PhS^+=O, respectively. These reactions are consistent with the cyclic structure proposed for **86**.

Eberlin and co-workers have shown that cyclic *N*-alkyl- and *N*-acyliminium cations **87** react with allyltrimethylsilane to form either a β-silyl cation *via* allyltrimthylsilyl addition **88** [eqn. (44)] or allyltrimethylsilyl ionic fragments.[199] The relative abundances of these channels provided information on the order of electrophilic reactivity of various cyclic *N*-alkyl- and *N*-acyliminium cations, which were found to be comparable with that observed in solution. Collisional activation of product β-silyl cations **88** results in dissociation exclusively by retro-addition (Grob fragmentation) to reform the reactant ion and allyltrimethylsilane. Pyridine reacts with β-silyl cations *via* either proton or trimethylsilyl abstraction [eqns. (45), (46)].

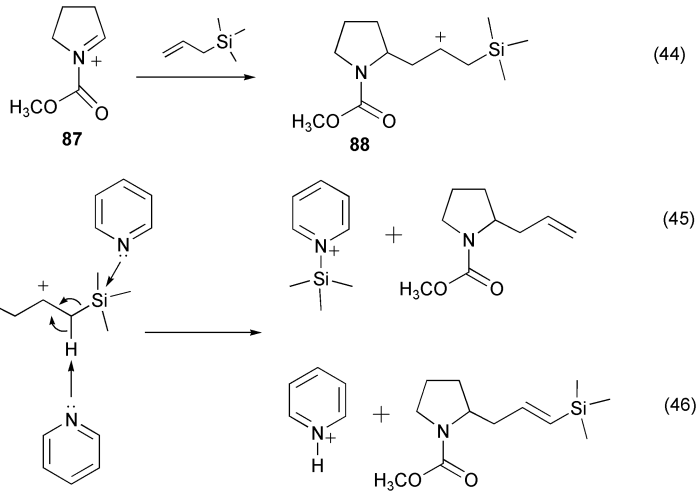

Canepa, Operti and co-workers have studied the reactivity of a number of $[Si_m,C_n,H_p]^+$ species (*e.g.* $SiC_2H_7^+$, $Si_2C_2H_7^+$, $Si_3H_5^+$ and $Si_4H_7^+$) with silane and propene.[200] Three types of reaction were observed with propene: (i) addition of propene and elimination of ethylene; (ii) addition of propene and elimination of acetylene; or (iii) addition of propene and elimination of silane. This chain propagation type reactivity was observed until the formation of larger clusters such as $Si_2C_5H_{13}^+$, $Si_3C_2H_{11}^+$ and $Si_4C_2H_{11}^+$ was attained. The same group have also studied the reactivity of related $[Ge_m,C_n,H_p]^+$ ions with ethane and germane.[201] The reactivities of CH_2=$Si(CH_3)$-$OSi(CH_3)_2^+$ towards acetaldehyde[202] and of the ethylsilylium cation towards ethylene[203] have also been studied.

Moraes and Eberlin have also prepared the first azaphosphirenium ion **91** *via* electron ionization and demetallation of ferriphosphaalkene **89**[eqn. (47)].[204] DFT calculations predict that the phosphavinyl cation **90** undergoes rapid cyclization to form the 3-(dimethylamino)-1,1-dimethyl-1*H*-azaphosphirenium cation **91**. This species was investigated *via* CID and ion–molecule reactions with N, O, P and S nucleophiles, as well as isoprene. Reaction with isoprene resulted in [4+2$^+$] cycloaddition followed by ring opening to form **92** [eqn. (48)].

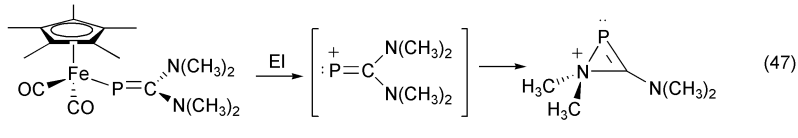

89 90 91 (47)

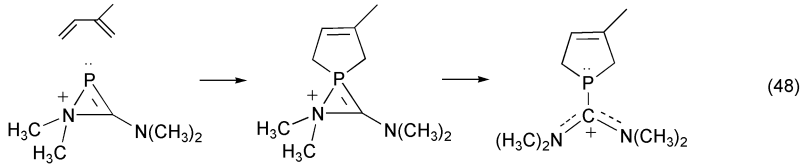

92 (48)

The *N*-methyl 2-azabutadienyl cation **93** reacts with alkyl, silyl and thio-enol ethers in a [4$^+$ + 2] cycloaddition reaction.[205] CID of these adducts **94** results in either retro-Diels–Alder reactions or loss of alcohol, silanol or thiol respectively [eqn. (49)]. These reactions enable isomeric enol ethers to be distinguished. For example, isomeric $C_3H_7OCH{=}CH_2$ and $C_2H_5OCH{=}CHCH_3$ react with **93** to form adducts of the same nominal mass, but these can be distinguished by the unique losses of propanol and ethanol under CID conditions.

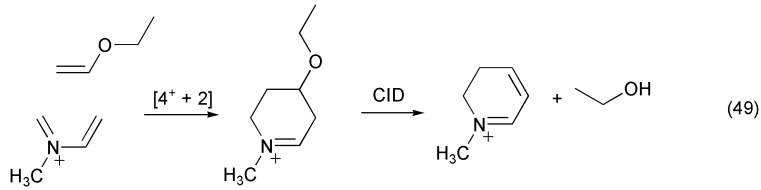

93 94 (49)

The products from association reactions between $HCNH^+$ and C_2H_2 or C_2H_4 have been studied experimentally and theoretically.[206] Reaction of $C_3H_4N^+$ (the acetylene adduct) with ethanol and HCN indicate the presence of two isomers of differing reactivity. High level G2(MP2) *ab initio* calculations suggest three possible structural isomers. Protonated acrylonitrile **95**, the most stable isomer, was ruled out on the basis of comparison of reactivity with the authentic species. It was concluded that the electrostatic bound species **96** accounts for one third of the $C_3H_4N^+$ ion

population, while the cyclic species **97** accounts for the other two thirds. In contrast, the association product from reaction of $HCNH^+$ with ethylene was found to have only one isomeric form.

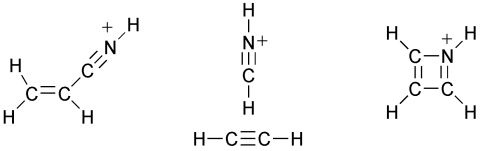

95, -244.2 kJ/mol **96**, -43.4 kJ/mol **97**, -73.8 kJ/mol

Bouchoux and co-workers have examined two competing unimolecular deamination reactions of protonated α,ω-alkanediamines, $NH_2CH_2(CH_2)_nNH_3^+$ **99** (n = 1–4): (i) intramolecular nucleophilic substitution and formation of a protonated cyclic amine **98** [eqn. (50)]; or (ii) hydride ion transfer to form a protonated imine species **100** [eqn. (51)].[207] The protonated cyclic amine ion is usually less stable than its acyclic isomer. However, comparisons of fragmentation patterns of resultant product ions with authentic protonated cyclic amine or protonated imine species reveal that the sole product is the thermodynamically unfavoured cyclic amine **98**. G2(MP2, SVP) *ab initio* calculations reveal that the transition state for formation of the acyclic imine ion is higher in energy than the transition state for formation of the cyclic amine species.

(50) 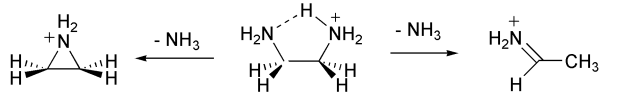 (51)

98 **99** **100**

The unimolecular fragmentation reactions of a variety of organic sulfate ester anions have been examined using a triple quadrupole mass spectrometer.[208] Three major pathways were observed: (i) cyclic *syn* elimination of the bisulfate anion, HSO_4^- (ii) loss of SO_3 or $SO_3^{-\bullet}$ and (iii) loss of $SO_4^{-\bullet}$. Competition between these pathways is controlled by the nature of the organic group attached to the sulfate moiety.

Grützmacher, Kirchhoff and Grützmacher have examined the unimolecular fragmentation reactions of triaryl pnictogen radical cations, $Ph_3E^{\bullet+}$ **101** (E = N, P, As, Sb, Bi).[209] Triphenylamine fragments *via* loss of sequential H atoms to generate a fragment ion with the azafluorene structure **102** [eqn. (52)]. Heavier triphenyl pnictogens (As, Sb, Bi) dissociate to almost completely generate $PhE^{\bullet+}$ **103** and eliminate biphenyl *via* the path in eqn. (53). This does not occur *via* the sequential loss of two successive phenyl radicals [eqn. (54)]. The triphenyl phosphane analogue is intermediate and shows dissociation *via* both these pathways. These results explain a previous observation that the appearance energy of $(C_6H_5)_2E^{\bullet+}$ **104** (E = As, Sb, Bi) is higher than that of $C_6H_5E^{\bullet+}$ **103**. In a separate study, the fragmentation of protonated tributylphosphate, $(C_4H_9O)_3POH^+$, was investigated.[210] Energy-resolved mass spectrometry and isotope labelling experiments allowed both competitive and consecutive mechanisms to be identified. The unimolecular gas phase chemistry of $(CH_3O)_2P(H)=O^{\bullet+}$ and $(CH_3O)_2P–OH^{\bullet+}$ has also been studied.[211]

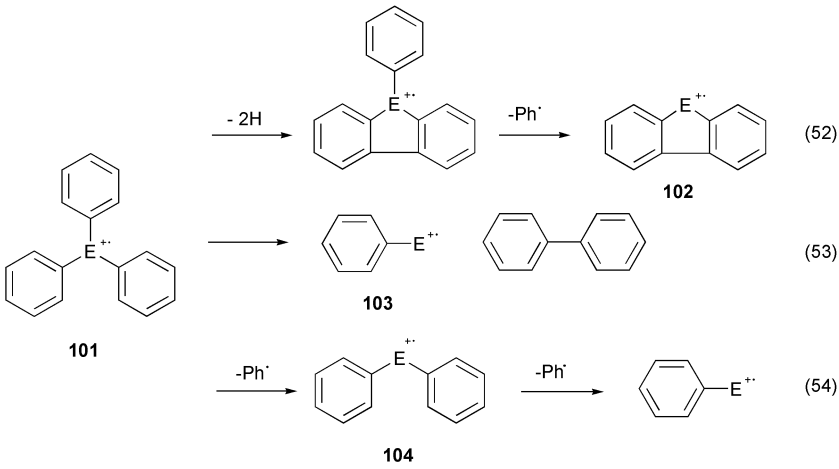

6 Reactions of organic compounds with inorganic ions

Reaction of XeF^+ with CH_3OH results in the formation of O-protonated methyl hypofluorite, $CH_3O(H)F^+$, and an adduct complex $(CH_3OH)XeF^+$.[212] Ion–molecule reactions of $CH_3O(H)F^+$ with methanol, 1,1-difluoroethylene, ethylene and hexafluorobenzene allowed the proton affinity of CH_3OF to be estimated as being in the range 648–680 kJ mol^{-1}, consistent with a theoretical prediction of 645 kJ mol^{-1}. Reaction of XeF^+ with acetylene results in the formation of $C_2H_2F^+$ and $C_2H_2Xe^+$.[213] $C_2H_2F^+$ was characterized as the 1-fluorovinyl cation, $CH_2{=}CF^+$, and its reactivity towards nucleophiles (CH_3COCH_3, CH_3CN, CH_3OH, C_2H_4) was investigated.

Arnold and Viggiano have studied the gas phase reactivity of SF_6^- with H_2O, CH_3OH and C_2H_5OH in a turbulent ion flow tube (TIFT) over the pressure range 50–500 Torr.[214] SF_6^- was found to be in equilibrium with a stable ion–neutral association complex, and products were formed *via* a bimolecular reaction of a second neutral with this complex. Final products for reaction with water included species such as $SOF_4^-(H_2O)_n$ and $F^-(HF)_2(H_2O)_n$. The kinetics of reaction between SF_6^- and O_3 have also been re-examined.[215] Kennedy and Mayhew have studied the reactivity of O_2^-, O^-, OH^-, CF_3^-, and F^- towards neutrals SeF_6 and TeF_6.[216] The same group have also studied the reactivity of positive ions of atmospheric interest (*e.g.* H_3O^+, NO^+, NO_2^+, O_2^+, H_2O^+, N_2O^+, O^+, CO_2^+, CO^+, N^+, N_2^+) towards SF_5CF_3.[217]

Viggiano and co-workers have studied the reactivity of NO^+ towards the four isomers of butene at temperatures from 225 to 500 K using a variable temperature SIFT.[218] Only charge transfer is observed for *cis*-2-butene and *trans*-2-butene, with both reactions occurring at the collision rate. Both charge transfer and association were observed for isobutene, while 1-butene undergoes a number of reaction channels including hydride transfer and charge transfer as well as more complex rearrangements.

Charge transfer dynamics of reaction between O^+ (^4S) and C_2H_2 have been examined experimentally using high-temperature guided ion beam measurements from 0 to

3 eV at 310 and 600 K, and variable temperature SIFT measurements at 193, 298 and 500 K.[219] High level *ab initio* theoretical calculations indicate that charge transfer occurs at an early stage *via* a non-adiabatic transition between quartet and doublet states.

Dotan and Viggiano have studied the reaction of O_2^+ with CH_4 over the temperature range 500–1400 K using a high temperature flowing afterglow apparatus.[220] Complex chemistry was observed, with seven primary products identified. Reaction rate constants were observed to increase dramatically over this temperature range, and reaction pathways and branching ratios were also highly temperature dependant. Four reaction pathways were investigated in a companion theoretical paper: (i) insertion of O_2^+ into C–H of CH_4; (ii) hydride abstraction from CH_4; (iii) charge transfer; and (iv) O–O cleavage.[221] CH_3OOH^+ was proposed as an important intermediate in this reaction.

Zare and co-workers have examined the reaction of vibrationally state selected NH_3^+ (v_2 = 1–9, 'umbrella') with CD_3NH_2 over the centre-of-mass collision energy range of 0.5–10 eV.[222] Five major products were observed: NH_4^+, NH_3D^+, $CD_2NH_2^+$, $CD_3NH_2^+$ and $CD_3NH_3^+$. The relative cross-section for each product formation was found to be a decreasing function of collisional energy. With the exception of $CD_2{=}NH_2^+$, the cross-section of each product was found to also decrease with increasing energy in the v_2 mode of NH_3^+. Ion–molecule reactions between state selected HCl^+ and CO, CO_2 and C_2H_4 have also been examined.[223,224]

Uggerud and co-workers have used CH_4 chemical ionization on H_2O_2 to generate protonated hydrogen peroxide, $HOOH_2^+$. The unimolecular and bimolecular reactivity of $HOOH_2^+$ was studied using a sector instrument (EBEB) and an FT-ICR apparatus.[225] Metastable $HOOH_2^+$ ions having internal energy sufficiently close to the dissociation threshold decompose spontaneously to form H_3O^+ and ^3O, consistent with previous theoretical predictions that ground state singlet $HOOH_2^+$ will decompose with loss of an oxygen atom *via* a spin change mechanism. A bond dissociation energy (BDE) of ≤150 kJ mol^{-1} for $HO–OH_2^+$ is inferred based on estimates of energy supplied during chemical ionization, in good agreement with previous theoretical predictions. Comparison with BDE(HO–OH) of 214 kJ mol^{-1} indicates that protonation activates the hydrogen peroxide molecule considerably. $HOOH_2^+$ reacted with alkanes (C_2H_6, C_3H_8, *i*-C_4H_{10}) *via* the hydride abstraction reaction [eqn. (55)], suggesting that similar reactions in solution may proceed *via* a

$$RH + HOOH_2^+ \longrightarrow R^+ + 2\,H_2O \qquad (55)$$

multistep process with initial hydride transfer, and not direct insertion of O into C–H as previously proposed. *Ab initio* direct dynamics calculations (for R = Et) reveal that the water molecule of the OH_2 group in $HOOH_2^+$ is expelled from the ion–molecule complex immediately after hydride abstraction, leaving a short lived $C_2H_5^+$–OH_2 complex. This complex dissociates to $C_2H_5^+$ and free H_2O after only 60 fs in approximately 80% of trajectories examined. Reaction of $HOOH_2^+$ with C_2D_6 results in almost exclusive formation of $C_2D_5^+$ (97%) and only a small amount of DH_2O^+ (3%), consistent with the extremely short-lived complex predicted by trajectory calculations. Reaction of $HOOH_2^+$ with $H_2{}^{18}O$ revealed only proton transfer to water, with no evidence of the identity S_N2 reaction occurring to form $HO^{18}OH_2^+$.

7 Thermochemistry and spectroscopy

A range of gas phase ion thermochemical and spectroscopic measurements of organic species were reported in 2001, but not all of these are reviewed here. Apart from the fact that these measurements provide fundamental information on species in the absence of solvent and counterions, they can provide useful information for analytical techniques. For example, information on the gas phase ion thermochemistry of 2,5-dihydroxybenzoic acid has been used to gain insight into the mechanisms associated with ion formation under MALDI conditions.[226] The NIST website continues to be regularly updated and is an invaluable tool for those interested in searching for gas phase thermochemistry of ions or neutrals.[227] In addition, several reviews dealing with gas phase ion thermochemistry and spectroscopy appeared in 2001.[39–47]

As discussed in Section 2B, photoionization–photoelectron experiments can provide highly accurate thermochemical data. A recent example has allowed the 0 K bond dissocation energies for the neutrals CH_3–Br (2.996 ± 0.002 eV) and CH_3–I (2.431 ± 0.003 eV) to be compared to their radical cations, CH_3–$Br^{+\bullet}$ (2.291 ± 0.002 eV) and CH_3-$I^{+\bullet}$ (2.731 ± 0.003 eV).[95] The thermokinetic method (previously used to determine proton affinities) has also been used to determine ionization energies for species such as benzene, cyclopentanone and vinyl alcohol.[228]

A Bond dissociation energies

Broadus and Kass have determined the heat of hydrogenation for acenaphthyne **105** to acenaphthylene **106** using a number of ingenious gas phase bracketing experiments.[229] Electrospray ionization (ESI) allows the 1,2-acenaphthylene dicarboxylate dianion **107** to be transferred to the gas phase. Sequential stages of CID yielded the acenaphthyne radical anion **108**, whose proton affinity (379 ± 2 kcal mol^{-1}) and electron binding energy (18.9 ± 1.6 kcal mol^{-1}) were determined. The acenaphthylene anion **109** was selectively generated *via* fluoride induced desilylation of 1-trimethylsilylacenaphthylene. **109** was found to have a proton affinity of 392 ± 3 kcal mol^{-1} and an electron binding energy of 39 ± 2 kcal mol^{-1}. Using these thermodynamic quantities, the heat of hydrogenation of acenaphthyne **105** was calculated to be 98 ± 4 kcal mol^{-1} *via* a thermodynamic cycle. Given that the heat of formation of acenaphthylene **106** is known, the heat of formation of acenaphthyne is calculated as 160 ± 4 kcal mol^{-1}. First and second C–H bond dissociation energies for acenaphthylene **106** of 117 ± 4 and 84 ± 2 kcal mol^{-1} were obtained. The gas phase reactivity of the acenaphthyne radical anion **108** towards a variety of neutral reagents was also reported.

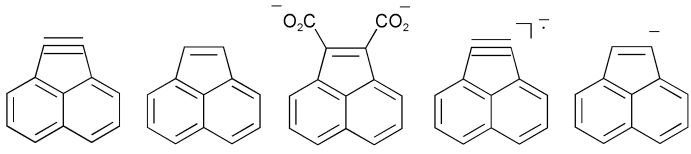

105 **106** **107** **108** **109**

Two separate studies have determined C–H bond dissociation energies for naphthalene using different approaches. These studies follow that of Reed and Kass described in last year's review. Lineberger, Ervin and co-workers determined the electron affinity of the naphthyl radical (1.403 ± 0.015 eV) *via* photoelectron spectroscopy of the naphthyl anion generated *via* deprotonation of naphthalene with NH_2^-.[230] Comparisons of Frank-Condon simulations with the photoelectron spectrum suggest the observed band could be attributed to the 1-$C_{10}H_7$ ⟵ 1-$C_{10}H_7^-$ transition, consistent with the expected stability of the 1-naphthyl anion over the 2-naphthyl anion. Combined with a revised value for the gas phase acidity of naphthalene ($\Delta_{acid}H_{298}$-(1-$C_{10}H_7$-H) = 1649 ± 14 kJ mol^{-1}), the bond dissociation energy of naphthalene was evaluated (BDE_{298}(1-$C_{10}H_7$-H) = 472 ± 14 kJ mol^{-1}). Wenthold and co-workers have used a different experimental approach to determine similar thermodynamic information.[231] Gas phase acidities for the 1-naphthalene anion (1648 ± 21 kJ mol^{-1}) and the 2-naphthalene anion (1664 ± 20 kJ mol^{-1}) were determined using the DePuy silane cleavage method. Electron affinities for the 1-naphthyl radical (1.43 ± 0.06 eV) and the 2-naphthyl radical (1.36 ± 0.04 eV) were determined using Cook's kinetic method *via* collision induced dissociation of 1- and 2-naphthylsulfinate adducts. These values provide naphthalene 1-C–H and 2-C–H bond dissociation energies of 473.6 ± 22 and 482.8 ± 21 kJ mol^{-1} respectively, in excellent agreement with the study by Lineberger, Ervin and co-workers.

By combining electron affinities of the peroxyl radicals determined *via* photoelectron spectroscopy on the parent hydroperoxide anions with the gas phase acidities of hydroperoxides measured in a FA-SIFT apparatus, the following alkyl hydroperoxide BDEs have been determined: $D_{H,298}(CH_3OO–H)$ = 87.8 ± 1.0 kcal mol^{-1}, $D_{H,298}(CD_3OO–H)$ = 87.9 ± 1.0 kcal mol^{-1} and $D_{H,298}(CH_3CH_2OO–H)$ = 84.8 ± 2.2 kcal mol^{-1}.[232]

Hammad and Wenthold have measured the heat of formation of 1,3,5-trimethylenebenzene **111** using an elaborate gas phase thermodynamic cycle.[233] This species is generated *via* CID of the chloromethyl-substituted *m*-xylylene anion **110**. Three major measurements were required for the thermodynamic cycle : (i) the heat of formation of the 5-chloromethyl-*m*-xylylene biradical (*i.e.* the neutral radical counterpart of **110**); (ii) the electron affinity of the 5-chloromethyl-*m*-xylylene biradical; and (iii) the threshold energy for chloride loss from **110** (*i.e.* **110** ⟶ **111** Scheme 14). A heat of formation of 111.0 ± 4.1 kcal mol^{-1} for **111** was proposed, implying a third C–H BDE in 1,3,5-trimethylbenzene of 88.2 ± 5.0 kcal mol^{-1}. This is indistinguishable from the C–H BDE in toluene or the first and second C–H BDEs in *m*-xylene, consistent with negligible interactions between the unpaired electrons in triradical **111**.

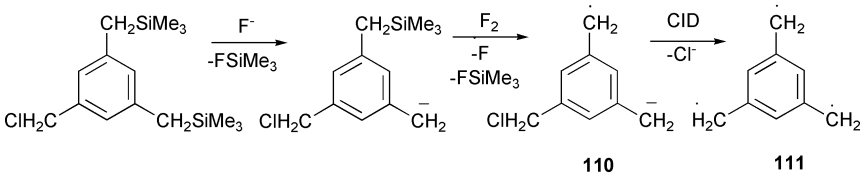

110 **111**

Scheme 14

Bouchoux and co-workers have used the thermokinetic method to determine proton affinities of the vinyloxy and acetonyl β-carbonyl radicals, PA($[CH_2CHO]^{\bullet}$) = 769.3 ± 2.6 kJ mol^{-1} and PA($[CH_2COCH_3]^{\bullet}$) = 813.0 ± 1.3 kJ mol^{-1}.[234] Combined with the known heats of formation of the ionized enols, these values allow the heat of formation of the radicals to be determined, $\Delta_f H°_{298}([CH_2CHO]^{\bullet})$ = 9.9 ± 3.9 and $\Delta_f H°_{298}([CH_2CHO]^{\bullet})$ = −34.6 ± 8.4 kJ mol^{-1}. Comparison with known heats of formation for relevant radical or neutral species also allowed selected bond dissociation energies to be estimated.

B Gas phase acidities and basicities

Cooks' kinetic method has been used to measure the primary and secondary isotope effects for H^+ affinities for a series of isotopomeric pairs (*e.g.* acetone, pyridine, acetonitrile).[235] For example, a normal secondary isotope effect of 1.32 was observed for dissociation of the CH_3CN/CD_3CN proton bound dimer **112A**, while an inverse primary isotope effect of 0.97 was observed for the $CH_3CN/CH_3C^{15}N$ pair **112B**. These results allow the PA ordering for acetonitrile isotopomers to be established: $CH_3{}^{15}CN > CH_3CN > CD_3CN$. Changes in zero point energies from DFT calculations were found to accurately predict the nature (*i.e.* normal or inverse) of the measured KIEs. In a related study, Cooks and co-workers have used the kinetic method with full entropy analysis to investigate the proton affinity of CH_3CN and CD_3CN and also find a normal secondary KIE ≈ 1.2, suggesting a difference in PA between CH_3CN and CD_3CN of ≈ 0.2 kcal mol^{-1}.[236]

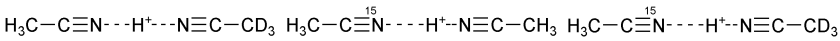

112A **112B** **112C**

Cao and Holmes have used the kinetic method to determine the proton affinity of secondary alcohols, (*i*-propanol, *c*-butanol, *c*-pentanol). Proton affinities of secondary alcohols are difficult to determine *via* the kinetic method, as their proton bound pairs with other alcohols often dissociate *via* H_2O or olefin loss. However, dissociation of proton bound trios, $A_2H^+B_n$ (A = ethanol, B = secondary alcohol) results in formation of the corresponding proton bound pairs, with no H_2O or olefin loss.[237] This technique allowed the kinetic method to be used to determine the proton affinity of secondary alcohols, PA(*i*-propanol) = 796 ± 6, PA(*c*-butanol) = 792 ± 6, PA(*c*-pentanol) = 798 ± 6 kJ mol^{-1}.

Several studies have examined the proton affinities of biomolecules. Cooks' kinetic method has been used to study the relative proton affinities of the naturally occurring amino acids.[238] A similar ordering to previous studies was reported, except for valine–aspartic acid, aspargine–glutamic acid and tryptophan–proline. Given these discrepancies, the extended kinetic method was used to determine the PA values for proline and tryptophan, determined as 219.9 kcal mol^{-1} and 221.6 kcal mol^{-1} respectively. These results are in agreement with the ordering from previous studies, and highlight limitations of the standard kinetic method. The kinetic method has also been used to evaluate the acidities and chloride affinities of isomeric monosaccharides,[239] and the

proton affinity of *N*-3-benzoyl-2-deoxycytidines.[240] Cassady and co-workers have continued their studies on the proton transfer reactions of protonated peptides[241]

The acidities of a number of substituted aryldimethylsilanes, determined *via* equilibrium measurements in an FT-ICR instrument, are linearly correlated with the standard substituent constant (σ°).[242] Dimethlyphenylsilane was found to be a stronger acid than dimethylsilane by only 2.7 kcal mol^{-1}, suggesting the acid enhancing effect of the phenyl group is smaller than that for the carbon analogue. Indeed, substituent effects for phenyl-substituted dimethyphenylsilane were found to be significantly smaller than analogous carbon acids.

Schlosser, Nibbering and co-workers have examined the acidity of nineteen different chloro-substituted benzenes using FT-ICR mass spectrometry.[243] Compared with results from a previous study on the oligofluorobenzenes, the chloro substituent was found to acidify the *ortho* position slightly less and the *meta* position slightly more than fluorine. Changes in acidity with three or more chloro substituents were not well described by an additive model. Gas phase acidities were compared with the reactivity of selected oligochloro-benzenes towards *sec*-butyllithium in THF at −100 °C, and a strong linear correlation between with logarithmic rates was found. Acidities for each of the chloro substituted benzenes were also determined theoretically *via ab initio* calculations.

Nibbering and co-workers have continued their studies on the light induced proton transfer from radical cations to reference bases.[244] Protonated naphthalene (PA = 803 kJ mol^{-1}) was excited using a 488 nm (2.54 eV) laser, and found to transfer a proton to bases having PA > 744 ± 2 kJ mol^{-1}. This suggests that ≈ 60 kJ mol^{-1} (0.6 eV) of the energy deposited into protonated naphthalene (2.54 eV) is available for proton transfer. This difference was explained using a complete randomization of the energy deposited in protonated naphthalene.

Bouchoux and co-workers have re-evaluated the gas phase basicities and proton affinities of ethyl halides using the thermokinetic method (C_2H_5X, X = Cl, Br, I), which suggest that current tabulated values for these molecules should be revised downward by between 10 and 14 kJ mol^{-1}.[245] High level *ab initio* G2 calculations were in excellent agreement with experiment, and suggest current estimates of PA(C_2H_5F) and GB(C_2H_5F) should also be revised downward by ≈ 30 kcal mol^{-1}.

Bartmess and co-workers have measured the gas phase acidity of 1,1,3,3-hexamethyl-1,3-disila-2-azacyclopentane **113**, and compared this species with its acyclic analogue, hexamethyldisilazane **114**.[246] **113** was found to be a 10.5 kcal mol^{-1} weaker acid than **114**. *Ab initio* calculations suggest that the geometry of **114** is altered significantly upon deprotonation, with rehybridization at nitrogen resulting in a linear Si–N–Si geometry. Similar geometry changes upon deprotonation are prevented in **113**.

Trends in the acidity of α,β-unsaturated alkanes, silanes, germanes and stannanes have been investigated using FT-ICR MS (*e.g.* CH_3–CH_2–XH_3, CH_2=CH–XH_3,

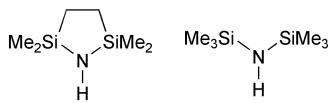

113 **114**

$HC{\equiv}C{-}XH_3$ X = C, Si, Ge, Sn).[247] As expected, acid strength was found to increase down the group. α,β-Unsaturated compounds were found to be stronger acids than their saturated counterparts, . $HC{\equiv}C{-}XH_3 > CH_2{=}CH{-}XH_3 > CH_3{-}CH_2{-}XH_3$. This was attributed to the greater electronegativity of unsaturated groups offering increasing stabilization of the conjugate anion. This effect was particularly strong for the carbon derivatives, but less pronounced for the silicon, germanium and tin derivatives. Resonance stabilization present in the allyl anion is considerably reduced for the Si-, Ge-, Sn- derivatives due to the inefficient π overlap of p-orbitals of different sizes. This results in a far greater increase in acidity upon moving from $CH_3{-}CH_2{-}XH_3$ to $CH_2{=}CH{—}XH_3$ for X = C than is observed when X = Si, Ge, Sn.

Brauman and co-workers have measured the acidities of α,ω-dithiols (*e.g.* $HS(CH_2)_nSH$, n = 2–4) and electron affinities of the corresponding dithiolate monoradicals.[248] Comparisons with related monothiols reveal that the aciditities and electron affinities of dithiol species are significantly enhanced over their monothiol counterparts (*e.g.* $n = 2$; $\Delta(\Delta G^\circ_{acid}) = 8.7$ kcal mol^{-1}, $\Delta(EA) = 6.7$ kcal mol^{-1}). This was attributed to increased stability of the dithiol anion due to the presence of an intramolecular hydrogen bond. *Ab initio* calculations supported this proposal, with cyclic dithiol anions involving a hydrogen bond predicted to be 3.4–5.0 kcal mol^{-1} lower in energy than their fully *anti* counterparts. This hydrogen bond is proposed to provide up to 9 kcal mol^{-1} extra stabilization.

A number of groups have used theoretical methods to investigate acidities and proton affinities of a wide variety of molecules. Only a selection of these studies from 2001 are listed here. Bouchoux and co-workers have used high level G2(MP2) *ab initio* calculations to investigate the protonation thermochemistry of α,ω-alkyldiamines.[249] Bernasconi and Wenzel have studied the identity proton transfer reactions from allene, ketene, ketenimine, thioketene,[250] propyne, acetimide, thioacetaldehyde and nitrosomethane[251] to their respective conjugate anions using a variety of theoretical methods. DFT has been used to study the proton affinity and gas phase basicity of proline,[252] and the structure, thermochemistry and unimolecular reactivity of protonated glycolaldehyde has been investigated theoretically.[253] The origins of the acidity of carboxylic acids have been re-evaluated,[254] and the effects of substituents on the gas phase acidity of alcohols and silanols have been explored.[255]

C Other ion affinities

Pulsed ionization high-pressure mass spectrometry (PHPMS) has been used to investigate the thermochemistry of clustering between halide ions and halide substituted organic molecules such as ethers and alkanes. PHPMS is one of the few experimental techniques able to obtain ΔS° values for gas phase clustering reactions.

McMahon and co-workers have studied the thermochemistry of clustering reactions between chloride and fluorinated dimethyl ether derivatives (CH_3OCH_3, CH_3OCF_3, CF_2HOCF_2H and CF_3OCF_2H).[256] Enthalpy and entropy changes determined experimentally were compared with *ab initio* calculated values for a number of different stable rotamers and isomers for each complex. Experimental ΔH° and ΔS° values were observed to be very dependent on the number and position of fluorine atoms in the ether. For example, the large negative ΔS° value obtained for

$Cl^-((CF_2H)_2O)$ formation was attributed to double hydrogen bond formation in the complex 'locking' the two CF_2H groups in position relative to the free neutral.

Hiraoka, Yamabe and co-workers have used a similar instrument to investigate clustering reactions between halide ions and methane, and chloride ions with chloromethanes (**1**,**2**).[257] Theoretical *ab initio* calculations predict highly symmetric geometries for the chloromethane systems. The chloride ion is proposed to coordinate linearly to the Cl–C of carbon tetrachloride due to charge transfer interactions. The same group has also studied the clustering reactions of halide ions with ethylene and propylene.[258] Binding energies of all cluster ions were found to be less than 10 kcal mol^{-1}, and no anion-initiated polymerization of C_2H_4 and C_3H_6 was observed. The association reactions and stability of adducts between chloride and three different dinitroalkanes have been studied using ion mobility mass spectrometry.[259] Finally, Grimsrud and co-workers have used PHPMS to determine equilibrium constants and free energies for the association reactions between SiF_4 and the anions of *p*-benzoquinone, benzophenone, nitrobenzene and 21 substituted nitrobenzenes.[260] The magnitude of Lewis acid–base interactions showed a strong inverse dependence on electron affinity of the parent molecule, and on the availability of Lewis base sites on the anion that could be closely approached by the Si atom of SiF_4.

The gas phase trimethylgermyl cation affinities of a series of acetophenones have been determined by equilibrium measurements [eqn. (56)].[261] The binding interaction between the Me_3Ge^+ cation and the carbonyl group of acetophenones has pronounced covalent character, resulting in a positive charge at the benzylic carbon atom. A strong correlation between the effects of ring substituents and Me_3Ge^+ cation affinities was observed.

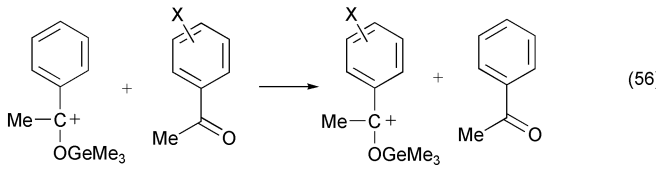

(56)

Interest in the gas phase binding affinities of various small organic and inorganic ligands towards the sodium cation continues and is largely prompted by the important role of the sodium cation in many biological systems.

Petrie has recently redressed the shortcomings of existing computational techniques for calculating sodium cation affinities and suggests three important principles: (i) the use of a sufficiently flexible basis set to accurately characterize both the sodium cation–ligand adduct and the separated species; (ii) correction for basis set superposition error (BSSE); and (iii) inclusion of the sodium 2s and 2p orbitals within the correlation space for single point calculations.[262] Amicangelo and Armentrout have examined bond dissociation energies for ligated sodium cation complexes using guided ion beam (GIB) mass spectrometry.[263] Competitive dissociation channels of complexes $L_1Na^+–L_2$ (L_1, $L_2 = H_2O$, C_6H_6, CH_3OH, CH_3OCH_3, NH_3 and C_2H_5OH, $L_1 \neq L_2$) were examined to yield absolute $L_1Na^+–L_2$ and relative $Na^+–L$ bond dissociation energies. Relative $Na^+–L$ binding affinities were anchored to the $Na^+–NH_3$ dissociation energy (determined previously) to provide absolute $Na^+–L$ bond

dissociation energies. Single ligand binding affinities were found to have the order: ethanol > ammonia > dimethyl ether > methanol > benzene > water, and span a range of only 20 kcal mol^{-1}. Rodgers and co-workers have used GIB mass spectrometry to determine the binding energy of acetonitrile ligands in $Na^+(CH_3CN)_n$ (n = 1–5) complexes.[264] These values were compared with previous literature values as well as theoretical predictions from *ab initio* (MP2) and DFT (B3LYP) calculations. Ligand binding energies were observed to decrease with increasing number of ligands, while the reliability of theory was also observed to decrease with increasing cluster size. Rodgers has also studied the binding energies of isomeric *o*-, *m*- and *p*-methylpyridines to alkali metal cations (Li^+, Na^+, K^+).[265] Dissociation energies were observed to decrease significantly with the size of the alkali metal cation. Typically, Li^+ binds ≈50% more strongly than Na^+, which in turn binds ≈35% more strongly than K^+. These trends were rationalized using changes in the charge density of the metal ion. The position of the methyl substituent was found to have a much smaller effect (*i.e.* <5 kJ mol^{-1}), and these effects were rationalized using the polarisability of the ligand. In a later study, the binding energies of aminopyridines to the same alkali metal cations were investigated.[266] Similar trends in binding energies upon variation of the metal cation were observed, however, a larger variation in binding energy with the position of the amino substituent was observed. This was attributed to chelation and resonance effects in the aminopyridine complexes. Finally, FT-ICR MS has been used to investigate the binding of Na^+ to alanine, alanine methyl ester and phenylalanine using ligand exchange measurements.[267] Phenylalanine binds 7 ± 2 kcal mol^{-1} more strongly than alanine, highlighting the importance of Na^+–π binding. Using the Na^+–pyridine affinity as an anchor, binding enthalpies of 38 ± 2 and 45 ± 2 kcal mol^{-1} were determined for alanine and phenylalanine, respectively.

The binding of other metal ions to organic molecules has also been extensively studied. Amunugama and Rodgers have also studied the binding of various metal ions (Mg^+, Al^+, Sc^+–Zn^+) to pyrimidine using threshold collision-induced dissociation[268] and DFT calculations while Satterfield and Broadbelt have studied the relative binding energies of pyridyl ligand–metal complexes using energy-variable CID in a quadrupole ion trap.[269] Threshold activation voltages for dissociation of pyridyl ligands such as 1,10-phenanthroline, 2,2′-bipyridine and 2,2′:6′,2″-terpyridine from a series of alkali, alkaline earth and transition metal ions (*e.g.* $[M^{I}L_2]^+$ or $[M^{II}L_3]^{2+}$) were determined. Again, a strong dependence on the metal ion was observed, with polarizability, steric hindrance, preorganization and chelating effects of the pyridyl ligands also being important factors. A correlation between ML_3 formation constants in solution and threshold dissociation voltages for $[M^{II}L_3]^{2+}$ complexes was observed.

Armentrout and co-workers have studied the dissociation of Cu^+–dimethyl ether complexes, $Cu^+((CH_3)_2O)_n$, n = 1–4.[270] Strong BDEs are observed for the first and second dimethyl ether ligands, while the third and fourth bind much more weakly, with BDEs of 1.92 ± 0.12, 2.00 ± 0.08, 0.57 ± 0.04, 0.47 ± 0.10 eV being measured for n = 1–4 respectively. The increase in binding energy of the second dimethyl ether was rationalized using 4s–3dσ hybridization of the Cu^+ cation resulting in reduced charge density of the metal along the bonding axis, thereby reducing metal–ligand repulsion. The same group have also studied the dissociation energies for ligand loss from Cu^+(dimethoxyethane) complexes, $Cu^+(CH_3OCH_2CH_2OCH_3)_n$ (n = 1, 2).[271] The first dimethoxyethane ligand is more strongly bound than the first dimethyl ether ligand

due to the bidentate nature of the dimethoxyethane complex. However, the second dimethoxyethane ligand cannot bind to Cu^+ to fully maximize the effects of 4s–3dσ hybridization, resulting in a slightly lower dissociation energy for the second dimethoxyethane ligand.

Yeh and co-workers have used photodissociation to study the photofragmentation and binding energies of M(furan)$^+$ (M = Cu, Ag, Au) complexes.[272] Based on ionization energy considerations, these complexes were formulated as Cu^+–furan, Ag^+–furan and Au–furan$^+$. Ligand-to-metal charge transfer resulting in formation of M and furan$^+$ was observed for Cu and Ag, while direct dissociation of furan$^+$ as well as activation of furan was observed for Au. Binding energies of 37 kcal mol^{-1} for Cu^+–furan, 28 kcal mol^{-1} for Ag^+–furan and 62 kcal mol^{-1} for Au–furan$^+$ were determined. These trends were qualitatively supported by CCSD(T)/MP2 *ab initio* calculations. In a separate study by the same group, the photodissociation of M^+–C_6H_6 and (M = V, Ta) complexes was investigated.[273] Photofragmentation of V^+–C_6H_6 produced exclusively V^+ ionic fragments, while photodissociation of Ta^+–C_6H_6 resulted in elimination of C_2H_2, with no Ta^+ formation.

Finally, Schröder, Schroeter and Schwarz have investigated the unimolecular decay of L′FeL$^{+/2+}$ species[274] (L = arene, *e.g.* benzene, pyridine, toluene, 4-picoline, fluorobenzene, chlorobenzene). Dicationic species were generated *via* charge stripping of the related cationic species. Based on branching ratios of ligand loss from metastable species, the Cooks kinetic method allowed a consistent order of relative affinities of Fe^+ for different arene ligands to be determined. Dissociation of dicationic species was considerably more complicated, with arene ligand loss ratios often being reversed relative to their monocationic counterparts. For example, the monocation (C_6H_6)-$Fe^+(C_6H_5F)$ dissociates with a 100-fold excess of C_6H_5F loss, while the dication $(C_6H_6)Fe^{2+}(C_6H_5F)$ dissociates with at least a 33-fold excess of C_6H_6 loss.

D Spectroscopy

Physical chemists and physicists are applying spectrospcopic techniques to a wide array of gas phase ions and neutral molecules (*e.g.* to probe conformations in neurotransmitters[275,276] or to probe tautomerism in nucleobases[277–279]). While many of these experiments require sophisticated instrumentation, they provide exciting results and benchmarks for theoretical models. Before discussing some interesting results for 2001, we note that spectroscopic studies providing information on the conformations of biomolecules are discussed in more detail in Section 9C.

Marshall and co-workers have measured the laser-induced fluorescence (LIF) excitation spectrum of $C_6F_6^+$ using ICR mass spectrometry based techniques.[280] Good agreement with previous results on the same ion using Penning ionization was observed. These results offer promise for the optical spectroscopy of a wide range of gas phase ions *via* ICR based techniques.

Apart from providing accurate electron affinities of radicals (often used in thermodynamic cycles discussed in Section 7A), anion photoelectron spectroscopy (PES) also provides information about vibrational frequencies and excited states of radicals generated upon ionization. Continetti and co-workers have used PES to investigate the effects of alkyl substitution on the energetics of enolate anions and radicals

(n-$C_3H_5O^-$, i-$C_3H_5O^-$, n-$C_3H_5O^-$, s-$C_3H_5O^-$, i-$C_3H_5O^-$).[281] Both the ground and first excited states of the radical were accessed *via* electron detachment from the anion, providing first excited state energies for radicals. Electron affinities and ground-excited state energy separations for the radical species were monitored as a function of both carbonyl and α-carbon substituents. Substitution at the carbonyl carbon produced a larger change in vibronic structure, while substitution at the α-carbon resulted in larger changes in energetics. High level CASPT2/CASSCF calculations were in good agreement with experiment. ZEKE photoelectron spectroscopy has also been used to investigate the *cis*- and *trans*-isomers of formanilide.[282]

Wild, Bieske and co-workers have used infrared vibrational predissociation spectroscopy to examine the $^{35}Cl^-$–H_2, $^{35}Cl^-$–D_2 and Br^-–D_2 complexes.[283,284] Spectra are consistent with linear equilibrium structures involving an H_2 (D_2) molecule attached to the halide anion *via* a linear hydrogen bond. Comparisons between the Br^-–D_2 bond and the Cl^-–D_2 bond reveal the Br^-–D_2 bond is longer (R_{cm} = 3.41 Å *vs.* 3.16 Å) and weaker (D_o = 364 *vs.* 570 cm^{-1}).

Johnson and co-workers have studied IR predissociation spectroscopy to study autodetachment and argon loss from the argon solvated nitromethane anion, $CH_3NO_2^-{\cdot}Ar_n$ (n = 1–4).[285] For smaller clusters (n = 1, 2) electron ejection is the dominant pathway, while for larger clusters (n = 3, 4) this is overwhelmed by a competing pathway involving Ar evaporation from the cluster. The same group have also used argon predissociation spectroscopy to study the hydrated superoxide anion, $O_2^{-\cdot}(H_2O)_n$ (n = 1–5).[286] Dopfer and co-workers have used a similar technique to investigate H_2O^+–He, HOD^+–He,[287] H_2O^+–Ne and HOD^+–Ne complexes.[288]

There have been several other reports on the gas phase infrared spectroscopy of cations. Many of these experiments are carried out by storing gas phase ions in an ion trap and irradiating them with IR light from a free electron laser. Multiphoton absorption and dissociation occurs when the IR light is in resonance with an IR-allowed vibration, and monitoring the amount of ionic fragmentation as a function of the IR wavelength yields the IR spectrum of the parent cation. This technique represents a powerful advance in determining the IR spectra of a range of species including inorganic and organic cations, and has been applied to the Ti_8C_{12} 'met-car'[289] as well as polycyclic aromatic hydrocarbon (PAH) species.[290–292] For example, the gas phase IR spectrum of the coronene cation was found to exhibit main absorption peaks at 849, 1327 and 1533 cm^{-1}, in good agreement with density functional theory calculations.[290] Other cationic PAHs studied with this technique include indane, acenaphthene, fluorene, and fluoranthene.[291,292] This technique is complementary to photo-induced cluster dissociation spectroscopy, which has also been used to study the IR spectra of the PAH model compound phenanthrene.[293]

By interacting ions with higher energy photons, UV–Vis spectra of gas phase species can be determined. These experiments are conceptually similar to the IR experiments discussed above except that the ions are stored in an electrostatic ion storage ring. Once again, this is a photodestructive spectroscopic technique whereby the absorption spectrum is generated by monitoring the yield of fragments formed as a function of the laser wavelength used. This technique has been used to examine the gas phase absorption spectrum of a model system **115** of the chromophore anion responsible for the behaviour of the green fluorescent protein found in jellyfish.[294] A remarkable finding is that this model chromophore has a gas phase absorption

maximum at 479 nm, which coincides with one of the two solution phase absorption peaks of the actual protein. In contrast, the solution phase absorption maximum of the model chromophore **115** is strongly influenced by the pH of the solution. This suggests that the actual envionment of the chromophore inside the protein cavity is much closer to vacuum than to bulk solution. Interestingly, while a range of factors govern the enhanced reactivity at enzyme sites (for some recent reviews see refs. 295–297), it is interesting to note that some time ago Dewar proposed that substrates at an enzyme active site experience an environment more akin to the gas phase than the condensed phase.[298]

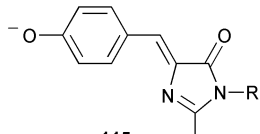

115

8 Bridging the gap between the gas and condensed phase

The advent of new techniques such as electrospray make bridging the gap between naked gas phase ions and the condensed phase a realistic proposition. Mass spectrometry based studies on the chemistry of solvated ions, nanodroplets and salts are providing important insights into the roles of solvent and counter ions in the condensed phases. These advances may also provide new opportunities for mass spectrometry based analysis (*e.g.* the formation of 'supercharged' protein and peptide ions[299]).

A Clusters and solvation phenomena

The structure and reactivity of neutral and ionic gas phase clusters continues to be the subject of intense research. Due to the size of this field, only a small selection of papers that highlight some of the various mass spectrometric and spectroscopic techniques used to examine gas phase clusters are discussed.

The neutralization of $[M + Li]^+$ ions ($M = NH_3$, H_2O) have been studied using NRMS and theoretical calculations.[300] NRMS experiments reveal that both neutral hypervalent $[M + Li]^{\bullet}$ complexes are stable, although dissociation to M and $Li^{\bullet}$ is observed. The dissociating fraction is larger for the water complex.

The structure and reactivity of ionic water clusters and water solvated ions has been the subject of a number of studies.[301–306] Water radical cations, $[(H_2O)_n]^{+\bullet}$ ($n = 2$–6), fragment *via* competitive loss of $HO^{\bullet}$ and H_2O, with the relative loss of H_2O increasing with the number of water molecules in the cluster.[302] This behaviour was interpreted as the formation of an $H_3O^+(HO^{\bullet})$ central core with additional H_2O ligands present in the first solvation shell. Protonated water clusters, $[H^+(H_2O)_n]$ ($n = 1$–7), have been studied in a swarm experiment.[303] A large abundance of the $n = 4$ ion was observed. Photodetachment photoelectron spectroscopy has been used to examine a range of small anionic species solvated by water molecules, including: (i) the

electron;[304] (ii) F^-;[305] (iii) SO_4^{2-}[306] and (iv) $C_2O_4^{2-}$.[306] Photoelectron spectra of the $[SO_4^{2-}(H_2O)_n]$ and $[C_2O_4^{2-}(H_2O)_n]$ clusters ($n = 4$–40) suggest that the solute dianions were in the centre of the water cluster. For smaller clusters, spectra were characteristic of the respective solutes. For larger clusters, with H_2O ligands beyond the first solvation shell ($n > 12$), features in the spectra from the solute were diminished and a new feature due to the ionization of water was apparent. For the largest clusters studied ($n \approx 30$–40) the solute photoemission features were absent, and spectra were dominated by the ionization of water. Thus, a smooth transition from gas phase clusters to bulk water was clearly revealed.

The hydration of gas phase metal ions continues to attract considerable interest. Shvartsburg and Siu have examined the stability of hydrated doubly charged metal cations in the gas phase.[307] As the second ionization potential of a metal atom usually exceeds the first ionization potential of a solvent molecule, a common feature of these species is dissociative charge transfer. Hydrated doubly charged cations of most common divalent metals (*e.g.* Mn, Fe, Co, Ni, Zn, Cd and Cu) were generated using electrospray and examined by CID. Monoaqua complexes were observed for all doubly charged metal ions, except Be, for which the smallest complex observed was the dihydrate. Wright *et al.* have examined the coordination chemistry of stable Cu(II) complexes in the gas phase with 20 different ligands, including water, ammonia, pyridine, tetrahydrofuran and benzene.[308] Considerable variation as a function of the composition and size of solvent molecule was observed, with evidence of stable coordination shells containing between two and eight molecules. In most instances, coordination shells containing more than four molecules can be attributed to the formation of an extended network of hydrogen bonding. Collisional activation of size-selected clusters reveals the presence of extensive ligand-to-metal electron transfer in the smaller complexes. In several cases, charge transfer is also accompanied by chemical reactivity. Solvated cluster ions $Co^{2+}(H_2O)_n$ ($n = 4$–7) have been generated *via* electrospray and studied using laser photofragment spectroscopy.[309] Similarities between the spectrum of gas phase $Co^{2+}(H_2O)_6$ and the absorption spectrum of aqueous cobalt(II) suggest that $Co^{2+}(H_2O)_6$ is responsible for the room-temperature absorption spectrum. Gas phase ion–molecule reactions of hydrated divalent alkaline earth metal ions with benzene have been examined using FT-ICR MS.[310] Rate constants for solvent-exchange reactions were determined as a function of hydration extent for $M^{2+}(H_2O)_n$ clusters (M = Mg, Ca, Sr, Ba; $n = 4$–7). Rates of reaction were observed to be dependent on both the metal cation and the number of water molecules in the cluster. Diminishing reactivity with increasing hydration was attributed to cation–π interaction between the metal ion and benzene being partially screened by surrounding water molecules. Cationic water clusters containing iodine have been investigated by FT-ICR mass spectrometry.[311] $[I(H_2O)_n]^+$ ($n \geq 13$) ions react with HCl by formation of the interhalide ICl and a protonated water cluster, in the reverse of a known solution-phase reaction. DFT calculations suggest that cationic $I(H_2O)_n^+$ is best regarded as a protonated water cluster in which one water molecule is replaced by hypoiodous acid (HOI).

The solvation of gas phase ions by amines has also been evaluated in several studies. Fox *et al.* have examined the thermal fragmentation of size-selected ionic ammonia clusters of H^+ and Ag^+.[312] Dissociation rates exhibit an overall linear dependence on the number of ligands. DFT calculations predict enthalpies for the addition of the

first and second CH_3CN ligands to Ag^+ to be 40.1 and 35.3 kcal mol^{-1}, while binding enthalpies for the third and fourth ligands are much smaller.[313] These results clarify why electrospray of $AgNO_3$ and acetonitrile in water predominantly yields $AgNCCH_3^+$ and $Ag(NCCH_3)_2^+$, and only small amounts of $Ag(CH_3CN)_3^+$. A guided ion beam instrument has been used to examine the binding energies of up to five acetonitrile ligands to Cu^+ ions.[314] Again, the first two CH_3CN ligands are more strongly bound than the third and following ligands.

Several studies have investigated hydration of the peptide bond *via* gas phase spectroscopy of both ionic and neutral water solvated amides.[315–319] Structures of the solvation shells of O-protonated formamide, $HCO(H)NH_2^+(H_2O)_n$ have been characterized by infrared spectroscopy (n = 3, 4) and *ab initio* calculations (n = 1–4).[315] Theoretical investigations on $HCO(H)NH_2^+(H_2O)_3$ indicate that filling of the first hydration shell with three water molecules to form **116** is less favoured than forming an H_3O^+ ion core solvated by three ligands, **117**. This is due to a hydrogen bond anticooperative effect disfavouring both NH bonds being involved in hydrogen bonding. Experiments on the cluster with four water molecules reveal a low-barrier proton transfer process that is expected to occur in aqueous solutions during acid-catalyzed amide hydrolysis. The observation of two different 1:1 complexes of water and *trans*-*N*-phenylformamide in a supersonic expansion has allowed the binding energy of H_2O at both the CO and NH sites to be determined .[316] At the CO site the water molecule acts as a proton donor, and the H-bond has an energy of 5.40 kcal mol^{-1}, while at the NH site the water molecules act as a proton acceptor and the H-bond has an energy of 5.65 kcal mol^{-1}. IR–UV ion-depletion and fluorescence spectroscopy has been used to show that hydration of 2-phenylacetamide by 1–3 water molecules leads to structures in which the water molecules link the amide NH and CO sites.[317] Bridging between the CO and NH sites by either water molecules,[318] ammonia molecules or mixtures of both[319] also occurs in amides that are constrained in the *cis* conformation.

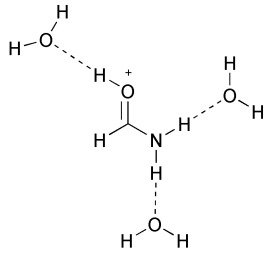

116

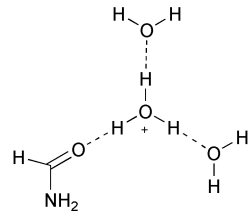

117

B Ion pairs, zwitterions, triple ions and salt bridges

Interest in ionic interactions in the gas phase has continued in 2001. This interest is largely driven by the important effect of ion-pair formation on the structure and reactivity of biomolecules in the gas phase. Strittmatter and Williams have used DFT calculations to evaluate the role that proton affinity, acidity and electrostatics have on the stability of neutral and ion-pair forms of five molecular dimers composed of a

basic molecule and a trifluoroacetic acid molecule.[320] Calculations suggest that the structures of the dimers change from a neutral pair to an ion pair as the proton affinity of the bases increases. This is consistent with previous experimental studies. Natural energy-decomposition analysis was used to investigate the electrostatic character of the interaction between the basic molecule and the trifluoroacetic acid molecule. The majority (69%–77%) of the attractive energy of the ion pair dimer can be attributed to the electrostatic component. ESI/MS has been used to examine the type and stability of ionic clusters formed from simple salts. For example, ESI of NaF produces a series $[Na(NaF)_n]^+$ and $[Na_2(NaF)_n]^{2+}$ cluster ions.[321] Evidence for 'magic cluster numbers' is provided by experiments involving alteration of the electrospray desolvation temperature and CID of mass selected clusters. The $Na_2(NaF)_n]^{2+}$ cluster ions fragment at higher source temperatures, while under CID conditions they decompose to singly charged clusters. Similar effects (including magic numbers) have been observed for alkali metal chlorides, ACl (A = Li^+, Na^+, K^+, Rb^+, Cs^+) as well as sodium salts NaB (B = I^-, $HCOO^-$, CH_3COO^-, NO_2^-, NO_3^-).[322]

The zwitterionic form of arginine in the gas phase continues to attract attention. Rak *et al.* have have used high level *ab initio* and DFT calculations to show that the five lowest energy structures of neutral arginine are all non-zwitterionic in nature and are clustered within a narrow energy range of 2.3 kcal mol^{-1}.[323] The lowest energy zwitterion structure is 4 kcal mol^{-1} higher in energy than the lowest energy non-zwitterion structure. It has been established that there are several ways of stabilizing a zwitterionic structure relative to its neutral structure, including: (i) binding of an electron; (ii) binding of another ion (to form a triple ion or salt bridge); (iii) hydration; and (iv) complexation to other species (*e.g.* formation of homo oligomers).

The effect of binding an electron has been demonstrated for arginine, where the zwitterionic form becomes more stable when bound to ('solvated by') an electron.[324]

Hoyau *et al.* have used *ab initio* calculations to evaluate the effect of binding another ion by studying the interactions between glycine and 15 atomic metal cations and dications.[325] In several cases, metal ion attachment results in a switch from the neutral form (the most stable form of gaseous glycine) to the zwitterionic form (the most stable form of glycine in solution). This effect mainly occurs with doubly charged cations. Metal ion properties such as charge, size, electron affinity and polarizability were invoked to explain these results.

Williams' group has used experiment and theory to examine the effect of metal ion and water coordination on the gas phase structure of valine.[326,327] Experiment and theory both suggest that the structure of the hydrated valine–lithium complex, $[Val + Li]^+(H_2O)_n$, changes as the degree of hydration increases. For complexes with one or two water molecules, the lithium is coordinated between the nitrogen and carbonyl oxygen of the non-zwitterionic form valine, and water molecules interact solely with the metal ion. In contrast, addition of a third water molecule changes the structure of the Val.Li^+ cluster significantly. The metal ion coordinates to the C-terminal end of the zwitterionic form of valine, and to two of the water molecules. The third water molecule interacts directly with valine *via* a hydrogen bond to the protonated N-terminus. This stabilizes the zwitterionic form of valine over the non-zwitterionic form.

The effect on the structure of amino acids of complexation of other species has been investigated by studying the salt bridge stabilization of charged zwitterionic

arginine aggregates in the gas phase.[328] Experiments carried out in a quadrupole ion trap provide evidence for the stability of arginine in the zwitterionic state. The protonated guanidinium group of one arginine interacts strongly with the carboxylate of another to form stable non-covalent complexes that are coordinated to either a cation or anion. Clusters of arginine with arginine, sodium, potassium, lithium, magnesium, chloride, fluoride, bromide, iodide and nitrate are observed. Cyclic trimers of arginine capped with either Cl^- or NO_3^- were found to possess exceptional stability.

Friess and Zenobi have exploited the stabilization induced by the protonated group of arginine to 'titrate' arginine residues in proteins using naphthalenesulfonic acid and related sulfonates in conjunction with matrix assisted laser desorption ionization (MALDI) MS analysis.[329] The data show that the number of complex adducts found equals the number of accessible arginine sites on the surface of folded peptides and proteins, plus the N-terminus. Buried arginine residues with hindered access, as well as Lys and His, are not complexed.

While salt bridges are known to play a role in some of the fragmentation reactions of protonated peptides, recent publications on the fragmentation reactions of deprotonated oligodeoxynucleotides suggest that salt bridges may also play a role in these systems.[330,331] Given the high acidity of the phosphate moiety, and the high basicity of nucleobase sites, this seems a reasonable proposition. It will be interesting to see if future experiments and theory provide support for this proposal.

C Molecular and chiral recognition in the gas phase

Molecular recognition and methods for determining enantiomeric excesses *via* chiral recognition have been studied in solution for some time. Recent efforts have focused on examining these processes in the gas phase, and progress has been reviewed.[53,54] Apart from the interest in fundamental reactivity in the absence of solvent and counter ions, an important aim is the development of mass spectrometry based methods to determine enantiomeric excesses on small amounts of sample (such as those formed in combinatorial libraries).

Nicoll and Dearden have examined the competition between self-exchange and complex formation for gas phase crown ether–alkali cation complexes, LM^+ (L = triglyme, 12-crown-4, 15-crown-5, 18-crown-6, and 21-crown-7; M = Li, Na, K, Rb, Cs).[332] For a given ligand, self-exchange rates generally decrease with increasing metal size, while complex formation ('sandwich complex') rates show a strong dependence on the relative sizes of metal cations and ligand cavities.

Julian and Beauchamp have used ESI-MS to examine molecular recognition between 18-crown-6 (18C6) and various functional groups present in amino acids, peptides and proteins.[333] Complexation of lysine with 18C6 represents a special case in which the 18C6 attaches to the N-terminus of lysine, with the complex deriving stability from the resulting salt-bridge structure. For peptides, 18C6 forms a stable supramolecular adduct with lysine by way of specific hydrogen bonding with the primary protonated amine on the side chain. However, competitive binding of 18C6 by other basic sites such as the N-terminus, histidine and arginine limits the utility of this technique for the molecular recognition of lysine. Nonetheless, adducts of 18C6 with proteins such as cytochrome-c and bovine pancreatic trypsin inhibitor reveal

structural information relevant to the accessibility of potential binding sites. Finally, the primary charge state and ion abundance of the analyte increases upon adduct formation with 18C6. This may be caused by a combination of increased surface activity of the peptide and inhibition of deprotonation during the ion desolvation process.

Host–guest formation has also been examined for more complex hosts using a combination of ESI-MS and theoretical calculations.[334,335] A particularly interesting system is decamethylcucurbit[5]uril, a 'pumpkin shaped' cyclic glyoluril polymer, which is known to trap molecules *via* the formation of an inclusion complex in the condensed phase. Hosts are trapped when cations of the right size form 'lids' by interacting with the rims of the cyclic glyoluril polymer. Kellersberger *et al.* have examined the role of these lids in trapping small guest molecules in the gas phase using ESI-MS.[335] Electrospray from various solutions (MeOH, MeCN, EtOH) provides evidence for small molecules (*e.g.* O_2, N_2, MeOH and MeCN but not EtOH) being trapped by two NH_4^+ lids.

A number of papers in 2001 have focused on the formation of protonated serine 'magic number' clusters.[336–339] Cooks *et al.* identified a series of higher-order clusters (metaclusters) corresponding to $[(Ser_8 + H)_n]^{n+}$ ($n = 1, 2, 3$) using ESI-MS.[336] A 'magic number' effect favouring formation of the protonated octamer over its homologues, as well as a strong preference for octamer formation from homochiral serine molecules, was observed. CID experiments suggest that the protonated octamer is composed of four hydrogen-bonded dimers which are stabilized by extensive hydrogen bonding. DFT calculations suggest a hydrogen-bonded drum-shaped structure of the octamer in which the serine molecules are in the non-zwitterionic forms. Calculations also suggest that the protonated homochiral octamer is energetically stabilized relative to its possible fragments (*e.g.* dimer plus protonated hexamer, *etc.*). Related $[(Ser_8 + Na)_n]^{n+}$ metaclusters ($n \geq 2$) were also generated by ESI, and their unique fused structures (hydrogen-bonded through the sticky ends of the drum-shaped octameric units) were examined using tandem mass spectrometry experiments and molecular mechanics calculations.[337] Hodyss *et al.* have also observed the same pronounced preference for homochirality in the protonated octamer of serine.[338] Based on the results of semiempirical calculations, Hodyss *et al.* suggested alternative stuctures for the octamer involving the zwitterionic form of serine forming an array of salt bridge interactions. Counterman and Clemmer have clarified the structure of the serine octamer through ion mobility measurements and molecular modelling simulations.[339] The measured cross section for the $[Ser_8 + H]^+$ ion is in close agreement with a value predicted from molecular modelling calculations based on tightly packed distorted block geometries comprised of zwitterionic amino acid units.[339]

A number of studies in 2001 have used mass spectrometry to study chiral recognition in the gas phase. These studies can be classified into three distinct methodologies: (i) use of gas phase ion–molecule ligand switching reactions of the analyte complexed to a host such as a cyclodextrin[340,341] (which appears to be more useful than thermal dissociation experiments[342]); (ii) use of the kinetic method in which CID is carried out on a preformed complex between a metal ion (M), the analyte (A) and typically two ancillary ligands (lig), $[M(A)(ref)]^+$;[343–348] and (iii) formation of jet-cooled diastereomeric complexes of two molecules with suitable chromophores, which are ionized by one-color resonant two-photon absorption and fragmentation patterns analysed

by time-of-flight mass spectrometry.[349–351] These three techniques have been successfully applied to discriminate chiral compounds ranging from simple amines and alcohols through to pharmaceuticals, amino acids (including phosphoserine) and peptides.

9 Bioorganic chemistry in the gas phase

The rapid growth of biological mass spectrometry has fuelled interest in fundamental studies in gas phase bioorganic and biophysical chemistry. Some studies focusing on the gas phase thermochemistry of gas phase bioorganic species have been discussed in Section 7, while aspects associated with zwitterions, salt bridges, molecular and chiral recognition were described in Section 8. The following topics are covered in this Section: (A) gas phase H/D exchange reactions and other ion–molecule reactions; (B) fragmentation mechanisms of protonated and deprotonated biomolecules; (C) conformational studies; (D) drug–DNA and related interactions. Due to the volume of studies in these areas, Sections 9B and 9D are not intended as comprehensive reviews. Various topics have been reviewed in 2001.[54,55]

A Gas phase ion–molecule, ion–electron and ion–ion reactions

H/D exchange reactions of biomolecules continue to be actively pursued. CH_3OD and D_2O react with protonated diglycine (GlyGly) *via* three fast, one moderate and one slow H/D exchange.[352] Based on comparisons with selectively methylated homologues (GlySar, GlyGly-OMe and GlySAr-OMe), these exchanges were identified as occurring at the N-terminal ammonium, amide hydrogen and carboxyl hydrogens, respectively. H/D exchange reactions of protonated peptides with reagents such as CH_3OD and ND_3 have also been studied.[353,354] On the short timescale of these experiments the following observations were made: (i) reaction of doubly protonated bradykinin with ND_3 results in three fast H/D exchanges and one slow exchange, while exchanges with CH_3OD are nearly 2 orders of magnitude slower; (ii) the more efficient exchange of doubly protonated des-Arg^9-bradykinin with ND_3 is accompanied by formation of collisionally stabilized $[M + 2H + ND_3]^{2+}$ complexes; and (iii) protonated leucine enkephalin undergoes four fast H/D exchanges and one slow exchange with ND_3 but is unreactive towards CH_3OD.[355] Using CID to produce b and y sequence ions provides information about the sites of H/D exchange. Doubly protonated bradykinin, which adopts a tightly folded structure in the gas phase, only undergoes H/D exchange with ND_3 at the protonated N-terminus amine group, with no exchange of the amide hydrogens. Additional H/D exchanges observed for doubly protonated des-Arg^9-bradykinin are due to complexation of its less compact structure *via* hydrogen-bonded intermediates that promote H/D exchange of amide hydrogens.

Solouki *et al.* have examined the effect of alkali metal cations on the rate and extent of H/D exchange in the simple tripeptide Arg-Gly-Asp.[355] The H/D exchange behaviour of $[M+Cat]^+$ with ND_3 differs from that of $[M + 2Cat\text{-}H]^+$ (Cat = H, Na, K, Ca). For $[M + Cat]^+$ the rates follow the order H > Cs > K > Na, while for $[M + 2Cat\text{-}H]^+$ they follow the order H > Na > K > Cs. These suggested changes in

the H/D exchange behaviour occur due to the peptide conformation being altered by both the number and type of complexing alkali metal ions.

The H/D exchange behaviour of protonated and deprotonated mononucleotides has been examined *via* FT-ICR MS.[356,357] ND_3 was found to be a more effective exchange reagent than D_2O and D_2S for protonated (deoxy)nucleoside-5′- and -3′-monophosphates (mononucleotides).[356] Most mononucleotides were observed to fully exchange their labile hydrogen for deuterium with ND_3, with the exception of deoxycytidine-3′-monophosphate, deoxyadenosine-5′-monophosphate, adenosine-5′-monophosphate and adenosine-3′-monophosphate. This attenuated exchange was rationalized by semiempirical calculations, which suggest the presence of hydrogen bonding in these protonated purine mononucleotides. H/D exchange rates differed between the deoxymononucleotides and the ribomononucleotides, indicating that the 2′-OH group plays an important role in the exchange process.

The conformational dependence of the gas phase hydrogen/deuterium (H/D) exchange of nucleotide-5-monophosphate anions with D_2S has been reported for species **118**–**121**.[357] Experiments suggest that no exchange occurs at the 2 position of the ribose sugar or the amino hydrogens on the nucleobase, but that **118** and **119** undergo exchange at the positions shown. Semiempirical molecular orbital calculations suggest that the phosphate anion site in **118** complexes with the exchange reagent to assists H/D exchange at the neighbouring 3′-OH site.

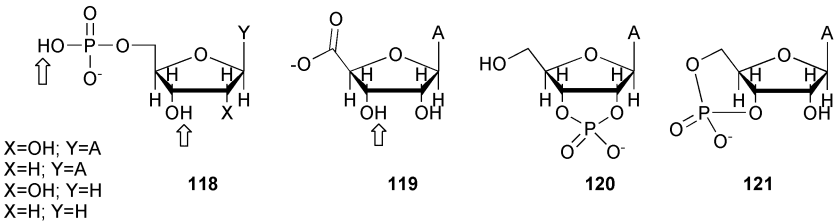

Reed and Kass have examined H/D exchange at non-labile sites under ESI conditions.[358] The conjugate bases of isophthalic acid [*m*-$C_6H_4(CO_2H)_2$], 2-oxoglutaric acid ($HO_2CCOCH_2CH_2CO_2H$), and 2-methylisophthalic acid [2-CH_3-1,3-$C_6H_4(CO_2H)_2$] undergo scrambling at 1, 2, and 3 carbon-centred hydrogens under a variety of conditions. Likewise, protonated 2-(*m*-methoxyphenyl)ethylamine [(*m*-$CH_3OC_6H_4$)CH_2-CH_2NH_2] undergoes up to 5 H/D exchanges upon gentle activation whereas the conjugate acid of 2-phenylethylamine ($C_6H_5CH_2CH_2NH_2$) requires the presence of ammonia-d_3 in order to undergo up to 8 H/D exchanges. This study suggests that the electrospray process can result in extensive movement of deuterium to carbon centres, and suggests caution is required in the interpretation of H/D exchange experiments using mass spectrometry as the analytical tool.

Gronert and Huang[359] have reported on a remarkable reaction between deprotonated amino acids and the dimethyl sulfide complex of borane which occurs *via* addition of the borane followed by elimination of H_2 to form a cyclic species. *Ab initio* calculations reveal that the mechanism of this reaction proceeds *via* initial addition to the neutral amino group to give a salt bridge structure (Scheme 15, path B) rather than addition to the deprotonated carboxylate position (Scheme 15, path A).

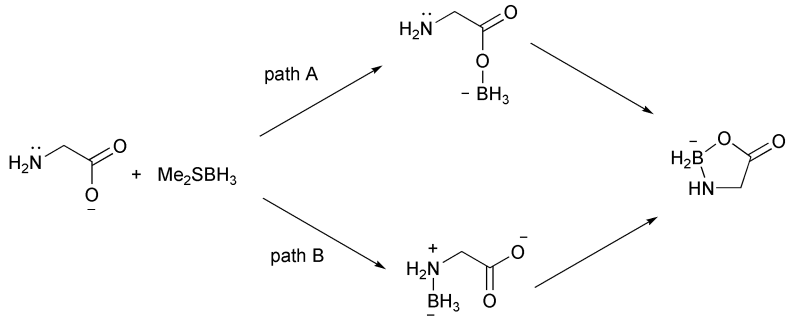

Scheme 15

Acylium ions RCO^+ [R = CH_3, CD_3, C_6H_5, C_6F_5, $(CH_3)_2N$], react with neutral alanylglycine in the gas phase *via* the formation of energized $[M + RCO]^+$ adduct ions **122** that fragment to yield b- and y-type sequence ions, including a modified b_1 ion.[360] Comparisons with fragmentation reactions of authentic *N*-acylated alanylglycine derivatives in conjuction with *ab initio* molecular orbital calculations indicate that gas phase derivatization of the peptide occurs at the N-terminal amine. The tetrapeptide valine-alanine-alanine-phenylalanine also reacts with the benzoyl cation to form similar types of product ions. The mechanism proposed for the formation of modified b_1 ions in the gas phase (Scheme 16) involves intramolecular proton transfer to form **123** followed by a neighbouring group process. This process has analogies with the ketalization reaction [eqn. (42)] as well as derivatization and N-terminal cleavage reactions employed in condensed-phase Edman degradation.

Two studies have examined the complexation of water to ions derived from biomolecules.[361,362] Previous reports have shown that ion–molecule reactions between small ligands (*e.g.* water, methanol) and metal complexes can be used to "titrate" the number of vacant coordination sites at the metal centre. Reactions of the $[M + Ag]^+$ ions of simple amino acids with background water and methanol (present from the electrospray solvent) provide information about the binding of the amino acid to the silver ions.[361] While $[M + Ag]^+$ ions of simple amino acids with no reactive side chains (*e.g.* alanine, valine, *tert*-leucine) do react with water or methanol to form adduct ions, those of phenylalanine, tyrosine and tryptophan undergo no reaction. These results suggest that the aromatic side chains can coordinate to the silver ion, and are supported by theoretical calculations. This is consistent with the coordination of metal ions to phenylalanine discussed in Section 7C.[267] Ion-mobility measurements have been used to measure the binding energies of a water molecule to the doubly protonated peptides bradykinin, angiotensin II and LHRH. Binding energies fall in the range -3.5 to -2.5 kcal mol^{-1}.[362] In contrast, the corresponding binding energies for the singly protonated ions are > -0.5 kcal mol^{-1} for angiotensin II and LHRH, and -2.6 kcal mol^{-1} for bradykinin. The stronger bonding of H_2O to the $[M + H]^+$ ion of bradykinin may be due to the presence of a salt bridge structure.

The chemistry that can occur within gas phase clusters of amino acids and other biologically relevant species is important in processes such as matrix assisted laser desorption ionization (MALDI). Grotemeyer and co-workers have continued their studies on the formation and ionization of clusters of several aromatic carboxylic

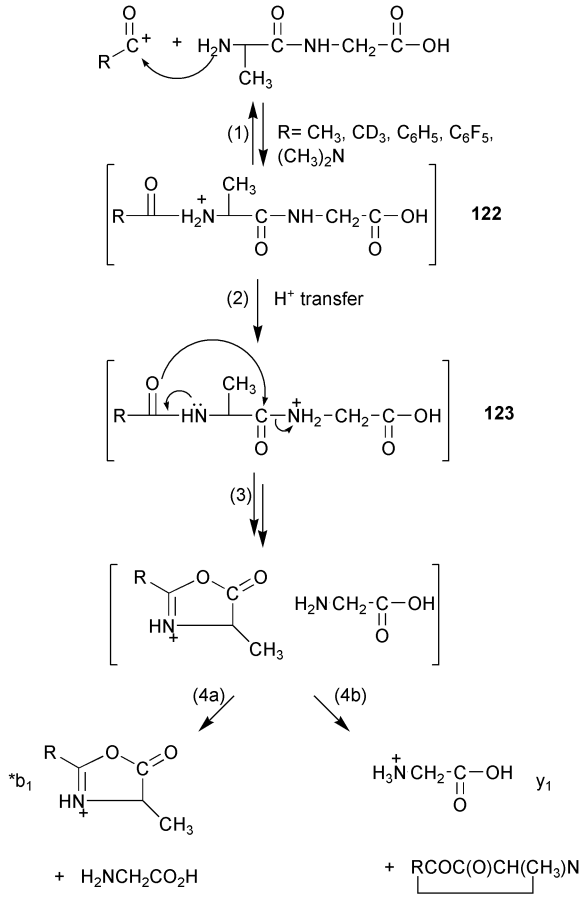

Scheme 16

acids (ferulic acid, vanillic acid, sinapinic acid, and 3,4-dihydroxybenzoic acid) *via* laser desorption into a supersonic beam followed by multiphoton ionization-time-of-flight mass spectrometry.[363] Homogenous and heterogeneous clusters with small amino acids have been studied. Under femtosecond ionization, both heterogeneous cluster ions as well as protonated amino acids were detected in the mass spectra. Since direct ionization of the free amino acids is not possible under these ionization conditions (they lack an adequate chromophore), these protonated amino acids are formed *via* an intracluster proton transfer.

The development on experimental techniques such as laser-induced acoustic desorption has renewed interest in the gas phase ion–molecule reactions of odd-electron biologically relevant species. The gas phase ion–molecule reactions of the radical cations of the nucleobases cytosine and adenine have been compared using FT-ICR mass spectrometry.[364] The cytosine radical cation undergoes facile hydrogen atom abstraction reactions with a variety of neutral reagents, even when electron

transfer reactions were expected to dominate. In contrast, the adenine radical cation only undergoes slow hydrogen atom abstraction in most of the cases studied. An ionic curve-crossing model was used to rationalize these results, and the thermodynamic and molecular properties of a radical cation that are favourable for efficient hydrogen atom abstraction were described. The competition between electron transfer and proton transfer within radical-cation clusters of guanosine and deoxyguanosine with substituted naphthalenes and sinapinic acid has been examined *via* tandem mass spectrometry.[365] The nucleobase guanine was much more easily oxidized when it is linked to a ribose moiety. Comparisons with migration of radical sites within stacking bases which causes DNA damage through depurination processes were made.

Aside from reactions with neutrals, reactions of biologically relevant ions with electrons or ions of opposite polarity have also been investigated. Reactions with electrons form the basis of the electron capture dissociation (ECD) technique. For multiply protonated proteins, electron capture results in highly energized radical cations (which can be regarded as $H^{\bullet}$ atom adducts), which fragment quite differently to their even-electron counterpart. This novel technique has been reviewed[366] and has recently been used to examine kinetic intermediates in the folding of gas phase protein ions.[367] Other types of radical cations of biomolecules can be formed by stripping an electron from protonated species through high energy collisions with O_2.[368,369] This technique has been used to study the formation of gas phase radical dications of protonated amino acids in a "microsolution" of water or acetonitrile. Reactivity towards the solvent[368] as well as electron loss from multiply protonated ions of the protein lysozyme[369] have been studied using this technique. Protonated amino acids, which yield radical dications under these conditions are Phe, His, Met, Tyr and Trp. When solvated by water or acetonitrile, $[M + H + S]^{2+\bullet}$ ions ($S = H_2O$, CH_3CN) are formed for Arg, His, Met, Tyr and Trp. The stability of the hydrogen-deficient amino acid $[M + H]^{2+\bullet}$ ion in these microsolvated complexes depends on the energetics of the electron transfer reaction [eqn. (57)], the hydrogen abstraction reaction [eqn. (58)] and the proton transfer reaction [eqn. (59)]. DFT calculations were used to investigate these three reactions in detail for M = Tyr, revealing that eqns. (57) and (58) are unfavourable, while eqn. (59) is favourable. However, a reverse Coulomb barrier exists for eqn. (59), which renders these complexes observable on the timescale of experiments (*i.e.* they have a life-time larger than 5 μs).

$$[M+H+S]^{2+\cdot} \longrightarrow [M+H]^{+} + S^{+\cdot} \quad (57)$$

$$[M+H+S]^{2+\cdot} \longrightarrow [M+2H]^{2+} + [S\text{-}H]^{\cdot} \quad (58)$$

$$[M+H+S]^{2+\cdot} \longrightarrow [M]^{+\cdot} + [S+H]^{+} \quad (59)$$

With regards to reactions with ions of opposite polarity, Payne and Glish have investigated the use of Fe^+ and $FeCO_2^-$ ions as gas phase cleavage reagents for oppositely charged peptide and protein ions.[370] Reaction products observed included charge exchange (lowering the charge states of the protein ions) and attachment (resulting in formation of a complex of the protein ion and the iron ion). It is unclear whether the formation of peptide and protein fragment ions observed is due to bond insertion by the iron ion, or due to the energetic reaction of oppositely charged species.

B Fragmentation mechanisms of protonated and deprotonated biomolecules

This Section focuses on studies that have used labelling experiments (deuterium and structural), multistage mass spectrometry, or theoretical calculations to investigate the role of charge site, charge mobility and structure in the fragmentation of biomolecules. Many studies have used a 'physical organic' approach to investigate fragmentation reactions of peptides (for sequence ion nomenclature, the reader is referred to ref. 371). MS/MS sequencing of tryptic peptides to yield structural information represents a 'bottom up' approach. However, methods are being developed which allow intact gas phase protein ions to be sequenced, representing a 'top down' approach to the analysis of protein structure.[372,373] At this early stage, it appears that some of the types of cleavages observed for peptides may also occur for proteins, suggesting similar mechanisms of fragmentation.[373]

Paizs and co-workers have continued their theoretical studies on the role of the "mobile proton", *cis-trans* isomerization of protonated amide bonds and neighbouring group interactions in the fragmentation reactions of simple peptides and model compounds.[374–376] Their studies of the fragmentation reactions of protonated glycylglycine highlight the useful insights that theory can provide. The key sequence ions observed experimentally for this species are the a_1, b_2 and y_1 ions (the b_1 acylium ions of aliphatic amino acids are unstable). Theory reveals that the a_1 and and y_1 ions are formed *via* extrusion of CO from the amide protonated form (Scheme 17, path A), rather than *via* the neighbouring group pathway (Scheme 17, path B).[376] Water loss to

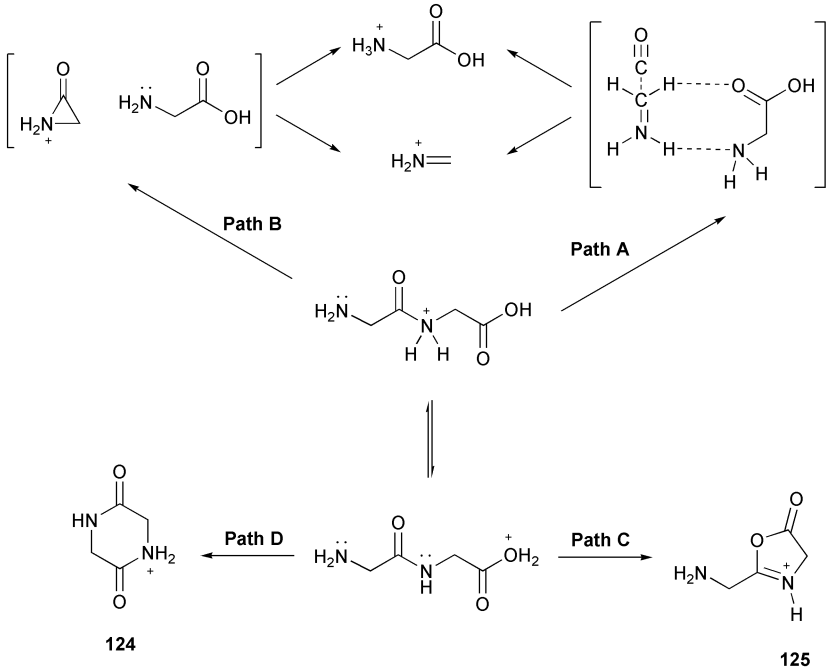

Scheme 17

form the b_2 ion proceeds *via* neighbouring group attack onto the OH protonated form. Of the two neighbouring group pathways available, attack by the amide to give an oxazolone species **125** (Scheme 17, path C) is favoured over attack by the N-terminal amine to give a diketopiperazine **124** (Scheme 17, path D).

Several studies have examined the modes of formation and structures of b_n ions. As noted previously, the acylium b_1 ions of structure **126** are unstable with respect to CO loss (in contrast, the acylium ion formed *via* loss of water from the side chain of glutamic acid is stable[377]). This suggests that formation of b_1 ions from species with nucleophilic side chains involves stabilization *via* ring formation through the side chain to yield structures of type **127**. Simple dipeptides and tripeptides with N-terminal histidine form such stabilized b_1 ions.[378] Theoretical calculations reveal that the N terminal lysine side chain of lysylglycine can promote peptide bond cleavage *via* formation of related side chain stabilized b_1 ions.[379]

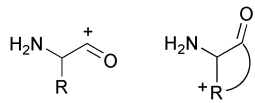

126 **127**

Farrugia *et al.* have used a combination of multistage mass spectrometry experiments and theoretical calculations to investigate the types of nucleophilic side chains that facilitate b_2 ion formation *via* structures related to **127** (as opposed to the conventional oxazolone type structure, *cf.* **125**, Scheme 17).[380] While the fragmentation reactions of b_2 ions of most systems involve loss of CO (consistent with an oxazolone structure), the b_2 ions of lysine and arginine do not fragment by loss of CO, suggesting an alternative cyclic structure related to **127**. *Ab initio* calculations suggest that cyclic structures involving the side chain are more stable than the oxazolone structures for arginine, histidine and lysine. In a related study, the role of histidine in facilitating b_2 ion formation in isomeric di- and tri-peptides of sequence GH, HG, GHG and HGG has been examined.[379] All b_2 ions give MS^3 spectra identical with the MS/MS spectrum of the protonated *cyclo*-glycylhistidine, consistent with a diketopiperazine structure (*cf.* **124**, Scheme 17). This suggests that the presence of a nucleophilic side chain alters the course of the reaction in Scheme 17 (*i.e.* path C is no longer favoured), and that the formation of the diketopiperazine structure is catalyzed *via* the histidine side chain. Side chains can also facilitate gas phase cleavage of adjacent peptide bonds to form higher b_n ions ($n > 2$). For example, Newton *et al.* have reported on a novel cleavage of the peptide bond between adjacent lysine-histidine residues in multiply protonated protein ions,[373] while Jonsson *et al.* have discovered a facile gas phase Gln-Gly cleavage with condensed phase analogies.[381]

Different fragmentation channels can often be accessed by changing the nature of the charge on the peptide. This can be achieved by fragmenting a metal cationized peptide ion, $[M + Cat]^+$, a deprotonated peptide ion, $[M - H]^-$, or a radical peptide ion, $[M]^{+\bullet}$, instead of the conventional protonated peptide ion, $[M + H]^+$. The gas phase chemistry of each of these alternatives is actively being examined.

Harrison has used deuterium labelling to examine the fragmentation reactions of deprotonated peptides and appears to have made the first analogy to an anionic

oxazolone-type neighbouring group pathway (*cf.* path C, Scheme 17).[382] Bowie and coworkers shown that the side chains of aspartic acid facilitate cleavage of the peptide backbone [eqn. (60)] *via* a different mechanism to glutamic acid [eqn. (61)].[383]

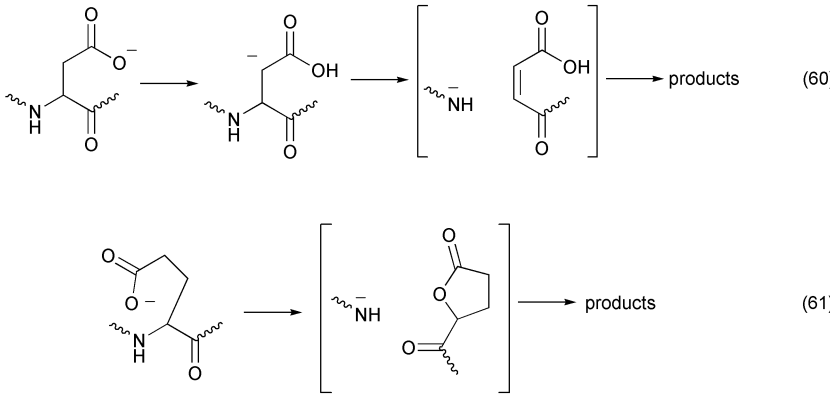

Metal cationized amino acids and peptides often fragment differently to their protonated counterparts. The deceptively simple losses of CO, CO_2 and $[H_2O + CO]$ from the zinc complex of glycinate $[Gly–H + Zn]^+$ formed *via* electrospray ionization are amongst the most complex gas phase reactions of glycine studied to date.[384,385] The main precursor to these $[Gly–H + Zn]^+$ ions is the solvent-bound $[Gly–H + Zn + MeOH]^+$ ion **128** (MeOH is the ESI solvent used). This precursor ion does not simply desolvate to yield **129**, but rather catalyzes the isomerization of the zinc bound glycine ligand to **130**, inducing fragmentation of the glycine framework to yield **131** (Scheme 18). Loss of methanol from this species produces an ion of identical stoichiometry to **129**, but with a vastly different structure. Theory and experiment reveal that the

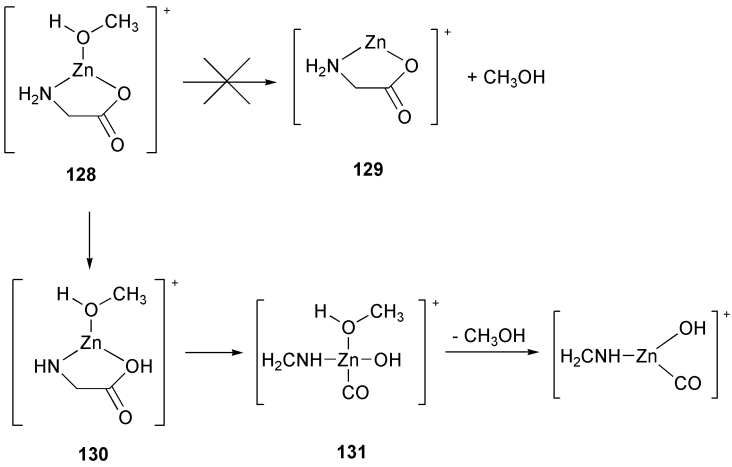

Scheme 18

$[M + Ni]^+$ ion of glycine also undergoes insertion into the C–C bond of glycine to form a complex related to **131**.[386]

Siu's group have continued their studies on the fragmentation reactions of the $[M + Ag]^+$ ions of amino acids and peptides. When M = proline, three main fragmentation channels are observed: (i) formation of a cyclic immonium ion *via* elimination of AgH; (ii) elimination of the combined elements of AgH and CO_2; and (iii) H_2 loss *via* a reductive–elimination reaction.[387] Deuterium labelling studies and DFT calculations provided insights into the mechanisms of these reactions. $[M + Ag]^+$ ions of peptides undergo similar fragmentation reactions to $[M + H]^+$ ions, forming $[b_n - H + Ag]^+$ and $[y_n - H + Ag]^+$ ions. DFT calculations on the $[b_2 - H + Ag]^+$ ions of gylcylglycine suggest oxazolone structures (*cf.* **125**), while MS/MS experiments on the $[y_n - H + Ag]^+$ ions indicated that these species are truncated peptides. In addition, $[b_n + OH + Ag]^+$ rearrangement ions are observed which involve extrusion of the [HNCHR + CO] from the C-terminal amino acid.[388] This same extrusion reaction dominates the fragmentation reactions of the $[M + Na]^+$ ions of peptides and provides a basis for a gas phase C-terminal sequencing strategy in which the $[b_n + OH + Na]^+$ ions are subjected to repeated stages of CID to "read out" the peptide sequence.[389]

Copper(II) complexes of peptides exhibit a diverse and interesting fragmentation behaviour in the gas phase. Fragmentation reactions are influenced by both the nature of the peptide and the ancillary ligand bound to copper.[390–392] If the ancillary ligand is a tridentate ligand such as diethylenetriamine (dien), the peptide complex $[Cu(II)(dien)M]^{2+\bullet}$ can fragment to form the radical cation of the peptide, $M^{+\bullet}$.[390] This exciting discovery allows the fragmentation behaviour of the $[M + H]^+$ and $M^{+\bullet}$ ions of peptides to be compared. The $M^{+\bullet}$ ions of peptides appear to be formed most readily *via* these copper complexes provided that M contains a tyrosyl or tryptophanyl residue and a basic residue, typically arginyl or lysyl. Fragmentation of $M^{+\bullet}$ ions is quite different to their $[M + H]^+$ counterparts, yielding prominent fragment ions due to elimination of the tyrosyl and tryptophanyl side chains with formation of glycyl radical residues on the remaining peptide ion. In contrast, when a peptide binds to a copper(II) centre with a bidentate ancillary ligand (*e.g.* 2,2′-bipyridine (bipy), $[Cu(bipy)M - H]^+$) ions typically undergo peptide fragmentation, with the charged fragements still binding to copper.[391] However, radical processes can still occur. For example, fragmentation of $[Cu(bipy)M - H - CO_2]^+$ (formed *via* decarboxylation $[Cu(bipy)M - H]^+$) allows distinction of the C-terminal leucine and isoleucine residues in isomeric tripeptides GGL [eqn. (62)] and GGI [eqn. (63)]. Toa *et al.* have used the kinetic method to quantitatively analyse isomeric mixtures of peptides (including those with Leu/Ile substitutions) by examining the fragmentation behaviour of $[Cu(ref)_2(A) - H]^+$ ions (A = the analyte, a mixture of isomeric peptides; ref = a reference compound).[392]

Radical cations or radical anions of peptides can also be accessed by allowing multiply protonated or deprotonated peptides to interact with an electron beam. As noted previously, this forms the basis of the electron capture dissociation (ECD) technique for positive ions. Electron detachment dissociation of peptide dianions has also recently been reported.[393] While complete mechanistic details of how species fragment under these conditions have not yet been established, the complementary fragmentation behaviour of ions subjected to ECD makes this a powerful technique

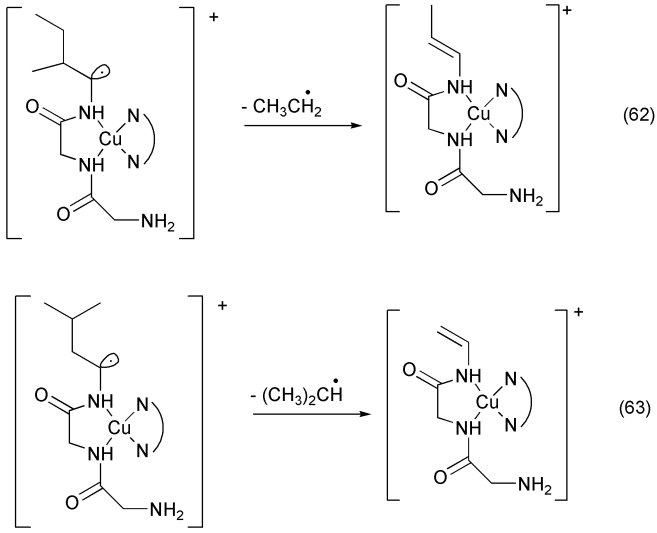

for analyis of post translational modifications (*e.g.* glycosylation [394] and phosphorylation [395]) in proteins not amenable to conventional MS/MS techniques.

Several studies have examined the fragmentation mechanisms of oligonucleotides.[330,331,396–398] Apart from deuterium labelling studies (which often hint at the role of salt bridges in the fragmentation of oligonucleotides), the role of the phosphate backbone moiety in fragmentation reactions of deprotonated oligonucleotides can be evaluated by replacing it with a methylphosphonate linkage.[396] Formation of $[a–B]^-$ ions requires transfer of an acidic proton from the 5′-phosphate to the departing base, and this is diminshed upon methylphosphonate substitution. When acidic protons are replaced by alkali and alkaline earth metal ions, a new mechanism involving 1,2-elimination operates for the formation of metallated $[a–B]^-$ ions.[397] This new fragmentation reaction has been applied to identify the sites of photomodification (to the *cis*,*syn*-cyclobutane pyrimidine dimer) in small oligonucleotides.[397,398]

C Conformational studies

Interplay between experiment and theory continues to play an important role in driving research into the conformations of small neutral amino acids and related systems, as well as the folding of larger multiply charged peptides, proteins and other biomolecules. Studies on the conformation of neutral molecules employ laser desorption methods to transfer neutrals to the gas phase where they can be investigated using a variety of spectroscopic techniques. This area has been the subject of two recent reviews.[45,46] Studies on the conformation of larger molecules (*e.g.* peptides, proteins, DNA) employ ion mobility measurements to determine the cross sections of ions (which are related to their ‘shape’) drifting through a buffer gas under the influence of an electric field.

Two independent studies have used experiment and theory to examine the conformations of neutral tryptophan in the gas phase. Compagnon *et al.* have used a matrix assisted laser desorption source and an electric beam deflection setup to measure the permanent electric dipole moment of tryptophan molecules cooled to 85 K.[399] The dominant conformation present in the molecular beam has a dipole moment that agrees with the lowest energy conformation found in calculations, **132**. This conformation exhibits $CO_2H \cdots NH_2$ hydrogen bonding and an interaction between the NH_2 group and the indole ring. The same conformation is the dominant conformation found by Snoek *et al.* using UV hole burning spectroscopy in conjunction with *ab initio* calculations.[400] This conformation is described as being stabilized by a "daisy chain" of hydrogen-bonded interactions. A different group has used a combination of theory and resonant ion-dip infrared spectroscopy to examine the conformational preferences of both tryptamine and 3-indolepropionic acid (simple model systems of tryptophan in which one of the functional groups is removed) in the absence[401] and in the presence of water molecules.[402] Seven conformations for tryptamine in the absence of water molecules were found, but only one conformer is observed for hydrated tryptamine$(H_2O)_n$ clusters (n = 1–3). Importantly, the most stable conformer changes upon solvation from **133** to bridged systems whereby the water molecules bridge the NH_2 group and the indole NH as shown for **134** and **135** (n = 2, 3 respectively). The first water molecule in the bridge from the NH_2 group also benefits from the interaction with the indole ring in structure **135**. In dramatic contrast to tryptamine, hydration of 3-indolepropionic acid does not change the conformational preference from the unhydrated species. These studies showcase the powerful interplay between modern spectroscopic experiments and theoretical calculations, and also highlight the

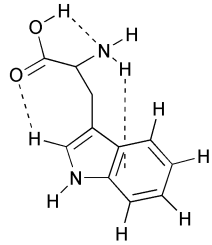

132

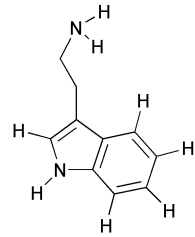

133

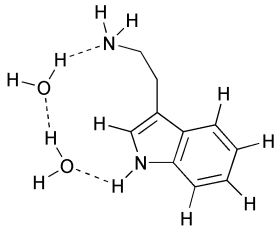

134

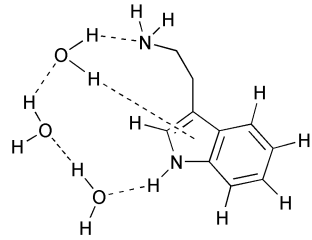

135

effect of interactions between amine groups, carboxylic acid groups, indole rings and solvent molecules in driving the conformational preference of tryptophan and other model systems.

Two groups have used laser induced fluorescence of the single tryptophan residue (Trp-59) in cytochrome c to examine the conformation of the protein within electrospray droplets.[403,404] Both induce protein denaturation chemically to investigate changes in detected fluorescence. In the first study, fluorescence was monitored as the concentration of denaturing alcohol was altered.[403] Comparison with analogous denaturation experiments in solution provide information about the relative protein conformations and differences between the bulk-solution and droplet environments. Both electrospray-plume and bulk-solution fluorescence measurements using solutions of low methanol concentration indicated the presence of folded protein structures, while at higher methanol concentration fluorescence measurements were consistent with the presence of partly denatured or unfolded conformations. A second study utilized changes in pH to induce protein denaturation.[404] While no fluorescence was observed for the electrospray of the solution at neutral pH, fluorescence due to unfolding was observed for acidified electrospray solutions.

Ion mobility measurements in conjunction with molecular dynamics simulations have been used to examine the gas phase conformations of ions derived from synthetic peptides,[405–409] naturally occuring peptides and proteins[410–412] and the dinucleotides dTG and dGT.[413]

Factors that govern helix formation in unsolvated peptides have been evaluated in a series of studies.[405–409] While $[Ac\text{-}K(AGG)_5 + H]^+$ exists as a globule (a compact, roughly spherical structure) over a wide temperature range, $[Ac\text{-}(AGG)_5K + H]^+$ forms both an α-helix and a globule at low temperature, with the α-helix unfolding as the temperature is raised.[405] Protonated polyalanine peptides form helices in the gas phase when their most basic protonation site (the N-terminus) is blocked by acetylation, while glycine analogues form random globules.[406] In a separate study, leucine residues were found to form helices more readily than alanine, but less readily than valine (*i.e.* an order of Val > Leu > Ala >> Gly).[407] Clemmer's group have compared conformations of $[Ala_n + 3H]^{3+}$ ions[408] with their $[Ala_n + 3Na]^{3+}$ counterparts.[409] For the protonated ions, two series of stable (non-interconverting) conformations were observed, consisting of a series of elongated structures (n = 18–39) and a series of more compact conformations (for n = 24–41). The more compact state becomes the dominant conformer for n > 32. Molecular modelling suggest the elongated ions have extended helical conformations. In contrast, the anhydrous sodiated polyalanine ions ($[Ala_n + 3Na]^{3+}$, n = 18–36) exist as highly extended conformations, with no evidence for the folded state observed for protonated polyalanines. Molecular dynamics simulations of $[Ala_n + 3Na]^{3+}$ ions indicate that extended structures are favoured with extensive helical regions being present. However, intramolecular charge solvation of the Na^+ cations disrupts the helical regions near the sites of cation attachment. Coupling an ion-trap to an an ion-mobility mass spectrometer has allowed changes in ion conformation over extended time periods (10–200 ms) in the ion trap to be examined. Such experiments have been carried out for the $[M + nH]^{n+}$ (where n = 7–10) ions of cytochrome c.[410]

Recent advances in high-field asymmetric waveform ion mobility spectrometry (FAIMS) have led to significant improvements in the application of this technology to

the study of peptide and protein conformers.[411,412] Gas phase conformers of the $[M + 2H]^{2+}$ ion of bradykin have been examined using a combination of FAIMS, H/D exchange, and energy-loss measurements.[411] When FAIMS data and H/D exchange data were analysed separately, the presence of only two conformers of the $[M + 2H]^{2+}$ ion of bradykinin could be detected. However, when FAIMS and H/D exchange are combined, at least four different conformers of the $[M + 2H]^{2+}$ ion of bradykinin are detected.

D Drug–DNA and other related interactions

ESI provides an attractive method of transferring intact solution phase non-covalent complexes into the gas phase. Unfortunately, the formation of non-covalent complexes by electrospray can also be the result of non-specific interactions of small molecules that have a high tendency to form hydrogen bonds. This suggests special precautions and additional experiments are required to identify the origin of non-covalent complexes sampled using electrospray. Lorenz *et al.* have used solution phase H/D exchange to determine the specificity of complexes of some common chemotherapy agents (paclitaxel, doxorubicin and etoposide).[414] By comparing the average number of exchanges for the monomer subunits to the average number of exchanges for the complex, one can distinguish if a specific complex is formed in solution. Gupta *et al*. have shown that factors influencing the observation of intact double-stranded DNA/drug complexes (*e.g.* cisplatin, daunomycin and distamycin) include: (i) careful choice of DNA sequences; (ii) use of a relatively high salt concentration; and (iii) use of low ESI desolvation temperatures.[415] Once complexes are transferred to the gas phase their gas phase stabilities can be evaluated. Gupta *et al.* have also shown that double stranded complexes with daunomycin and distamycin are more stable to strand separation in the gas phase than double stranded DNA alone, paralleling the solution phase behaviour of these systems.[415] Gabelica and De Pauw have also compared the solution-phase stability and gas phase kinetic stability of oligodeoxynucleotide duplexes, finding that both hydrogen bonding and base stacking interactions present in solution are maintained in the gas phase.[416] Indeed, breaking double-helix structure is a multistep process that in larger systems is often less likely than covalent bond cleavage of nucleobases. Another study has shown that double-helical RNA complexes can also be retained in the gas phase using microelectrospray mass spectrometry.[417]

The binding energies of the gas phase ions for non-covalent protein complexes of bovine pancreatic trypsin inhibitor and its target enzymes have been assessed using CID experiments.[418] Ordering differs from that observed for the solution phase complexes, suggesting that the solution structure of these complexes is not preserved in the gas phase.

McLuckey's group have examined the loss of charged *versus* neutral heme from the various charge states (+10 to +2) of gaseous holomyoglobin ions using CID.[419] Charged heme loss was dominant for +10 to +4 holomyoglobin ions, while neutral heme loss was dominant for charge states +3 and +2. For a given charge state, activation of holomyoglobin ions from a solution containing primarily ferromyoglobin yielded significantly more abundant neutral heme-loss products than

was observed for activation of ions from solutions containing primarily ferrimyoglobin. Given that the relative concentrations of the different oxidation states are apparently affected by redox chemistry within the nano-electrospray source, this suggests caution is required when examining metalloenzymes which are sensitive to redox changes. Finally, the precursor ions of a given charge state were shown to contain a mixture of two populations, with ferromyoglobin giving rise to neutral heme loss upon dissociation and ferrimyoglobin yielding charged heme. The same group have also examined dissociation reactions of gaseous ferro-, ferri- and apocytochrome c ions under similar conditions.[420] Electrochemical reduction of the iron bound in the heme group of cytochrome c was found to occur in the nano-electrospray capillary when the protein was sprayed from neutral water using a steel wire as the electrical contact. Again, dissociation reactions of gas phase cytochrome c ions are influenced by the oxidation state of the iron, with the oxidized Fe(III) form dissociating *via* sequence-specific amide bond cleavage, while the reduced Fe(II) form dissociates almost exclusively by loss of protonated heme. These studies reinforce the possibility of changes in metal oxidation state during the electrospray process.

Several studies have reported on the gas phase dissociation of various protein complexes.[421–423] Versluis and Heck have used CID to examine protein assemblies of hemoglobin, examining the gas phase disassembly of holo-hetero-dimers and holo-tetramers of bovine, porcine and human hemoglobin.[421] Gas phase dissociation patterns are in sharp contrast with the known solution phase behaviour, providing a further indication that caution is required when relating gas phase data to solution phase properties.

Felitsyn *et al.* have used black body infrared dissociation (BIRD) to examine the thermal decomposition of the B_5 pentamer of the Shiga-like toxin and its complexes with small oligosaccharide ligands.[422] These studies provide information on the Arrhenius parameters for dissociation as a function of the charge state of the complex. Dissociation of the protonated pentamer, $[B_5 + nH]^{n+}$ (n = 11–14), proceeds almost exclusively by the loss of a single subunit (B) with a disproportionately large fraction (30–50%) of the parent ion charge. The degree of charge enrichment of the leaving subunit increases with increasing parent ion charge state. A simple electrostatic model was used to provide an explanation for the magnitude of the Arrhenius parameters observed and the origin of the asymmetric dissociation behaviour of the complexes. In this model, charge enrichment leads to Coulombic repulsion-induced denaturation of the subunits and disruption of the intersubunit interactions.

In a separate study, dissociation of complexes between calmodulin, four calcium ions and a synthetic peptide derived from the phosphorylation site of smooth-muscle myosin light-chain kinase was studied using CID.[423] It was proposed that the gas phase dissociation of the calmodulin complex reflects the existence of gas phase salt bridges.

McLuckey's group has shown that gas phase ion–ion reactions between protein ions of opposite polarity leads to proton transfer from the $[M + nH]^{n+}$ ions to the deprotonated protein ions, as well as formation of protein–protein complexes.[424] It will be fascinating to see how the gas phase ion chemistry of these complexes compares with analogous complexes formed in solution.

References

1 R. A. J. O'Hair, *Annu. Rep. Prog. Chem., Sect. B*, 2001, **97**, 393.
2 J. O. Lay, *Mass Spectrom. Rev.*, 2001, **20**, 172.
3 C. Fenselau and P. A. Demirev, *Mass Spectrom. Rev.*, 2001, **20**, 157.
4 S. D. Richardson, *Chem. Rev.*, 2001, **101**, 211.
5 S. D. Hanton, *Chem. Rev.*, 2001, **101**, 527.
6 *Proteome Research: Mass Spectromerty*, ed. P. James, Springer-Verlag, Berlin, 2001.
7 R. Aebersold and D. R. Goodlett, *Chem. Rev.*, 2001, **101**, 269.
8 M. Mann, R. C. Hendrickson and A. Pandey, *Annu. Rev. Biochem.*, 2001, **70**, 437.
9 J. R. Engen and D. L. Smith, *Anal. Chem.*, 2001, **73**, 256A.
10 S. D. Maleknia and K. Downard, *Mass Spectrom. Rev.*, 2001, **20**, 388.
11 H. Hernandez and C. V. Robinson, *J. Biol. Chem.*, 2001, **276**, 46685.
12 R. C. Murphy, J. Fiedler and J. Hevko, *Chem. Rev.*, 2001, **101**, 479.
13 K. L. Busch, *Spectroscopy*, 2000, **15**, 30.
14 V.M. Bierbaum, *Chem. Rev.*, 2001, **101**, 209.
15 S. Gronert, *Chem. Rev.*, 2001, **101**, 329.
16 W.Y. Feng and S. Gronert, *Annu. Rep. Prog. Chem., Sect. B*, 1999, **95**, 349.
17 W.Y. Feng and S. Gronert, *Annu. Rep. Prog. Chem., Sect. B*, 2000, **96**, 445.
18 K. L. Busch, *Spectroscopy*, 2001, **16**, 28.
19 M. L. Vestal, *Chem. Rev.*, 2001, **101**, 361.
20 N. B. Cech and C. G. Enke, *Mass Spectrom. Rev.*, 2001, **20**, 362.
21 M. Vincenti, *Int. J. Mass Spectrom.*, 2001, **212**, 505.
22 S. A. McCluckey and J. M. Wells, *Chem. Rev.*, 2001, **101**, 571.
23 C. Hao and R. E. March, *Int. J. Mass Spectrom.*, 2001, **212**, 337.
24 K. B. Tomer, *Chem. Rev.*, 2001, **101**, 297.
25 *Current Practice of Gas Chromatography–Mass Spectrometry*, ed. W. M. A. Niessen, Marcel Dekker Inc., New York, 2001.
26 C. Lifshitz, *Chem. Soc. Rev.*, 2001, **30**, 186.
27 J. Laskin and C. Lifshitz, *J. Mass Spectrom.*, 2001, **36**, 459.
28 V. Grill, J. Shen, C. Evans and R. G. Cooks, *Rev. Sci. Instrum.*, 2001, **72**, 3149.
29 A. S. Danell and G. L. Glish, *Int. J. Mass. Spectrom.*, 2001, **212**, 219.
30 J. H. Bowie, *Int. J. Mass. Spectrom.*, 2001, **212**, 249.
31 R. N. Compton and N. I. Hammer, *Adv. Gas Phase Ion Chem.*, 2001, **4**, 257.
32 Z. Herman, *Int. J. Mass. Spectrom.*, 2001, **212**, 413.
33 A. A. Viggiano and S. Williams, *Adv. Gas Phase Ion Chem.*, 2001, **4**, 85.
34 R. J. Green and S. L. Anderson, *Int. Rev. Phys. Chem.*, 2001, **20**, 165.
35 W. Lindinger, R. Fall and T. G. Karl, *Adv. Gas Phase Ion Chem.*, 2001, **4**, 1.
36 F. M. Bickelhaupt, *Mass Spectrom. Rev.*, 2001, **20**, 347.
37 G. I. Yranzo, J. Elguero, R. Flammang and C. Wentrup, *Eur. J. Org. Chem.*, 2001, **12**, 2209.
38 T. H. Morton, *Adv. Gas Phase Ion Chem.*, 2001, **4**, 213.
39 K. M. Ervin, *Chem. Rev.*, 2001, **101**, 391.
40 J.-F. Gal, P-C. Maria and E. D. Raczynska, *J. Mass Spectrom.*, 2001, **36**, 699.
41 L.-S. Wang, *Comments Mod. Phys.*, 2001, **2**, D207.
42 H. Sato, *Chem. Rev.*, 2001, **101**, 2687.
43 P. D. Kleiber, *Adv. Met. Semiconduct. Clust.*, 2001, **5**, 267.
44 C. A. De Lange, *Adv. Chem. Phys.*, 2001, **117**, 1.
45 E. G. Robertson and J. P. Simons, *Phys. Chem. Chem. Phys.*, 2001, **3**, 1.
46 T. S. Zwier, *J. Phys. Chem. A*, 2001, **105**, 8827.
47 M. S. de Vries in *Atomic and Molecular Beams*, ed. R. Campargue, Springer-Verlag, Berlin, 2001, 805.
48 S. Iwata and T. Tsurusawa, *Adv. Met. Semiconduct. Clust.*, 2001, **5**, 39.
49 K. Fuke, K. Hashimoto and R. Takasu, *Adv. Met. Semiconduct. Clust.*, 2001, **5**, 1.
50 A. A. Shvartsburg, R. R. Hudgins, P. Dugourd and M. F. Jarrold, *Chem. Soc. Rev.*, 2001, **30**, 26.
51 D. V. Dearden, Y. Liang, J. B. Nicoll and K. A. Kellersberger, *J. Mass Spectrom.*, 2001, **36**, 989.
52 C. A. Schalley, *Mass Spectrom. Rev.*, 2001, **20**, 253.
53 C. B. Lebrilla, *Acc. Chem. Res.*, 2001, **34**, 653.
54 S. A. Hofstadler and R. H. Griffey, *Chem. Rev.*, 2001, **101**, 377.
55 J. L. Beck, M. L. Colgrave, S. F. Ralph and M. M. Sheil, *Mass Spectrom. Rev.*, 2001, **20**, 61.
56 M. Alcamí, O. Mó and M. Yáñez, *Mass Spectrom. Rev.*, 2001, **20**, 195.
57 R. C. Dougherty, *Mass Spectrom. Rev.*, 2001, **20**, 142.
58 *Mass Spectrometry in Drug Discovery*, ed. D.T. Rossi and M.W. Sinz, Marcel Dekker, New York, 2001.
59 R. A. J. O'Hair in *Mass Spectrometry in Drug Discovery*, ed. D.T. Rossi and M.W. Sinz, Marcel Dekker, New York, 2001, ch. 4, p. 85.

60 D. H. Chace, *Chem. Rev.*, 2001, **101**, 445.
61 D. B. Kassel, *Chem. Rev.*, 2001, **101**, 255.
62 L. A. Posey, *Adv. Met. Semiconduct. Clust.*, 2001, **5**, 145.
63 A. J. Stace, *Phys. Chem. Chem. Phys.*, 2001, **3**, 1935.
64 V. E. Bondybey, M. Beyer, U. Achatz, B. Fox and G. Niedner-Schatterburg, *Adv. Met. Semiconduct. Clust.*, 2001, **5**, 295.
65 K. Fisher, *Prog. Inorg. Chem.*, 2001, **50**, 343.
66 A. J. Stace, *Adv. Met. Semiconduct. Clust.*, 2001, **5**, 121.
67 P. B. Armentrout, *Ann. Rev. Phys. Chem.*, 2001, **52**, 423.
68 M. Peschke, A. T. Blades and P. Kebarle, *Adv. Met. Semiconduct. Clust.*, 2001, **5**, 77.
69 A.I. Boldyrev and L.-S. Wang, *J. Phys. Chem. A*, 2001, **105**, 10759.
70 V. E. Bondybey and M. K. Beyer, *J. Phys. Chem. A*, 2001, **105**, 951.
71 I. Kretzschmar, D. Schroder, H. Schwarz and P. B. Armentrout, *Adv. Met. Semiconduct. Clust.*, 2001, **5**, 347.
72 D. A. Plattner, *Int. J. Mass Spectrom.*, 2001, **207**, 125.
73 P. Ehrenfreund and S. B. Charnley, *Ann. Rev. Astron. Astrophys.*, 2000, **38**, 427.
74 R. Navarro-Gonzalez, S. I. Ramirez, J. G. De la Rosa, P. Coll and F. Raulin, *Adv. Space Res.*, 2001, **27**, 271.
75 Z. Tang, Z. J. Zhang, K. Narumi, Y. Xu, H. Naramoto, S. Nagai and K. Miyashita, *J. Appl. Phys.*, 2001, **89**, 1959.
76 P. G. Wenthold and X. Liu, *Int. J. Mass Spectrom.*, 2001, **207**, 69.
77 V. G. Anicich and M. J. McEwan, *Icarus*, 2001, **154**, 522.
78 Y. Tanaka and M. Tsuji, *Bull. Chem. Soc. Jpn*, 2001, **74**, 839.
79 M. Eckert-Maksic, Z. Glasovac, N. Novak Coumbassa and Z. B. Maksic, *J. Chem. Soc., Perkin Trans. 2*, 2001, 1091.
80 T. A. Kochina, D. V. Vrazhnov, E. N. Sinotova, M. Y. Katsup and B. F. Shchegolev, *Russ. J. Gen. Chem.*, 2001, **71**, 1557.
81 R. W. Holman, J. Plocica, L. Blair, D. Giblin and M. L. Gross, *J. Phys. Org. Chem.*, 2001, **14**, 17.
82 A. Filippi, N. A. Trout, P. Brunell, W. Adcock, T. S. Sorensen and M. Speranza, *J. Am. Chem. Soc.*, 2001, **123**, 6396.
83 E. Marotta and C. Paradisi, *J. Mass Spectrom.*, 2001, **36**, 1195.
84 R. Flammang, Y. Van Haverbeke, P. Gerbaux and M. T. Nguyen, *Tetrahedron Lett.*, 2001, **42**, 669.
85 C. Q. Jiao, B. Ganguly, C. A. DeJoseph Jr and A. Garscadden, *Int. J. Mass Spectrom.*, 2001, **208**, 127.
86 L. A. B. Moraes, M. A. Mendes, R. Sparrapan and M. N. Eberlin, *J. Am. Soc. Mass Spectrom.*, 2001, **12**, 14.
87 H.-F. Wu, L.-W. Chen and C.-H. Chen, *Rapid Commun. Mass Spectrom.*, 2001, **15**, 1977.
88 V. Gabelica, D. Lemaire, O. Laprévote and E. De Pauw, *Int. J. Mass Spectrom.*, 2001, **210/211**, 113.
89 J. Chen, Y. Jiang, H. Fu, Y. Chen, C.-M. Cheng and Y.-F. Zhao, *Rapid Commun. Mass Spectrom.*, 2001, **15**, 1489.
90 T. A. Kochina, E. O. Kalinin, E. N. Sinotova, I. S. Ignat'ev and A. A. Kinebas, *Russ. J. Gen. Chem.*, 2001, **71**, 934.
91 I. S. Ignatyev and T. Sundius, *J. Phys. Chem. A*, 2001, **105**, 4535.
92 Y.-P. Tu and J. L. Holmes, *J. Chem. Soc., Perkin Trans. 2*, 2001, 1378.
93 K.-M. Weitzel, G. K. Jarvis, M. Malow, T. Baer, Y. Song and C. Y. Ng, *Phys. Rev. Lett.*, 2001, **86**, 3526.
94 Y. Song, X.-M. Qian, K.-C. Lau and C. Y. Ng, *Chem. Phys. Lett.*, 2001, **347**, 51.
95 Y. Song, X.-M. Qian, K.-C. Lau, C. Y. Ng, J. Liu and W. J. Chen, *J. Chem. Phys.*, 2001, **115**, 4095.
96 L. Cooper, L. G. Shpinkova, E. E. Rennie, D. M. P. Holland and D. A. Shaw, *Int. J. Mass Spectrom.*, 2001, **207**, 223.
97 K. Takeuchi, T. Okazaki, T. Kitagawa, T. Ushino, K. Ueda, T. Endo and R. Notario, *J. Org. Chem.*, 2001, **66**, 2034.
98 B. Chiavarino, M. E. Crestoni, A. A. Fokin and S. Fornarini, *Chem. Eur. J.*, 2001, **7**, 2916.
99 M. Mormann and D. Kuck, *Int. J. Mass Spectrom.*, 2001, **210/211**, 531.
100 R. D. Bowen, S. J. Mandeville, M. A. Trikoupis and J. K. Terlouw, *Int. J. Mass Spectrom.*, 2001, **210/211**, 447.
101 R. D. Bowen, M. A. Trikoupis and J. K. Terlouw, *Eur. J. Mass Spectrom.*, 2001, **7**, 225.
102 S. Nakajima, T. Asakawa, O. Sekiguchi, S. Tajima and N. M. M. Nibbering, *Eur. J. Mass Spectrom.*, 2001, **7**, 47.
103 R. Chawla, A. Shukla and J. Futrell, *J. Phys. Chem. A*, 2001, **105**, 349.
104 T. Fiegele, C. Mair, P. Scheier, K. Becker and T. D. Märk, *Int. J. Mass Spectrom.*, 2001, **207**, 145.
105 V. G. Zaikin, R. S. Borisov and V. V. Luzhnov, *Eur. J. Mass Spectrom.*, 2001, **7**, 63.
106 K. Pihlaja, H. Agirbas and P. Valtamo, *J. Mass Spectrom.*, 2001, **36**, 754.
107 V. V. Ovcharenko, K. Pihlaja and D. Matosiuk, *Rapid Commun. Mass Spectrom.*, 2001, **15**, 2502.
108 L. Ceraulo, V. Di Stefano, M. Ferrugia, K. Ludányi, S. Segreto and K. Vékey, *Rapid Commun. Mass Spectrom.*, 2001, **15**, 433.

109 S. Prabhakar, P. Kar, S. P. Mirza, V. V. S. Lakshmi, K. Nagaiah and M. Vairamani, *Rapid Commun. Mass Spectrom.*, 2001, **15**, 2127.
110 Y. H. Kim, J. C. Choe and M. S. Kim, *J. Phys. Chem. A*, 2001, **105**, 5751.
111 S. Tajima, D. Watanabe, S. Nakajima, O. Sekiguchi and N. M. M. Nibbering, *Int. J. Mass Spectrom.*, 2001, **207**, 217.
112 H. T. Le, R. Flammang, P. Gerbaux, G. Bouchoux and M. T. Nguyen, *J. Phys. Chem. A*, 2001, **105**, 11582.
113 H.-T. Kim, J. Liu and S. L. Anderson, *J. Chem. Phys.*, 2001, **115**, 1274.
114 H.-T. Kim, J. Liu and S. L. Anderson, *J. Chem. Phys.*, 2001, **115**, 5843.
115 H.-T. Kim, J. Liu and S. L. Anderson, *J. Chem. Phys.*, 2001, **114**, 7838.
116 G. van der Rest, J. Chamot-Rooke, P. Mourgues, T. B. McMahon and H. E. Audier, *J. Am. Mass Spectrom.*, 2001, **12**, 938.
117 P. Mourgues, J. Chamot-Rooke, G. van der Rest, H. Nedev, H. E. Audier and T. B. McMahon, *Int. J. Mass Spectrom.*, 2001, **210/211**, 429.
118 M. A. Trikoupis, P. C. Burgers, P. J. A. Ruttink and J. K. Terlouw, *Int. J. Mass Spectrom.*, 2001, **210/211**, 489.
119 P. Mourgues, J. Chamot-Rooke, H. Nedev and H.-E. Audier, *J. Mass Spectrom.*, 2001, **36**, 102.
120 P. Gerbaux, M. Barbieux-Flammang, J. K. Terlouw and R. Flammang, *Int. J. Mass Spectrom.*, 2001, **206**, 91.
121 R. Flammang, M. Barbieux-Flammang, E. Gualano, P. Gerbaux, H. T. Le, M. T. Nguyen, F. Turecek and S. Vivekananda, *J. Phys. Chem. A*, 2001, **105**, 8579.
122 R. Flammang, M. Barbieux-Flammang, H. T. Le, P. Gerbaux, J. Elguero and M. T. Nguyen, *Chem. Phys. Lett.*, 2001, **347**, 465.
123 D. J. Lavorato, T. K. Dargel, W. Koch, G. A. McGibbon, H. Schwarz and J. K. Terlouw, *Int. J. Mass. Spectrom.*, 2001, **210/211**, 43.
124 A. Nixdorf and H.-F. Grützmacher, *Chem. Eur. J.*, 2001, **7**, 1248.
125 R. W. Holman, B. Atkins, D. Giblin, D. Rempel and M. Gross, *Int. J. Mass Spectrom.*, 2001, **210/211**, 569.
126 Y. B. Pithawalla, M. Meot-Ner, J. Gao, M. S. El Shall, V. I. Baranov and D. K. Bohme, *J. Phys. Chem. A*, 2001, **105**, 3908.
127 H. Hu and P. G. Wenthold, *J. Am. Soc. Mass Spectrom.*, 2001, **12**, 840.
128 A. T. Radosevich and O. Wiest, *J. Org. Chem.*, 2001, **66**, 5808.
129 A. T. Lebedev, I. V. Dianova, S. S. Mochalov, V. V. Lobodin, T. Y. Samguina, R. A. Gazzaeva and T. Blumenthal, *J. Am. Soc. Mass Spectrom.*, 2001, **12**, 956.
130 C. H. Kwon, M. S. Kim and J. C. Choe, *J. Am. Soc. Mass Spectrom.*, 2001, **12**, 1120.
131 S. Kato, G. E. Davico, H. S. Lee, C. H. DePuy and V. M. Bierbaum, *Int. J. Mass Spectrom.*, 2001, **210/211**, 223.
132 L. A. Angel and K. M. Ervin, *J. Phys. Chem. A*, 2001, **105**, 4042.
133 S. Gronert, L. M. Pratt and S. Mogali, *J. Am. Chem. Soc.*, 2001, **123**, 3081.
134 R. Gareyev, S. Kato and V. M. Bierbaum, *J. Am. Soc. Mass Spectrom.*, 2001, **12**, 139.
135 A. M. McAnoy, S. Dua, K. Rees and J. H. Bowie, *Int. J. Mass Spectrom.*, 2001, **210/211**, 557.
136 P. R. Tiller, C. Raab and C. E. C. A. Hop, *J. Mass Spectrom.*, 2001, **36**, 344.
137 T. D. Fridgen, J. D. Keller and T. B. McMahon, *J. Phys. Chem. A*, 2001, **105**, 3816.
138 R. A. Ochran and P. M. Mayer, *Eur. J. Mass Sepctrom.*, 2001, **7**, 267.
139 J. A. D. McCormack and P. M. Mayer, *Int. J. Mass Spectrom.*, 2001, **207**, 183.
140 T. D. Fridgen and T. B. McMahon, *J. Phys. Chem. A*, 2001, **105**, 1011.
141 T. D. Fridgen and T. B. McMahon, *J. Am. Chem. Soc.*, 2001, **123**, 3980.
142 L. Bache-Andreassen and E. Uggerud, *Int. J. Mass Spectrom.*, 2001, **210/211**, 459.
143 X. Zheng, W. A. Tao and R. G. Cooks, *J. Am. Soc. Mass Spectrom.*, 2001, **12**, 948.
144 J. S. Brodbelt, J. Isbell, J. M. Goodman, H. V. Secor and J. I. Seeman, *Tetrahedron Lett.*, 2001, **42**, 6949.
145 A. Filippi and M. Speranza, *J. Am. Chem. Soc.*, 2001, **123**, 6077.
146 A. Filippi, F. Gasparrini and M. Speranza, *J. Am. Chem. Soc.*, 2001, **123**, 2251.
147 C. Barckholtz, T. P. Snow and V. M. Bierbaum, *Astrophys. J.*, 2001, **547**, L171.
148 S. J. Blanksby, A. M. McAnoy, S. Dua and J. H. Bowie, *Mon. Not. R. Astron. Soc.*, 2001, **328**, 89.
149 M. Tulej, F. Güthe, M. V. Pachkov, K. Tikhomirov, R. Xu, M. Jungen and J. P. Maier, *Phys. Chem. Chem. Phys.*, 2001, **3**, 4674.
150 H.-Y. Wang, R.-B. Huang, H. Chen, M.-H. Lin and L.-S. Zheng, *J. Phys. Chem. A*, 2001, **105**, 4653.
151 G. Pascoli and H. Lavendy, *Int. J. Mass Spectrom.*, 2001, **206**, 153.
152 Z. Tang and J. J. BelBruno, *Int. J. Mass Spectrom.*, 2001, **208**, 7.
153 Z. Cao and S. D. Peyerimhoff, *Phys. Chem. Chem. Phys.*, 2001, **3**, 1403.
154 G. A. Rechtsteiner, O. Hampe and M. F. Jarrold, *J. Phys. Chem. B*, 2001, **105**, 4188.
155 C. O. Kappe, D. Kvaskoff, D. W. J. Moloney, R. Flammang and C. Wentrup, *J. Org. Chem.*, 2001, **66**, 1827.
156 C. T. Pedersen, E. Fanghanel and R. Flammang, *J. Chem. Soc., Perkin Trans. 2*, 2001, 356.
157 C. T. Pedersen, M. W. Wong and R. Flammang, *J. Chem. Soc., Perkin Trans. 2*, 2001, 2047.
158 Y. Keheyan, *Chem. Phys. Lett.*, 2001, **340**, 405.
159 V. Le Page, T. P. Snow and V. M. Bierbaum, *Astrophys. J., Supp. Ser.*, 2001, **132**, 233.
160 M. J. Dibben, D. Kage, J. Szczepanski, J. R. Eyler and M. Vala, *J. Phys. Chem. A*, 2001, **105**, 6024.

161 J. Szczepanski, M. J. Dibben, W. Pearson, J. R. Eyler and M. Vala, *J. Phys. Chem. A*, 2001, **105**, 9388.
162 D. Schroder, J. Loos, H. Schwarz, R. Thissen, D. V. Preda, L. T. Scott, D. Caraiman, M. V. Frach and D. K. Bohme, *Helv. Chim. Acta*, 2001, **84**, 1625.
163 Y. V. Vasil'ev, R. R. Absalimov, S. K. Nasibullaev, A. S. Lobach and T. Drewello, *J. Phys. Chem A*, 2001, **105**, 661.
164 G. A. Grieves, J. W. Buchanan, J. E. Reddic and M. A. Duncan, *Int. J. Mass Spectrom.*, 2001, **204**, 223.
165 T. Peres, B. Cao, W. Cui, A. Khong, R. J. Cross Jr., M. Saunders and C. Lifshitz, *Int. J. Mass Spectrom.*, 2001, **210/211**, 241.
166 T. Sugai, M. Inakuma, R. Hudgins, P. Dugourd, J. L. Fye, M. F. Jarrold and H. Shinohara, *J. Am. Chem. Soc.*, 2001, **123**, 6427.
167 D. Caraiman, G. K. Koyanagi, L. T. Scott, D. V. Preda and D. K. Bohme, *J. Am. Chem. Soc.*, 2001, **123**, 8573.
168 B. Cao, T. Peres, R. J. Cross, Jr., M. Saunders and C. Lifshitz, *J. Phys. Chem. A*, 2001, **105**, 2142.
169 S. Peppe, S. Dua and S. J. H. Bowie, *J. Phys. Chem. A*, 2001, **105**, 10139.
170 S. Dua, S. Peppe and J. H. Bowie, *J. Chem. Soc., Perkin Trans. 2*, 2001, 2244.
171 S. Dua and J. H. Bowie, *J. Chem. Soc., Perkin Trans. 2*, 2001, 827.
172 M. Polásek and F. Turecek, *J. Phys. Chem. A*, 2001, **105**, 1371.
173 M. Polásek, F. Turecek, P. Gerbaux and R. Flammang, *J. Phys. Chem. A*, 2001, **105**, 995.
174 E. A. Syrstad and F. Turecek, *J. Phys. Chem. A*, 2001, **105**, 11144.
175 S. Vivekananda, J. K. Wolken and F. Turecek, *J. Phys. Chem. A*, 2001, **105**, 9130.
176 J. K. Wolken, E. A. Syrstad, S. Vivekananda and F. Turecek, *J. Am. Chem. Soc.*, 2001, **123**, 5804.
177 J. K. Wolken and F. Turecek, *J. Phys. Chem. A*, 2001, **105**, 8352.
178 J. Wu and C. Wesdemiotis, *J. Am. Soc. Mass Spectrom.*, 2001, **12**, 1229.
179 M. C. Hare, S. S. Marimanikkuppam and S. R. Kass, *Int. J. Mass Spectrom.*, 2001, **210/211**, 153.
180 A. M. Cardoso, L. E. Ramos and A. J. Ferrer-Correia, *Int. J. Mass Spectrom.*, 2001, **210/211**, 563.
181 E. A. Stemmler, E. Yoshida, Y. J. Pacheco, J. Brunton, E. Woodbury and T. Solouki, *J. Am. Soc. Mass Spectrom.*, 2001, **12**, 694.
182 E. A. Stemmler and C. Segovis, *J. Mass Spectrom.*, 2001, **36**, 685.
183 Y. Gimbert, R. Arnaud, E. de Hoffman and J. C. Tabet, *J. Phys. Chem. A*, 2001, **105**, 5221.
184 S. M. Schulze, N. Santella, J. J. Grabowski and J. K. Lee, *J. Org. Chem.*, 2001, **66**, 7247.
185 K. M. Broadus, S. Han and S. R. Kass, *J. Org. Chem.*, 2001, **66**, 99.
186 S. Dua and J. H. Bowie, *Rapid Commun. Mass Spectrom.*, 2001, **15**, 1304.
187 S. Dua, J. H. Bowie and J. M. Hevko, *Eur. J. Mass Spectrom.*, 2001, **7**, 7.
188 L. E. Ramírez-Arizmendi, L. Guler, J. J. Ferra Jr, K. K. Thoen and H. I. Kenttämaa, *Int. J. Mass Spectrom.*, 2001, **210/211**, 511.
189 J. L. Heidbrink, L. E. Ramírez-Arizmendi, K. K. Thoen, L. Guler and H. I. Kenttämaa, *J. Phys. Chem. A*, 2001, **105**, 7875.
190 S. E. Tichy, K. K. Thoen, J. M. Price, J. J. Ferra Jr, C. J. Petucci and H. I. Kenttämaa, *J. Org. Chem.*, 2001, **66**, 2726.
191 E. D. Nelson, A. Artau, J. M. Price, S. E. Tichy, L. Jing and H. I. Kenttämaa, *J. Phys. Chem. A*, 2001, **105**, 10155.
192 E. D. Nelson and H. I. Kenttämaa, *J. Am. Soc. Mass Spectrom.*, 2001, **12**, 258.
193 S. E. Tichy, B. T. Hill, J. L. Cambell and H. I. Kenttämaa, *J. Am. Chem. Soc.*, 2001, **123**, 7923.
194 E. C. Meurer, L. A. B. Moraes and M. N. Eberlin, *Int. J. Mass Spectrom.*, 2001, **212**, 445.
195 Z. Guan and J. M. Liesch, *J. Mass Spectrom.*, 2001, **36**, 264.
196 L. A. B. Moraes and M. N. Eberlin, *J. Am. Soc. Mass Spectrom.*, 2001, **12**, 150.
197 A. M. Seldes, N. D. D'Accorso, M. F. Souto, M. Martins Alho and C. G. Arabehety, *J. Mass Spectrom.*, 2001, **36**, 1069.
198 X. Zheng, W. A. Tao and R. G. Cooks, *J. Chem. Soc., Perkin Trans. 2*, 2001, 350.
199 M. G. M. D'Oca, L. A. B. Moraes, R. A. Pilli and M. N. Eberlin, *J. Org. Chem.*, 2001, **66**, 3854.
200 C. Canepa, A. Maranzana, L. Operti, R. Rabezzana and G. A. Vaglio, *Organometallics*, 2001, **20**, 4593.
201 P. Antoniotti, C. Canepa, A. Maranzana, L. Operti, R. Rabezzana, G. Tonachini and G. A. Vaglio, *Organometallics*, 2001, **20**, 382.
202 D. Leblanc, J. P. Denhez and H. E. Audier, *Eur. J. Mass Spectrom.*, 2001, **7**, 343.
203 E. V. Shchukin, T. A. Kochina, E. N. Sinotova and I. S. Ignat'ev, *Russ. J. Gen. Chem.*, 2001, **71**, 206.
204 L. A. B. Moraes and M. N. Eberlin, *Organometallics*, 2001, **20**, 4863.
205 E. C. Meurer and M. N. Eberlin, *Int. J. Mass Spectrom.*, 2001, **210/211**, 469.
206 D. B. Milligan, C. G. Freeman, R. G. A. R. Maclagan, M. J. McEwan, P. F. Wilson and V. G. Anicich, *J. Am. Soc. Mass Spectrom.*, 2001, **12**, 557.
207 G. Bouchoux, N. Choret, F. Berruyer-Penaud and R. Flammang, *J. Phys. Chem. A*, 2001, **105**, 9166.
208 A. B. Attygalle, S. Garcia-Rubio, J. Ta and J. Meinwald, *J. Chem. Soc., Perkin Trans 2*, 2001, 498.
209 H.-F. Grützmacher, D. Kirchhoff and H. Grützmacher, *Organometallics*, 2001, **20**, 3738.
210 D. Lesage, H. Virelizier, J. C. Tabet and C. K. Jankowski, *Rapid Commun. Mass Spectrom.*, 2001, **15**, 1947.
211 L. N. Heydorn, Y. Ling, G. De Oliveira, J. M. L. Martin, C. Lifshitz and J. K. Terlouw, *Z. Phys. Chem.*, 2001, **215**, 141.

212 M. Attinà, F. Cacace, A. Cartoni and M. Rosi, *J. Mass Spectrom.*, 2001, **36**, 392.
213 F. Cacace, M. Attinà, A. Cartoni and F. Pepi, *Chem. Phys. Lett.*, 2001, **339**, 71.
214 S. T. Arnold and A. A. Viggiano, *J. Phys. Chem. A*, 2001, **105**, 3527.
215 V. Catoire, C. Stépien, D. Labonnette, J.-C. Rayez, M.-T. Rayez and G. Poulet, *Phys. Chem. Chem. Phys.*, 2001, **3**, 193.
216 R. A. Kennedy and C. A. Mayhew, *Phys. Chem. Chem. Phys.*, 2001, **3**, 5511.
217 C. Atterbury, R. A. Kennedy, C. A. Mayhew and R. P. Tuckett, *Phys. Chem. Chem. Phys.*, 2001, **3**, 1949.
218 A. J. Midley, S. Williams and A. A. Viggiano, *J. Phys. Chem. A*, 2001, **105**, 1574.
219 K. Fukuzawa, T. Matsushita, K. Morokuma, D. J. Levandier, Y.-H. Chiu, R. A. Dressler, E. Murad, A. Midey, S. Williams and A. A. Viggiano, *J. Chem. Phys.*, 2001, **115**, 3184.
220 I. Dotan and A. A. Viggiano, *J. Chem. Phys.*, 2001, **114**, 6112.
221 S. Irle and K. Morokuma, *J. Chem. Phys.*, 2001, **114**, 6119.
222 J. E. Flad, M. A. Everest, J. C. Poutsma and R. N. Zare, *J. Chem. Phys.*, 2001, **115**, 124.
223 M. Michel, M. V. Korolkov, M. Malow, K. Brembs and K.-M. Weitzel, *Phys. Chem. Chem. Phys.*, 2001, **3**, 2253.
224 M. Malow, K. Brembs and K.-M. Weitzel, *Z. Phys. Chem.*, 2001, **215**, 737.
225 Å. M. Leere Øiestad, A. C. Peterson, V. Bakken, J. Vedde and E. Uggerud, *Angew. Chem., Int. Ed.*, 2001, **40**, 1305.
226 S. Bourcier, S. Bouchonnet and Y. Hoppilliard, *Int. J. Mass Spectrom.*, 2001, **210/211**, 59.
227 http://webbook.nist.gov/chemistry.
228 G. Bouchoux, D. Leblanc and M. Sablier, *Int. J. Mass Spectrom.*, 2001, **210/211**, 189.
229 K. M. Broadus and S. R. Kass, *J. Am. Chem. Soc.*, 2001, **123**, 4189.
230 K. M. Ervin, T. M. Ramond, G. E. Davico, R. L. Schwartz, S. M. Casey and W. C. Lineberger, *J. Phys. Chem. A*, 2001, **105**, 10822.
231 H. A. Lardin, R. R. Squires and P. G. Wenthold, *J. Mass Spectrom.*, 2001, **36**, 607.
232 S. J. Blanksby, T. M. Ramond, G. E. Davico, M. R. Nimlos, S. Kato, V. M. Bierbaum, W. C. Lineberger, G. B. Ellison and M. Okumura, *J. Am. Chem. Soc.*, 2001, **123**, 9585.
233 L. A. Hammad and P. G. Wenthold, *J. Am. Chem. Soc.*, 2001, **123**, 12311.
234 G. Bouchoux, J. Chamot-Rooke, D. Leblanc, P. Mourgues and M. Sablier, *CHEMPHYSCHEM*, 2001, 235.
235 F. Cesar Gozzo and M. N. Eberlin, *J. Mass Spectrom.*, 2001, **36**, 1140.
236 T. I. Williams, J. W. Denault and R. G. Cooks, *Int. J. Mass Spectrom.*, 2001, **210/211**, 133.
237 J. Cao and J. L. Holmes, *Eur. J. Mass Spectrom.*, 2001, **7**, 243.
238 S. P. Mirza, S. Prabhaker and M. Vairamani, *Rapid Commun. Mass Spectrom.*, 2001, **15**, 957.
239 J. Zhu and R. B. Cole, *J. Am. Soc. Mass Spectrom.*, 2001, **12**, 1193.
240 L. Di Donna, A. Napoli and G. Sindona, *Int. J. Mass Spectrom.*, 2001, **210/211**, 165.
241 N. P. Ewing, G. A. Pallante, X. Zhang and C. J. Cassady, *J. Mass Spectrom.*, 2001, **36**, 875.
242 M. Irie, K. Kikukawa, N. Shimizu and M. Mishima, *J. Chem. Soc., Perkin Trans. 2*, 2001, 923.
243 M. Schlosser, E. Marzi, F. Cottet, H. H. Büker and N. M. M. Nibbering, *Chem. Eur. J.*, 2001, **7**, 3511.
244 F. H. W. van Amerom, D. van Duijn, W. J. van der Hart and N. M. M. Nibbering, *J. Am. Soc. Mass Spectrom.*, 2001, **12**, 359.
245 G. Bouchoux, F. Caunan, D. Leblanc, M. T. Nguyen and J.-Y. Salpin, *CHEMPHYSCHEM*, 2001, 604.
246 P. R. Higgins, R. J. Hinde, D. T. Grimm, J. E. Bloor and J. E. Bartmess, *Int. J. Mass Spectrom.*, 2001, **210/211**, 231.
247 J.-F. Gal, M. Decouzon, P.-C. Maria, A. I. González, O. Mó, M. Yáñex, S. El Chaouch and J.-C. Guillemin, *J. Am. Chem. Soc.*, 2001, **123**, 6353.
248 J. M. Karty, Y. Wu and J. I. Brauman, *J. Am. Chem. Soc.*, 2001, **123**, 9800.
249 G. Bouchoux, N. Choret and F. Berruyer-Penaud, *J. Phys. Chem. A*, 2001, **105**, 3989.
250 C. F. Bernasconi and P. J. Wenzel, *J. Am. Chem. Soc.*, 2001, **123**, 7146.
251 C. F. Bernasconi and P. J. Wenzel, *J. Org. Chem.*, 2001, **66**, 968.
252 T. Marino, N. Russo, E. Tocci and M. Toscano, *Eur. J. Mass Spectrom.*, 2001, **7**, 301.
253 G. Bouchoux, F. Penaud-Berruyer and W. Bertrand, *Eur. J. Mass Spectrom.*, 2001, **7**, 351.
254 O. Exner and P. Carsky, *J. Am. Chem. Soc.*, 2001, **123**, 9564.
255 P. Pérez, *J. Phys. Chem. A*, 2001, **105**, 6182.
256 B. Bogdanov, H. J. S. Lee and T. B. McMahon, *Int. J. Mass Spectrom.*, 2001, **210/211**, 387.
257 K. Hiraoka, T. Mizuno, T. Iino, D. Eguchi and S. Yamabe, *J. Phys. Chem. A*, 2001, **105**, 4887.
258 K. Hiraoka, J. Katsuragawa, T. Sugiyama, T. Kojima and S. Yamabe, *J. Am. Soc. Mass Spectrom.*, 2001, **12**, 144.
259 A. H. Lawrence, P. Neudorfl and J. A. Stone, *Int. J. Mass Spectrom.*, 2001, **209**, 185.
260 D. H. Williamson, W. B. Knighton and E. P. Grimsrud, *Int. J. Mass Spectrom.*, 2001, **206**, 53.
261 Mustanir and M. Mishima, *J. Chem. Soc., Perkin Trans. 2*, 2001, 798.
262 S. Petrie, *J. Phys. Chem. A*, 2001, **105**, 9931.
263 J. C. Amicangelo and P. B. Armentrout, *Int. J. Mass Spectrom.*, 2001, **212**, 301.
264 A. B. Valina, R. Amunugama, H. Huang and M. T. Rodgers, *J. Phys. Chem. A*, 2001, **105**, 11057.
265 M. T. Rodgers, *J. Phys. Chem. A*, 2001, **105**, 2374.

266 M. T. Rodgers, *J. Phys. Chem. A*, 2001, **105**, 8145.
267 A. Gapeev and R. C. Dunbar, *J. Am. Chem. Soc.*, 2001, **123**, 8360.
268 R. Amunugama and M. T. Rodgers, *J. Phys. Chem. A*, 2001, **105**, 9883.
269 M. Satterfield and J. S. Brodbelt, *Inorg. Chem.*, 2001, **40**, 5393.
270 H. Koizymi, X.-G. Zhang and P. B. Armentrout, *J. Phys. Chem. A*, 2001, **105**, 2444.
271 H. Koizumi and P. B. Armentrout, *J. Am. Soc. Mass Spectrom.*, 2001, **12**, 480.
272 P.-H. Su, F.-W. Lin and C.-S. Yeh, *J. Phys. Chem. A*, 2001, **105**, 9643.
273 H.-F. Lee, F.-W. Lin and C.-S. Yeh, *J. Mass Spectrom.*, 2001, **36**, 493.
274 D. Schröder, K. Schroeter and H. Schwarz, *Int. J. Mass Spectrom.*, 2001, **212**, 327.
275 P. Butz, R. T. Kroemer, N. A. Macleod, E. G. Robertson and J. P. Simons, *J. Phys. Chem. A*, 2001, **105**, 1050.
276 P. Butz, R. T. Kroemer, N. A. Macleod and J. P. Simons, *J. Phys. Chem. A*, 2001, **105**, 544.
277 C. Pluetzer, E. Nir, M. S. de Vries and K. Kleinermanns, *Phys. Chem. Chem. Phys.*, 2001, **3**, 5466.
278 E. Nir, C. Janzen, P. Imhof, K. Kleinermanns and M. S. de Vries, *J. Chem. Phys.*, 2001, **115**, 4604.
279 E. Nir, K. Kleinermanns, L. Grace and M. S. de Vries, *J. Phys. Chem. A*, 2001, **105**, 5106.
280 Y. Wang, C. L. Hendrickson and A. G. Marshall, *Chem. Phys. Lett.*, 2001, **334**, 69.
281 L. S. Alconcel, H.-J. Deyerl and R. E. Continetti, *J. Am. Chem. Soc.*, 2001, **123**, 12675.
282 S. Ullrich, G. Tarczay, X. Tong, C. E. H. Dessent and K. Müller-Dethlefs, *Phys. Chem. Chem. Phys.*, 2001, **3**, 5450.
283 D. A. Wild, P. S. Weiser, E. J. Bieske and A. Zehnacker, *J. Chem. Phys.*, 2001, **115**, 824.
284 D. A. Wild, P. S. Weiser and E. J. Bieske, *J. Chem. Phys.*, 2001, **115**, 6394.
285 J. M. Weber, W. H. Robertson and M. A. Johnson, *J. Chem. Phys.*, 2001, **115**, 10718.
286 J. M. Weber, J. A. Kelley, W. H. Robertson and M. A. Johnson, *J. Chem. Phys.*, 2001, **114**, 2698.
287 D. Roth, O. Dopfer and J. P. Maier, *Phys. Chem. Chem. Phys.*, 2001, **3**, 2400.
288 O. Dopfer, D. Roth and J. P. Maier, *J. Chem. Phys.*, 2001, **114**, 7081.
289 D. van Heijnsbergen, M. A. Duncan, G. Meijer and G. von Helden, *Chem. Phys. Lett.*, 2001, **349**, 220.
290 J. Oomens, B. G. Sartakov, A. G. G. M. Tielens, G. Meijer and G. von Helden, *Astrophys. J.*, 2001, **560**, L99.
291 J. Oomens, G. Meijer and G. von Helden, *J. Phys. Chem. A*, 2001, **105**, 8302.
292 T. Pino, P. Bréchignac, E. Dartois, K. Demyk and L. d'Hendecourt, *Chem. Phys. Lett.*, 2001, **339**, 64.
293 J. A. Piest, J. Oomens, J. Bakker, G. von Helden and G. Meijer, *Spectrochim. Acta, Part A*, 2001, **57A**, 717.
294 S. B. Nielsen, A. Lapierre, J. U. Andersen, U. V. Pedersen, S. Tomita and L. H. Andersen, *Phys. Rev. Lett.*, 2001, **87**, 228102.
295 A. Warshel, *J. Biol. Chem.*, 1998, **273**, 27035.
296 W. W. Cleland, P. A. Frey and J. A. Gerlt, *J. Biol. Chem.*, 1998, **273**, 25529.
297 W. R. Cannon and S. J. Benkovic, *J. Biol. Chem.*, 1998, **273**, 26257.
298 M. J. S. Dewar and D. M. Storch, *Proc. Natl. Acad. Sci. U. S. A.*, 1985, **82**, 2225.
299 A. T. Iavarone, J. C. Jurchen and E. R. Williams, *Anal. Chem.*, 2001, **73**, 1455.
300 J. Wu, M. J. Polce and C. Wesdemiotis, *Int. J. Mass Spectrom.*, 2001, **204**, 125.
301 D. N. Shin, J. W. Wijnen, J. B. F. N. Engberts and A. Wakisaka, *J. Phys. Chem. B*, 2001, **105**, 6759.
302 L. Angel and A. J. Stace, *Chem. Phys. Lett.*, 2001, **345**, 277.
303 T. Wróblewski, E. Gazda, J. Mechlinska-Drewko and G. P. Karwask, *Int. J. Mass Spectrom.*, 2001, **207**, 97.
304 J. M. Weber, J. Kim, E. A. Woronowicz, G. H. Weddle, I. Becker, O. Cheshnovsky and M. A. Johnson, *Chem. Phys. Lett.*, 2001, **339**, 337.
305 X. Yang, X.-B. Wang and L.-S. Wang, *J. Chem. Phys.*, 2001, **115**, 2889.
306 X.-B. Wang, X. Yang, J. B. Nicholas and L.-S. Wang, *Science*, 2001, **294**, 1322.
307 A. A. Shvartsburg and K. W. M. Siu, *J. Am. Chem. Soc.*, 2001, **123**, 10071.
308 R. R. Wright, N. R. Walker, S. Firth and A. J. Stace, *J. Phys. Chem. A*, 2001, **105**, 54.
309 K. P. Faherty, C. J. Thompson, F. Aguirre, J. Michne and R. B. Metz, *J. Phys. Chem. A*, 2001, **105**, 10054.
310 S. E. Rodriguez-Cruz and E. R. Williams, *J. Am. Soc. Mass Spectrom.*, 2001, **12**, 250.
311 U. Achatz, B. S. Fox, M. K. Beyer and V. E. Bondybey, *J. Am. Chem. Soc.*, 2001, **123**, 6151.
312 B. S. Fox, M. K. Beyer and V. E. Bondybey, *J. Phys. Chem. A*, 2001, **105**, 6386.
313 T. Shoeib, H. El Aribi, K. W. M. Siu and A. C. Hopkinson, *J. Phys. Chem. A*, 2001, **105**, 710.
314 G. Vitale, A. B. Valina, V. H. Huang, R. Amunugama and M. T. Rodgers, *J. Phys. Chem. A*, 2001, **105**, 11351.
315 C. Chaudhuri, J. C. Jiang, C.-C. Wu, X. Wang and H.-C. Chang, *J. Phys. Chem. A*, 2001, **105**, 8906.
316 M. Mons, I. Dimicoli, B. Tardivel, F. Piuzzi, E. G. Robertson and J. P. Simons, *J. Phys. Chem. A*, 2001, **105**, 969.
317 E. G. Robertson, M. R. Hockridge, P. D. Jelfs and J. P. Simons, *Phys. Chem. Chem. Phys.*, 2001, **3**, 786.
318 J. R. Carney, A. V. Federov, J. R. Cable and T. S. Zwier, *J. Phys. Chem. A*, 2001, **105**, 3487.
319 A. V. Federov, J. R. Cable, J. R. Carney and T. S. Zwier, *J. Phys. Chem. A*, 2001, **105**, 8162.
320 E. F. Strittmatter and E. R. Williams, *Int. J. Mass Spectrom.*, 2001, **212**, 287.
321 M. P. Ince, B. A. Perera and M. J. Van Stipdonk, *Int. J. Mass Spectrom.*, 2001, **207**, 41.
322 C. Hao, R. E. March, T. R. Croley, J. C. Smith and S. P. Rafferty, *J. Mass Spectrom.*, 2001, **36**, 79.
323 J. Rak, P. Skurski, J. Simons and M. Gutowski, *J. Am. Chem. Soc.*, 2001, **123**, 11695.

324 P. Skurski, J. Rak, J. Simons and M. Gutowski, *J. Am. Chem. Soc.*, 2001, **123**, 11073.
325 S. Hoyau, J.-P. Pélicier, F. Rogalewicz, Y. Hoppilliard and G. Ohanessian, *Eur. J. Mass Spectrom.*, 2001, **7**, 303.
326 R. A. Jockusch, A. S. Lemoff and E. R. Williams, *J. Am. Chem. Soc.*, 2001, **123**, 12255.
327 R. A. Jockusch, A. S. Lemoff and E. R. Williams, *J. Phys. Chem. A*, 2001, **105**, 10929.
328 R. R. Julian, R. Hodyss and J. L. Beauchamp, *J. Am. Chem. Soc.*, 2001, **123**, 3577.
329 S. D. Friess and R. Zenobi, *J. Am. Soc. Mass Spectrom.*, 2001, **12**, 810.
330 J. Gross, F. Hillenkamp, K. X. Wan and M. L. Gross, *J. Am. Soc. Mass Spectrom.*, 2001, **12**, 180.
331 K. X. Wan, J. Gross, F. Hillenkamp and M. L. Gross, *J. Am. Soc. Mass Spectrom.*, 2001, **12**, 193.
332 J. B. Nicoll and D. V. Dearden, *Int. J. Mass Spectrom.*, 2001, **204**, 171.
333 R. R. Julian and J. L. Beauchamp, *Int. J. Mass Spectrom.*, 2001, **210/211**, 613.
334 C. Collette, D. Dehareng, E. De Pauw and G. Dive, *J. Am. Soc. Mass Spectrom.*, 2001, **12**, 304.
335 K. A. Kellersberger, J. D. Anderson, S. M. Ward, K. E. Krakowiak and D. V. Dearden, *J. Am. Chem. Soc.*, 2001, **123**, 11316.
336 R. G. Cooks, D. Zhang, K. J. Koch, F. C. Gozzo and M. N. Eberlin, *Anal. Chem.*, 2001, **73**, 3646.
337 K. J. Koch, F. C. Gozzo, D. Zhang, M. N. Eberlin and R. G. Cooks, *Chem. Commun.*, 2001, 1854.
338 R. Hodyss, R. R. Julian and J. L. Beauchamp, *Chirality*, 2001, **13**, 703.
339 A. E. Counterman and D. E. Clemmer, *J. Phys. Chem. B*, 2001, **105**, 8092.
340 S. Ahn, J. Ramirez, G. Grigorean and C. B. Lebrilla, *J. Am. Soc. Mass Spectrom.*, 2001, **12**, 278.
341 G. Grigorean and C. B. Lebrilla, *Anal. Chem.*, 2001, **73**, 1684.
342 B. Garcia, J. Ramirez, S. Wong and C. B. Lebrilla, *Int. J. Mass Spectrom.*, 2001, **210/211**, 215.
343 W. A. Tao and R. G. Cooks, *Angew. Chem., Int. Ed.*, 2001, **40**, 757.
344 D. Zhang, W. A. Tao and R. G. Cooks, *Int. J. Mass Spectrom.*, 2001, **204**, 159.
345 W. A. Tao, F. C. Gozzo and R. G. Cooks, *Anal. Chem.*, 2001, **73**, 1692.
346 G. Fago, A. Filippi, A. Giardini, A. Lagana, A. Paladini and M. Speranza, *Angew. Chem., Int. Ed.*, 2001, **40**, 4051.
347 A. Paladini, C. Calcagni, T. Di Palma, M. Satta, M. Speranza, D. Scuderi, A. Lagana, G. Fago and A. G. Guidoni, *Int. J. Photoen.*, 2001, **3**, 217.
348 A. Paladini, C. Calcagni, T. Di Palma, M. Speranza, A. Lagana, G. Fago, A. Filippi, M. Satta and A. G. Guidoni, *Chirality*, 2001, **13**, 707.
349 A. Filippi, A. Giardini, A. Latini, S. Piccirillo, D. Scuderi and M. Speranza, *Int. J. Mass Spectrom.*, 2001, **210/211**, 483.
350 A. G. Guidoni, S. Piccirillo, D. Scuderi, M. Satta, T. M. Di Palma, M. Speranza, A. Filippi and A. Paladini, *Int. J. Photoen.*, 2001, **3**, 223.
351 A. G. Guidoni, S. Piccirillo, D. Scuderi, M. Satta, T. M. Di Palma, M. Speranza, A. Filippi and A. Paladini, *Chirality*, 2001, **13**, 727.
352 F. He, A. G. Marshall and M. A. Freitas, *J. Phys. Chem. B*, 2001, **105**, 2244.
353 E. Levy-Seri, G. Koster, A. Kogan, K. Gutman, B. G. Reuben and C. Lifshitz, *J. Phys. Chem. A*, 2001, **105**, 5552.
354 P. Ustyuzhanin, A. Kogan, B. G. Reuben and C. Lifshitz, *Int. J. Chem. Kinetics*, 2001, **33**, 707.
355 T. Solouki, R. C. Fort Jr., A. Alomary and A. Fattahi, *J. Am. Soc. Mass Spectrom.*, 2001, **12**, 1272.
356 K. B. Green-Church, P. A. Limbach, M. A. Freitas and A. G. Marshall, *J. Am. Soc. Mass Spectrom.*, 2001, **12**, 268.
357 M. A. Freitas and A. G. Marshall, *J. Am. Soc. Mass Spectrom.*, 2001, **12**, 780.
358 D. R. Reed and S. R. Kass, *J. Am. Soc. Mass Spectrom.*, 2001, **12**, 1163.
359 S. Gronert and R. Huang, *J. Am. Chem. Soc.*, 2001, **123**, 8606.
360 G. E. Reid, S. E. Tichy, J. Pérez, R. A. J. O'Hair, R. J. Simpson and H. I. Kenttämaa, *J. Am. Chem. Soc.*, 2001, **123**, 1184.
361 B. A. Perera, M. P. Ince, E. R. Talaty and M. J. Van Stipdonk, *Rapid Commun. Mass Spectrom.*, 2001, **15**, 615.
362 T. Wyttenbach, P. R. Kemper and M. T. Bowers, *Int. J. Mass Spectrom.*, 2001, **212**, 13.
363 A. Meffert and J. Grotemeyer, *Isr. J. Chem.*, 2001, **41**, 79.
364 J. M. Price, C. J. Petzold, H. C. M. Byrd and H. I. Kenttämaa, *Int. J. Mass Spectrom.*, 2001, **212**, 455.
365 A. Liguori, A. Napoli and G. Sindona, *J. Am. Soc. Mass Spectrom.*, 2001, **12**, 176.
366 F. W. McLafferty, D. M. Horn, K. Breuker, Y. Ge, M. A. Lewis, B. Cerda, R. A. Zubarev and B. K. Carpenter, *J. Am. Soc. Mass Spectrom.*, 2001, **12**, 245.
367 D. M. Horn, K. Breuker, A. J. Frank and F. W. McLafferty, *J. Am. Chem. Soc.*, 2001, **123**, 9792.
368 M. Sørensen, J. S. Forster, P. Hvelplund, T. J. D. Jørgensen, S. B. Nielsen and S. Tomita, *Chem. Eur. J.*, 2001, **7**, 3214.
369 P. Hvelplund, S. B. Nielsen, M. Sørensen, J. U. Andersen and T. J. D. Jørgensen, *J. Am. Soc. Mass Spectrom.*, 2001, **12**, 889.
370 A. H. Payne and G. L. Glish, *Int. J. Mass Spectrom.*, 2001, **204**, 47.
371 I. A. Papayannopoulos and K. Biemann, *Acc. Chem. Res.*, 1994, **27**, 370.
372 Y. Ge, D. M. Horn and F. W. McLafferty, *Int. J. Mass Spectrom.*, 2001, **210/211**, 203.

373 K. A. Newton, P. A. Chrisman, G. E. Reid, J. M. Wells and S. A. McLuckey, *Int. J. Mass Spectrom.*, 2001, **212**, 359.
374 B. Paizs, I. P. Csonka, G. Lendvay and S. Suhai, *Rapid Commun. Mass Spectrom.*, 2001, **15**, 637.
375 B. Paizs and S. Suhai, *Rapid Commun. Mass Spectrom.*, 2001, **15**, 2307.
376 B. Paizs and S. Suhai, *Rapid Commun. Mass Spectrom.*, 2001, **15**, 651.
377 A. G. Harrison, *Int. J. Mass Spectrom.*, 2001, **210/211**, 361.
378 J. M. Farrugia, T. Taverner and R. A. J. O'Hair, *Int. J. Mass Spectrom.*, 2001, **209**, 99.
379 I. P. Csonka, B. Paizs, G. Lendvay and S. Suhai, *Rapid Commun. Mass Spectrom.*, 2001, **15**, 1457.
380 J. M. Farrugia, R. A. J. O'Hair and G. E. Reid, *Int. J. Mass Spectrom.*, 2001, **210/211**, 71.
381 A. P. Jonsson, T. Bergman, H. Jörnvall, W. J. Griffiths, P. Bratt and N. Strömberg, *J. Am. Soc. Mass Spectrom.*, 2001, **12**, 337.
382 A. G. Harrison, *J. Am. Soc. Mass Spectrom.*, 2001, **12**, 1.
383 C. S. Brinkworth, S. Dua, A. M. McAnoy and J. H. Bowie, *Rapid Commun. Mass Spectrom.*, 2001, **15**, 1965.
384 Y. Hoppilliard, F. Rogalewicz and G. Ohanessian, *Int. J. Mass Spectrom.*, 2001, **204**, 267.
385 F. Rogalewicz, Y. Hoppilliard and G. Ohanessian, *Int. J. Mass Spectrom.*, 2001, **206**, 45.
386 L. Rodriguez-Santiago, M. Sodupe and J. Tortajada, *J. Phys. Chem. A*, 2001, **105**, 5340.
387 T. Shoeib, A. C. Hopkinson and K. W. M. Siu, *J. Phys. Chem. B*, 2001, **105**, 12399.
388 I. K. Chu, T. Shoeib, X. Guo, C. F. Rodriquez, T.-C. Lau, A. C. Hopkinson and K. W. M. Siu, *J. Am. Soc. Mass Spectrom.*, 2001, **12**, 163.
389 T. Lin, A. H. Payne and G. L. Glish, *J. Am. Soc. Mass Spectrom.*, 2001, **12**, 497.
390 I. K. Chu, C. F. Rodriquez, A. C. Hopkinson, K. W. M. Siu and T.-C. Lau, *J. Am. Soc. Mass Spectrom.*, 2001, **12**, 1114.
391 T. Vaiser, C. L. Gatlin, R. D. Rao, J. L. Seymour and F. Turecek, *J. Mass Spectrom.*, 2001, **36**, 306.
392 W. A. Tao, L. Wu and R. G. Cooks, *J. Am. Soc. Mass Spectrom.*, 2001, **12**, 490.
393 B. A. Budnik, K. F. Haselmann and R. A. Zubarev, *Chem. Phys. Lett.*, 2001, **342**, 299.
394 K. Hkansson, H. J. Cooper, M. R. Emmett, C. E. Costello, A. G. Marshall and C. L. Nilsson, *Anal. Chem.*, 2001, **73**, 4530.
395 S. D.-H. Shi, M. E. Hemling, S. A. Carr, D. M. Horn, I. Lindh and F. W. McLafferty, *Anal. Chem.*, 2001, **73**, 19.
396 K. X. Wan and M. L. Gross, *J. Am. Soc. Mass Spectrom.*, 2001, **12**, 580.
397 Y. Wang, J.-S. Taylor and M. L. Gross, *J. Am. Soc. Mass Spectrom.*, 2001, **12**, 550.
398 Y. Wang, J.-S. Taylor and M. L. Gross, *J. Am. Soc. Mass Spectrom.*, 2001, **12**, 1174.
399 I. Compagnon, F. C. Hagemeister, R. Antoine, D. Rayane, M. Broyer, P. Dugourd, R. R. Hudgins and M. F. Jarrold, *J. Am. Chem. Soc.*, 2001, **123**, 8440.
400 L. C. Snoek, R. T. Kroemer, M. R. Hockridge and J. P. Simons, *Phys. Chem. Chem. Phys.*, 2001, **3**, 1819.
401 J. R. Carney and T. S. Zwier, *Chem. Phys. Lett.*, 2001, **341**, 77.
402 J. R. Carney, B. C. Dian, G. M. Florio and T. S. Zwier, *J. Am. Chem. Soc.*, 2001, **123**, 5596.
403 S. E. Rodriguez-Cruz, J. T. Khoury and J. H. Parks, *J. Am. Soc. Mass Spectrom.*, 2001, **12**, 716.
404 S. Ideue, K. Sakamoto, K. Honma and D. E. Clemmer, *Chem. Phys. Lett.*, 2001, **337**, 79.
405 B. S. Kinnear, M. R. Hartings and M. F. Jarrold, *J. Am. Chem. Soc.*, 2001, **123**, 5660.
406 D. T. Kaleta and M. F. Jarrold, *J. Phys. Chem. B*, 2001, **105**, 4436.
407 B. S. Kinnear and M. F. Jarrold, *J. Am. Chem. Soc.*, 2001, **123**, 7907.
408 A. E. Counterman and D. E. Clemmer, *J. Am. Chem. Soc.*, 2001, **123**, 1490.
409 J. A. Tarasza, A. E. Counterman and D. E. Clemmer, *Int. J. Mass Spectrom.*, 2001, **204**, 87.
410 E. R. Badman, C. S. Hoaglund-Hyzer and D. E. Clemmer, *Anal. Chem.*, 2001, **73**, 6000.
411 R. W. Purves, D. A. Barnett, B. Ells and R. Guevremont, *Rapid Commun. Mass Spectrom.*, 2001, **15**, 1453.
412 R. W. Purves, D. A. Barnett, B. Ells and R. Guevremont, *J. Am. Soc. Mass Spectrom.*, 2001, **12**, 894.
413 J. Gidden, J. E. Bushnell and M. T. Bowers, *J. Am. Chem. Soc.*, 2001, **123**, 5610.
414 S. A. Lorenz, E. P. Maziarz III and T. D. Wood, *J. Am. Soc. Mass Spectrom.*, 2001, **12**, 795.
415 R. Gupta, A. Kapur, J. L. Beck and M. M. Sheil, *Rapid Commun. Mass Spectrom.*, 2001, **15**, 2472.
416 V. Gabelica and E. De Pauw, *J. Mass Spectrom.*, 2001, **36**, 397.
417 P. R. Hoyne, L. M. Benson, T. D. Veenstra, L. J. Maher III and S. Naylor, *Rapid Commun. Mass Spectrom.*, 2001, **15**, 1539.
418 V. J. Nesatyy, *J. Mass Spectrom.*, 2001, **36**, 950.
419 P. A. Chrisman, K. A. Newton, G. E. Reid, J. M. Wells and S. A. McLuckey, *Rapid Commun. Mass Spectrom.*, 2001, **15**, 2334.
420 J. M. Wells, G. E. Reid, B. J. Engel, P. Pan and S. A. McLuckey, *J. Am. Soc. Mass Spectrom.*, 2001, **12**, 873.
421 C. Versluis and A. J. R. Heck, *Int. J. Mass Spectrom.*, 2001, **210/211**, 637.
422 N. Felitsyn, E. N. Kitova and J. S. Klassen, *Anal. Chem.*, 2001, **73**, 4647.
423 M. Nousiainen, P. Vainiotalo, X. Feng and P. J. Derrick, *Eur. J. Mass Spectrom.*, 2001, **7**, 393.
424 J. M. Wells, P. A. Chrisman and S. A. McLuckey, *J. Am. Chem. Soc.*, 2001, **123**, 12428.